

TECHNISCHE UNIVERSITÄT MÜNCHEN

Fachgebiet Molekulare Katalyse

**Building Blocks for
Organometallic Frameworks and Ionic Liquids**

Sara Abbassi

Vollständiger Abdruck der von der Fakultät für Chemie der Technischen Universität
München zur Erlangung des akademischen Grades eines

Doktors der Naturwissenschaften (Dr. rer. nat.)

genehmigten Dissertation.

Vorsitzende(r): Prof. Dr. Klaus Köhler

Prüfer der Dissertation: 1. Prof. Dr. Fritz E. Kühn
2. Prof. Dr. Ghada Bassioni

Die Dissertation wurde am 20.07.2016 bei der Technischen Universität München eingereicht
und durch die Fakultät für Chemie am 28.07.2016 angenommen.

Die vorliegende Arbeit entstand in der Zeit von November 2012 bis Dezember 2015 am Anorganisch-Chemischen Institut, Fachgebiet Molekulare Katalyse, der Technischen Universität München.

Diese Arbeit wurde durch die Bayerische Forschungstiftung gefördert.

I would like to express the deepest gratitude to my academic supervisor

Prof. Dr. Fritz E. Kühn

for giving me the opportunity to work in his research group, his guidance and all his kind support in regards to the research work, scholarship and other daily issues which were crucial for the success of this thesis.

ACKNOWLEDGMENTS

Without the supporting of the following people the completion of this work could not be possible. Therefore, my special thanks go to:

Dr. Alexander Pöthig, Dr. Eberhardt Herdtweck, Dr. Teresa Meister and Dr. Marlene Kaposi for crystal measurements.

Dr. Iulius Markovits for all his advices and technical support in ionic liquid project.

Dr. Markus Drees for his support on IT related issues.

Ms. Bircan Dilki, Ms. Ulrike Ammari and Ms. Petra Ankenbauer for the characterization of the countless compound and their nice cooperation.

Dr. Gabriele Raudaschl-Sieber, Jürgen Kudermann and Maria Weindl for NMR and GC-MS measurements.

Ms. Rodica Dumitrescu for mass spectroscopic measurements.

Mr. Martin Schellerer for chemical supply and shipment as well as technical support.

Dr. Viktor Hlukhyy for his support on magnetic susceptibility and X-ray powder diffraction measurements.

My internship students who assisted me in the lab, especially **Ms. Pei Shan Tan** for her good cooperation.

All my nice colleagues in ACI group who helped me during my PhD studies, especially **Dr. Robert Reich, Dr. Claudia Hille, Mr. Markus Anneser, Dr. Xumin Cai and Ms. Esther Bayon**.

All secretaries, **Ms. Ulla Hifinger, Ms. Irmgard Grötsch, Ms. Roswitha Kaufmann and Ms. Renate Schuhbauer-Gerl**, for their support in administrative cases.

I would also like to thank my dear husband, **Morteza**, who has made this journey as smooth as possible with his unlimited love and support. I express my deepest appreciation to my parents, **Khosrow and Hourieh**, as well who have always supported and encouraged me, and my sister, **Sanaz**, for her inspiring role through all times.

Abstract

The research work described in this thesis is divided in two major parts. The first one deals with potential building blocks for metal-organic frameworks (MOFs), the second part focusses on the synthesis of novel ionic liquids (ILs).

In the first part of the work chromium complexes are examined, since their molybdenum derivatives have been successfully applied for the synthesis of MOFs. Chromium acetates and chromium nitrile complexes were selected as starting materials. Due to the high reactivity of the latter compound, not all reactions yielded the intended products. In any case, the resulting compounds were characterized and examined. Five crystal structures could be obtained as well. Due to the size of the compounds and associated solvent molecules the structures are of different quality levels, but allow at least a structural proof of the respective compounds' composition. Due to the high precursor reactivity, a chemistry of similar usefulness as in the case of Mo could not be established.

In the second part of the research, differently substituted imidazolium and pyrrolidinium based ionic liquids with bromides as counter ions were synthesized and anion exchange was executed for several examples to broaden the scope of available ionic liquids. After obtaining a sufficiently high level of purity of the products, electrochemical properties of the synthesized ILs were examined by CV and LSV measurements in order to use them later as electrolytes or electrolyte additives of Li-ion or Na based batteries. For the electrochemical tests, a certain amount of each of the ILs was dissolved in selected electrolytes. The resulted electrochemical windows were compared to the used commercial electrolyte consequently. This research was conducted in cooperation with a battery research group at the Nanyang Technological University (NTU) in Singapore. Unfortunately, most of the work performed at NTU was not finished when this thesis was written.

Kurzfassung

Die vorliegende Arbeit ist in zwei Themenbereiche unterteilt. Während sich der erste Teil mit potentiellen Grundbausteinen für metallorganische Netzwerke (MOFs) beschäftigt, konzentriert sich der zweite Teil auf die Synthese neuer ionischer Flüssigkeiten (ILs).

Im ersten Teil dieser Arbeit wurden Chromkomplexe untersucht, da deren Molybdän-Derivate bereits erfolgreich zur Synthese von MOFs angewendet werden konnten. Als Ausgangsverbindungen dienten hierbei Chromazetat und Chromnitril-Komplexe. Aufgrund der hohen Reaktivität der letzteren Verbindung, führten einige Reaktionen nicht zu den erhofften Produkten. Jedoch wurden die jeweils erhaltenen Verbindungen charakterisiert und untersucht. Fünf Kristallstrukturen konnten erhalten werden. Aufgrund der Größe der Verbindungen sowie darin enthaltener Lösungsmittelmoleküle erlauben diese Strukturen teilweise keine detailliertere Diskussion der Bindungsabstände und Bindungswinkel, ermöglichen aber einen Beweis für die Zusammensetzung der Verbindungen. Eine weiterführende Chemie, ähnlich der des Molybdäns konnte aufgrund der hohen Reaktivität der Startverbindungen aber im Rahmen dieser Arbeit nicht etabliert werden.

Im zweiten Teil wurden unterschiedlich substituierte ionische Flüssigkeiten auf der Basis von Imidazol- und Pyrrol-Grundgerüsten mit Bromiden als Gegenionen synthetisiert. Anionenaustausch wurde ausgeführt, um ein breiteres Spektrum an ionischen Flüssigkeiten zu erhalten. Die elektrochemischen Eigenschaften der gereinigten Produkte wurden mittels CV- und LSV-Messungen untersucht, um sie später als Elektrolyte bzw. Elektrolytadditive für Natrium bzw.- Lithiumionenbatterien einzusetzen.

Für die Durchführung der elektrochemischen Tests wurden die ionischen Flüssigkeiten in ausgewählten Elektrolyten gelöst und die resultierenden elektrochemischen Fenster (EWs) daraufhin mit dem des verwendeten, handelsüblichen Elektrolyten verglichen. Diese Messungen wurden in Zusammenarbeit mit einer Batterieforschungsgruppe an der Nanyang Technological University (NTU) in Singapur durchgeführt. Leider waren die an der NTU durchgeführten Untersuchungen zum Zeitpunkt des Verfassens dieser Arbeit noch nicht beendet.

Abbreviations

δ	chemical shift
$^{\circ}\text{C}$	degree centigrade
μ_{B}	bohr magneton
\AA	angstrom
Ar	aromatic group
Bn	benzyl
Bn^{F}	2',3',4',5',6'-pentafluorobenzyl
bpy	2,2'-bipyridyl
Bu	n-butyl
$t\text{Bu}$	tertio-butyl
CV	cyclic voltammetry
d	doublet (NMR)
DCM	dichloromethane
DEC	diethyl carbonate
DPPF	1,1'-bis(diphenylphosphino)ferrocene
EC	ethylene carbonate
Et_2O	diethyl ether
equiv.	equivalent(s)
Fc	ferrocene
FCA	ferrocene monocarboxylic acid
g	gram(s)
h	hour(s)
Hz	Hertz
IL	ionic liquid
IR	infrared (spectroscopy)
J	coupling constant
K	kelvin
L	ligand

L _{ax}	axial ligand
LSV	linear sweep voltammetry
M	molar, metal
m	multiplet (NMR), medium (IR)
mbipy	5,5'-Dimethyl-2,2'-bipyridine
Me	methyl
MHz	megahertz
mL	millilitre(s)
mmol	millimole(s)
MOFs	metal-organic frameworks
m.p.	melting point
NMR	nuclear magnetic resonance (spectroscopy)
OTf	trifluoromethanesulfonate
Ph	phenyl
ppm	parts per million
R	any alkyl or aryl group
RT	room temperature
RTIL	room temperature ionic liquid
S	spin quantum number
s	singlet (NMR), strong (IR), second
SC-XRD	single crystal X-ray diffraction
sep	septet (NMR)
t	triplet (NMR)
T	tesla
TFSI	bis(trifluoromethane)sulfonimide; bistriflimide
THF	tetrahydrofuran
UV-Vis	ultraviolet–visible (spectroscopy)
V	volt(s)
w	week (IR)

Glossary of Ionic Liquids

[BMIm]	1-butyl-3-methylimidazolium
[MBnIm]	1-benzyl-3-Methylimidazolium
[MMBnIm]	1-benzyl-2,3-dimethylimidazolium
[MBn ^F Im]	1-methyl-3-(2',3',4',5',6'-pentafluorobenzyl)imidazolium
[MMBn ^F Im]	1,2-dimethyl-3-(2',3',4',5',6'-pentafluorobenzyl)imidazolium
[BnBnIm]	1,3-dibenzylimidazolium
[Bn ^F Bn ^F Im]	1,3-bis-(2', 3', 4', 5', 6'-pentafluorobenzyl)imidazolium
[MBnPyr]	1-benzyl-1-methylpyrrolidinium
[MBn ^F Pyr]	1-methyl-1-(2',3',4',5',6'-pentafluorobenzyl)pyrrolidinium
PipGuan	N,N,N',N'-tetramethyl-N'',N''-pentamethyleneguanidinium

Table of Contents

1. Introduction.....	1
1.1. Metal-Organic Frameworks.....	2
1.1.1. Metal-Organic Frameworks and their Applications.....	2
1.1.2. Paddle-wheel Complexes as Building Units of MOFs.....	3
1.1.3. Dichromium Tetraacetate Complexes.....	4
1.1.4. Trimeric Chromium Acetates Complexes.....	8
1.1.5. Nitrile Ligated Chromium Complexes and their Applications.....	9
1.2. Ionic Liquids.....	11
1.2.1. A Brief History of Ionic Liquids (ILs) and their Applications.....	11
1.2.2. Electrochemical Potential of ILs.....	14
1.2.3. Application of ILs in Batteries.....	15
1.2.4. Application of ILs in Lithium-ion Cells.....	15
1.2.5. Electrochemical Windows of RTILs.....	16
2. Objective.....	17
2.1. Chromium-based Building Blocks for Metal-Organic Frameworks.....	18
2.2. Ionic Liquids in Li-ion Batteries.....	18
3. Results and Discussion.....	19
3.1. Chromium Complexes.....	20
3.1.1. A Review of the Performed Research on Chromium Complexes.....	20
3.1.2. Chromium (III) Complexes.....	23
3.1.2.1. $[\text{Cr}(\text{mbpy})_3][\text{BF}_4]_3$	23
3.1.2.2. $[\text{Cr}_3\text{O}(\text{O}_2\text{C-Fc})_6(\text{THF})_3]^{+1}$ Complexes.....	26
3.1.3. Chromium (II) Complex of $\text{Cr}(\text{DPPF})(\text{Cl})_2$	27
3.2. Ionic Liquids.....	28
3.2.1. Synthesis.....	28
3.2.1.1. Preparation of the Ionic Liquid Halide Salts.....	28
3.2.1.2. Anion Exchange.....	30
3.2.1.2.1. ILs with BF_4 , OTf, PF_6 and TFSI counter anions.....	30
3.2.1.2.2. Preparation of BF_4 , OTf, PF_6 and TFSI Salts of ILs.....	31
3.2.2. Characterization.....	33
3.2.3. Electrochemical Tests.....	36
3.2.3.1. Preparation.....	36
3.2.3.2. Electrochemical Window Results.....	37
4. Conclusion and Summary.....	39
5. Experimental Details.....	44
5.1. General Procedure.....	45
5.2. Chromium Complexes.....	46
5.2.1. Synthesis of $\text{Cr}_2(\text{O}_2\text{C-Fc})_4$ Complex.....	46
5.2.1.1. Substitution of the Acetate Group in $\text{Cr}_2(\text{O}_2\text{CCH}_3)_4$ Complex.....	46
5.2.1.2. Using Chromium Metal as the Starting Material.....	47
5.2.1.3. Using Tetrakis(nitrile)chromium(II) Complex as the Starting Material.....	47
5.2.1.4. Using Chromocene as the Starting Material.....	48

5.2.2. Synthesis of $[\text{Cr}_3\text{O}(\text{O}_2\text{C-Fc})_6(\text{THF})_3]^{+1}$ Complexes	48
5.2.2.1. $[\text{Cr}_3\text{O}(\text{O}_2\text{C-Fc})_6(\text{THF})_3][\text{CrCl}_4(\text{THF})_2]$	48
5.2.2.2. $[\text{Cr}_3\text{O}(\text{O}_2\text{C-Fc})_6(\text{THF})_3]\text{I}_3$	48
5.2.3. Reactions of $\text{Cr}_2(\text{O}_2\text{CCH}_3)_4$ with Long Carbon Chain Dicarboxylic Acids	49
5.2.3.1. $\text{Cr}_2(\text{O}_2\text{CCH}_3)_4$ + Adipic acid	49
5.2.3.2. $\text{Cr}_2(\text{O}_2\text{CCH}_3)_4$ + Sebacic acid.....	49
5.2.4. Reactions of Tetrakis(nitrile)chromium(II) tetrafluoroborate Complex of $[\text{Cr}(\text{NCPh})_4][\text{BF}_4]_2$	50
5.2.4.1. Reaction of $[\text{Cr}(\text{NCPh})_4][\text{BF}_4]_2$ with 5,5'-Dimethyl-2,2'-bipyridine.....	50
5.2.4.2. Reaction of $[\text{Cr}(\text{NCPh})_4][\text{BF}_4]_2$ with Diethylenetriamine.....	50
5.2.4.3. Reaction of $[\text{Cr}(\text{NCPh})_4][\text{BF}_4]_2$ with N,N,N',N'-Tetrakis(di-phenylphosphanyl) ethane-1,2-diamine	51
5.2.4.4. Reaction of $[\text{Cr}(\text{NCPh})_4][\text{BF}_4]_2$ with 1,1'-Bis(diphenylphosphino)ferrocene (DPPF)	51
5.3. Ionic liquids	51
5.3.1. Synthesis and General Procedure.....	51
5.3.2. Analysis.....	52
5.3.2.1. Imidazolium-based ILs	52
5.3.2.2. Pyrrolidinium-based ILs	62
5.3.3. Electrochemical Measurements	65
6. References	67
7. Appendix	80

Table of Figures

Figure 1.1. Schematic representation of a tri-nuclear node forming highly connected metal-organic frameworks	3
Figure 1.2. “Paddle-wheel” structure of chromium acetate (Cr: blue, O: red, C: grey)	4
Figure 1.3. Formation of a 3D porous network	4
Figure 1.4. Molecular structure of dichromium tetraacetate with the ‘paddle-wheel’ motif	5
Figure 1.5. The formation of infinite chains of $\text{Cr}_2(\text{O}_2\text{CR})_4$ by oxygen bridges bonding	5
Figure 1.6. Self-association of $\text{Cr}_2(\text{O}_2\text{CR})_4(\text{O}_2\text{Cbiph})_4$ molecules	6
Figure 1.7. Parallel infinite chains between neighboring Cr pairs	6
Figure 1.8. $\text{Cr}_2(\text{O}_2\text{CAr})_4$ molecule (hydrogen atoms omitted for clarity)	7
Figure 1.9. Plot of E_{ST} gap for some $\text{Cr}_2(\text{O}_2\text{CR})_4\text{L}_2$ compounds	7
Figure 1.10. The structure of $[\text{Cr}_3(\mu\text{-O})(\mu\text{-RCO}_2)_6(\text{L})_3]^+$	8
Figure 1.11. Catalytically active homochiral MOF CMIL-1	9
Figure 1.12. $[\text{Cr}(\text{RCN})_4][\text{BF}_4]_2$ complex	10
Scheme 1.1. Polymerization of cyclopentadiene in the presence of $[\text{M}(\text{MeCN})_n][(\text{BF}_4)]_2$ complexes	10
Figure 1.13. Homoleptic tris(2,2'-bipyridine) metal complex	11
Figure 1.14. Typical cations and anions in ionic liquids	12
Figure 1.15. 1-butylpyridinium chloride- aluminum chloride	13
Scheme 3.1. Performed reactions in order to synthesize $\text{Cr}_2(\text{O}_2\text{C-Fc})_4$ complex	20
Scheme 3.2. Desired reaction for replacing two neighboring carboxylate groups of $\text{Cr}_2(\text{O}_2\text{CCH}_3)_4$ with a proper dicarboxylic acid	21
Scheme 3.3. Reaction of dichromium tetraacetate complex with adipic acid	21
Scheme 3.4. Reaction of dichromium tetraacetate complex with sebacic acid	22
Scheme 3.5. Performed reactions of $[\text{Cr}(\text{NCR})_4][\text{BF}_4]_2$ with carboxylic acids and multidentate ligands	23
Figure 3.6. Comparison of the resulting $^1\text{H-NMR}$ spectra for diluted and concentrated solutions of compound 3a in CD_3CN	24
Figure 3.7. Crystal structure of complex 3b	25
Figure 3.8. Crystal structure of complex 3c (Cr: blue, C: grey, N: yellow, F: light green, B: pink)	25
Figure 3.9. Crystal structure of complex 3d (Cr: blue, O: red, C: grey, Cl: green)	27
Figure 3.10. Crystal structure of complex 3e (Cr: blue, O: red, C: grey, I: violet)	27
Figure 3.11. Crystal structure of complex 3f (Cr: blue, Fe: red, C: grey, P: orange, Cl: green)	28
Figure 3.12. Synthesized imidazolium, pyrrolidinium and guanidinium-piperidinium cations	28
Scheme 3.6. General procedure for synthesis of imidazolium bromides	29
Scheme 3.7. General procedure for synthesis of pyrrolidinium bromides	29
Scheme 3.8. Synthesis of imidazolium bromide by quaternization reaction of 1-(trimethylsilyl)-1H-imidazole	30
Scheme 3.9. Synthesis procedure for PipGuan-based ionic liquid	30
Figure 3.13. $^1\text{H-NMR}$ spectrum of $[\text{MMBnIm}][\text{Br}]$	33
Figure 3.14. $^1\text{H-NMR}$ of $[\text{MBnPyr}][\text{Br}]$	34
Figure 3.15. $^1\text{H-NMR}$ spectrum of $[\text{BMIm}][\text{Br}]$	35
Figure 3.16. $^1\text{H-NMR}$ spectrum of $[\text{BMIm}][\text{OTf}]$	35
Figure 3.17. $^{13}\text{C-NMR}$ spectra of $[\text{BMIm}][\text{Br}]$ (a) and $[\text{BMIm}][\text{OTf}]$ (b) (# peaks belong to OTf anion)	36

1. Introduction

1.1. Metal-Organic Frameworks

1.1.1. Metal-Organic Frameworks and their Applications

Metal-organic frameworks (MOFs) are also known as metal-ligand coordination polymers and porous coordination polymers (PCPs).¹ The first compound which can be considered as a member of this family was reported by Kinoshita et al. in 1959.² Other reports of coordination polymers followed in the early 1960's³⁻⁵ and the topic has even been reviewed in 1964.⁶ However, these compounds did not receive much attention until the late 1990's, when the subject was "re-discovered". Pioneering work was done by Robston et al.,⁷⁻⁹ demonstrating that the formation of porous frameworks was easily achievable.

MOFs have regular pores ranging from micro to mesopores,^{10,11} resulting in a large pore surface area and a highly designable framework, pore shape, pore size and surface functionality. Their structures are based on organic ligands as linkers and metal centers as connectors. The choice of linkers and metals has a significant effect on the properties of MOFs. The rich functionality and designability of the organic ligands and physical properties of metal ions are fascinating for the design of various functions, not only conventional adsorptive functions such as gas storage,¹²⁻¹⁶ gas separation¹⁷⁻²⁰ and catalysis,²¹⁻²⁴ but also other physical and chemical functions that can be integrated in the frameworks. In addition to coordination bonds, MOFs are also connected by other weak interactions or noncovalent bonds such as H-bonds, π -electron stacking and van der Waals interactions. These interactions lead to structural flexibility and dynamics in the crystalline state, which also promotes the unique character of MOFs in the field of porous materials.¹ The metal-linker coordination bonds are stronger than the other (rather weak) interactions. Therefore, it is possible to completely remove solvent molecules from the pores without structural collapse of the frameworks.²⁵

MOFs can provide various frameworks constructed from one, two or three dimensional networks.²⁶ Three-dimensional metal-organic networks incorporating uniform pores usually include guest species introduced during synthesis. If this guests can be removed under vacuum or at elevated temperature and permanent porosity is retained, then guest molecules such as hydrogen, nitrogen, carbon dioxide or methane can be re-introduced into the network.²⁷ In fact, the vast surface area characteristic of MOFs enables large gas storage capacities that soak up as a sponge. Therefore, gas molecules have large quantity of absorption sites. Molecules which are adsorbed and immobilized in the material, occupy lesser volume than when they are free to move as a gas. Therefore, at a given pressure a tank filled with MOFs material can store much more gas than an empty tank. The porosity also allows to separate and filter gases, thus the specific structure of MOFs can be designed to capture certain gases and chemicals, while letting others pass through. This technology has been a great interest for "green" fuels such as natural gas.²⁸

The design of MOFs for catalytic applications has emerged as an important research field. MOFs are functionalized catalytically in different ways: (1) metal as catalytic sites; (2) functional linkers as catalytic sites; (3) homochiral MOFs; (4) MOF-encapsulated catalytically active guest molecules or clusters; (5) mesoporous MOFs.²⁹

The nontoxic porous crystalline of MOFs are attractive for use in biomedicine. Most MOFs are

biodegradable and their stability lasts from a few hours up to some weeks. This function reduces their accumulation after biomedical use in the body. Iron oxo-centered polycarboxylate-based MOFs are nontoxic after intravenous administration of high doses in rats. The dual hydrophilic/hydrophobic character of MOFs and the presence of Lewis acid metal sites and functional linkers make these materials suitable candidates to host active therapeutic molecules and can then release them in a control manner under physiological conditions.³⁰

MOFs can be used in sensors as their micro- and mesoporosity provide a considerable surface area and in some cases their responsive properties make them functional material for sensing. To provide a recognition layer with a selectivity to the desired species they can be designed with respect to both size and chemical functionality of the internal coordination space available for hosting guest molecules.³¹⁻³³

The study of MOFs is a field of research that has rapidly risen to the forefront of modern chemistry. The area has grown from initial reports of Robson⁷⁻⁹ toward advanced design strategies,³⁴⁻³⁶ structural appreciation and topological analysis^{37,38} and has afforded a range of fascinating materials properties.³⁹⁻⁴⁴ The building block approach can be used to design and synthesize metal-organic frameworks of high connectivity. The frameworks in which at least one of the nodes within the network adopts a connectivity greater than six or in other words a node is connected to more than six nearest neighbor nodes are termed as highly connected metal-organic frameworks.⁴⁵ Figure 1.1.1. shows a tri-nuclear node forming such frameworks.

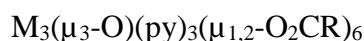
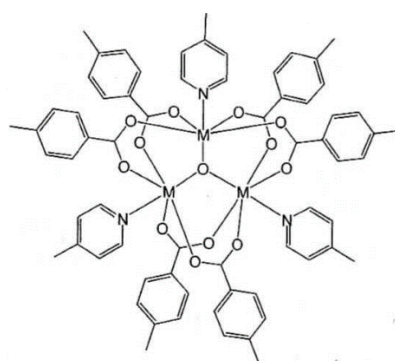


Figure 1.1. Schematic representation of a tri-nuclear node forming highly connected metal-organic frameworks

1.1.2. Paddle-wheel Complexes as Building Units of MOFs

A paddle-wheel (PW) type di-metal cluster is a popular building unit to construct frameworks. Many transition metals can form this type of cluster.¹ This term is derived from the long-known di-nuclear PW complexes of the type $M_2(\mu-O_2CR)_4$ (with or without a metal-metal bond), where each metal has an octahedral coordination sphere and four bidentate ligands which adopt the equatorial sites of the octahedral. (see figure 1.2)

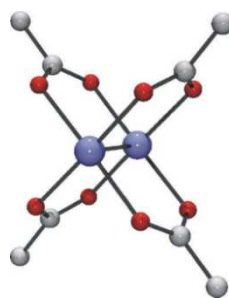


Figure 1.2. "Paddle-wheel" structure of chromium acetate (Cr: blue, O: red, C: grey)

The reactions of paddle-wheel complexes with organic linkers lead to one-, two-, or three-dimensional macro-molecular complexes or networks, which serve as building blocks for the rational synthesis of MOFs.⁴⁶ (Figure 1.3)

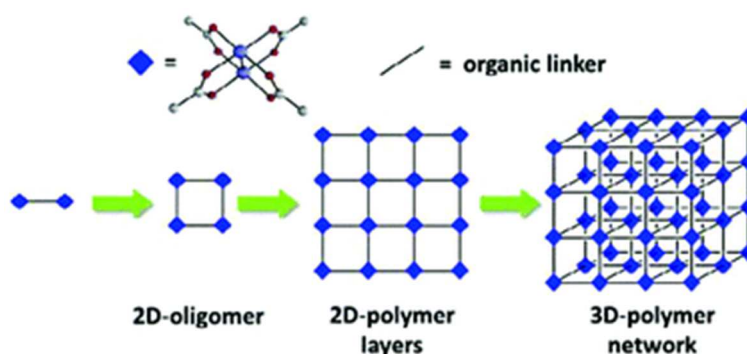


Figure 1.3. Formation of a 3D porous network

During the last few decades, a variety of macro-molecular coordination compounds and metal-organic frameworks (MOFs) containing di-nuclear paddle-wheel (PW) units based on metal-metal-bonded entities have been synthesized. Coordinating sites include both equatorial and axial ligands.⁴⁶⁻⁵⁶ Particularly widespread among the M^{2n+} -based metal-metal-bonded compounds are chromium-based systems. The Cr_2^{4+} unit has a formal $\sigma^2\pi^4\delta^2$ electron configuration and is connected by a quadruple bond. The strengths of these bonds is widely different from 1.83 Å to about 2.60 Å, depending on the Cr-Cr distance.⁵⁷

1.1.3. Dichromium Tetraacetate Complexes

As mentioned earlier in this chapter, among the elements of the first transition series, chromium has the ability to form compounds with quadruple bonds based on Cr_2^{4+} moieties with a paddlewheel structure. This has led to choosing dichromium tetracarboxylate complex as the starting material. The early 1844, Peligot^{58,59} reported the synthesis of " $CrC_4H_4O_5$ ", which we now know to be $Cr_2(O_2CCH_3)_4(H_2O)_2$ and the structure of which has been depicted in Figure 1.4.

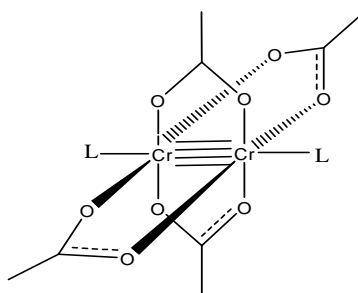


Figure 1.4. Molecular structure of dichromium tetraacetate with the 'paddle-wheel' motif

Peligo could isolate small red crystals which could be decomposed by exposure to air for a few moments from the blue aqueous solution of chromium (II) ions, upon addition of sodium or potassium acetate. The extension of this work to the preparation and non-structural characterization of the large number of similar compounds were reported,⁶⁰⁻⁶³ especially by Herzog and Kalies in 1964 who published a series of papers.⁶⁴⁻⁶⁹ In more recent years, additional compounds have been made, but dichromium tetraacetates did not become integrated with M-M multiple bond structure until 1970 when an accurate measurement of the crystal structure of $\text{Cr}_2(\text{O}_2\text{CR})_4(\text{H}_2\text{O})_2$ was carried out. This showed that Cr-Cr distance is 2.362(1) Å and made it reasonable for the quadruple M-M interaction.^{70,71}

In 2000, crystallographic characterization of a $\text{Cr}_2(\text{O}_2\text{CR})_4$ molecule with no axial ligand and a super short bond of 1.966 Å were carried out.⁷²

Dichromium tetracarboxylato complexes are generally air-sensitive, especially in solution and must be prepared and handled in an inert atmosphere although a report which has been published in 2012 by Levy et al. gives a preparation method for $\text{Cr}_2(\text{O}_2\text{CR})_4$ with no axial ligands under air.⁷³

$\text{Cr}_2(\text{O}_2\text{CR})_4$ complexes can be obtained difficultly without axial coordination as these kind of complexes have a strong tendency to coordinate electron pair donors in the axial positions. These compounds are insufficiently soluble in non-coordinating solvents preventing the growth of good quality crystals. Additionally, if they can be solved in coordination solvents, remains of solvent molecules could be found in each axial site. Using vacuum sublimation also cannot provide crystals with a high quality. Evidence shows that even when no independent ligands are present, $\text{Cr}_2(\text{O}_2\text{CR})_4$ molecules tend to connect with themselves and axial coordination occurs by association of the molecules to form an infinite chain.^{57,72} (Figure 1.5.)

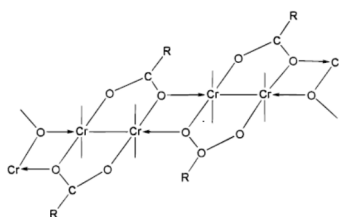


Figure 1. 5. The formation of infinite chains of $\text{Cr}_2(\text{O}_2\text{CR})_4$ by oxygen bridges bonding (RCO_2 groups which are above and below each Cr_2 units are not fully shown)

Although it had been attempted to employ an R group with different sizes and shapes to prevent any access to axial sites, as the position of R group is not close to the axial sites and the bond rotation between the carbonyl group and the α -carbon atom of R group doesn't allow any interference with axial positions, avoiding axial coordination was not achieved.^{74,75} Even with sterically appropriate R group, there is the question of sufficient solubility and other factors which are involved to obtain X-ray quality crystals. In the next stages of the research, it was attempted to prevent just the access of carbonyl oxygen atoms to axial sites. But the molecules still could have some axial coordination. An example of such situation has been illustrated in the report of Cotton et al in 1981 when 2-phenylphenyl was chosen as R group and although the ends of two $\text{Cr}_2(\text{O}_2\text{CR})_4(\text{O}_2\text{Cbiph})_4$ were blocked, a dimer product was achieved.⁷⁶ This could be seen in Fig. 1.6.

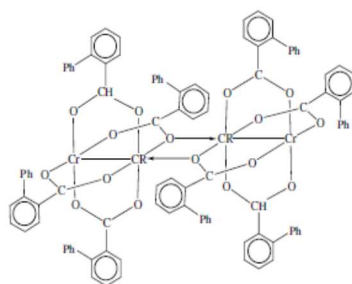


Figure 1.6. Self-association of $\text{Cr}_2(\text{O}_2\text{CR})_4(\text{O}_2\text{Cbiph})_4$ molecules

In 1988 in another report from Cotton et al. triphenylmethyl was chosen as the R group and the product was crystallized from benzene. But the axial ligation occurred and parallel infinite chains (shown in fig. 1.7) with a benzene molecule centred between every neighboring Cr pairs perpendicular to the chain direction were obtained.⁷⁷

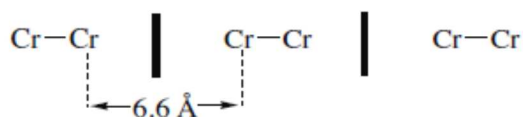


Figure 1.7. Parallel infinite chains between neighboring Cr pairs

In general, although finally, in 2000, a $\text{Cr}_2(\text{O}_2\text{CR})_4$ compound with R = 2,4,6-triisopropylphenyl and no axial ligation was characterized by X-ray (Fig. 1.8.),⁷² as mentioned previously most of $\text{Cr}_2(\text{O}_2\text{CR})_4$ compounds have axial coordination. This makes Cr-Cr distance longer.

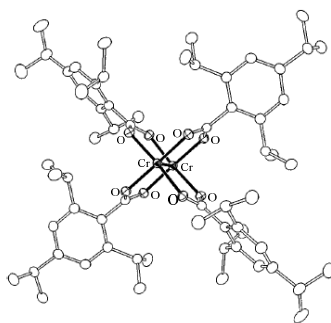


Figure 1.8. $\text{Cr}_2(\text{O}_2\text{CAR})_4$ molecule (hydrogen atoms omitted for clarity)

$\text{Cr}_2(\text{O}_2\text{CR})_4(\text{L}_{\text{ax}})_2$ complexes display paramagnetism (usually 3 - 0.5 μ_{B}). In some cases, at least part of this may be due to Cr^{III} impurities but in general where Cr-Cr distances are long, Cr_2^{4+} unit displays paramagnetism of its own, attributed to thermal population of a paramagnetic excited state.^{78,79} It was recognised in 1992 that if the single-triplet gap is sufficiently small relative to kT at room temperature, it would cause anomalous temperature dependence of ^1H -NMR spectrum, according to the equation below:

$$\Delta = \frac{CA}{kT} \left(3 + e^{\frac{E_{\text{ST}}}{kT}} \right)^{-1}$$

Where Δ is the shift in the magnetic field at which resonance is observed at a fixed frequency, C is collection of fundamental constants, A is the hyperfine coupling constant and T is the temperature in kelvin (K).

E_{ST} values were obtained for several $\text{Cr}_2(\text{O}_2\text{CR})_4\text{L}_2$ according to this equation at various temperature levels. Fig. 1.9. shows the linear plot of the singlet-triplet gap (E_{ST}) against Cr-Cr distance.⁸⁰

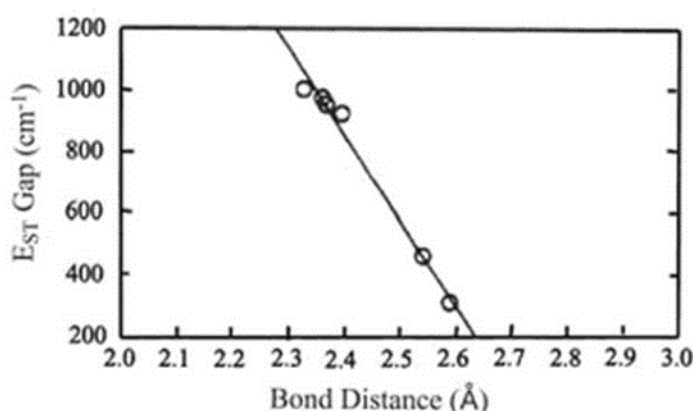


Figure 1.9. Plot of E_{ST} gap for some $\text{Cr}_2(\text{O}_2\text{CR})_4\text{L}_2$ compounds

1.1.4. Trimeric Chromium Acetates Complexes

The trimeric octahedral μ_3 -O chromium cluster⁸¹ is another type of building unit to construct frameworks. This kind of cluster exists in the structure of chromium (III) acetate. The trinuclear core has a central O atom and can be coordinated to three ligands. The three Cr^{III} atoms form vertices of a nearly equilateral triangle. Each of the six acetate carboxylate groups bridges a Cr-O-Cr fragment, in the way that two carboxylate groups bridge each of the sides of the equilateral triangle (Figure. 1.10.).^{82,83} The clusters of trimeric metal acetates shared by μ_3 -O, with various physical properties can be obtained with a large number of transition metals, such as chromium, iron, vanadium, ruthenium, manganese and cobalt.^{84,85,86}

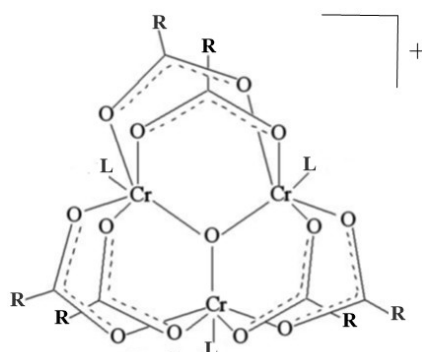


Figure 1.10. The structure of $[\text{Cr}_3(\mu\text{-O})(\mu\text{-RCO}_2)_6(\text{L})_3]^+$

Trimeric Cr^{III} acetate clusters are stable in solution from 25 °C to 200 °C without modification which allows exchange reactions to be performed in this range of temperature and gives rise to interesting structures.^{82,87,88}

The magnetic properties of both magnetically dilute and magnetically concentrated systems have been studied. In the first case, the magnetic interaction between a magnetic ion and any other such ion is negligible, therefore normal paramagnetism results can be observed. In the second system, each magnetic ion interacts with other ions and ferro- and antiferro-magnetism arise in this way.⁸⁴

In order to make 3D frameworks, trimeric acetate building units should be introduced to dicarboxylic acids and by increasing the temperature and presence of base, an exchange between monocarboxylic acid and dicarboxylic acid would be occurred while the trimeric SBU remains intact.⁸²

The investigations were carried out by Ferey's group on the chromium-based 3D MOFs MIL-100⁸⁹ and MIL-110⁹⁰. Both of these materials present potential open metal sites at Cr^{III} clusters which are occupied by water molecules in their as-synthesized form. The preparation of alcohol-decorated MIL-100 by reaction of the dehydrated MOF with methanol at room temperature was supported by infrared studies, showing the stability of the post-functionalized material even after being evacuated overnight at 737 K.⁹¹ A similar approach was used on MIL-101 to insert organic multifunctional amines, such as ethylenediamine, diethylenetriamine and

3-aminopropyltriethoxysilane.⁹² These newly obtained materials were found to be active as catalysts for the Knoevenagel condensation. More recently, Banerjee et al. reported the post-modification of MIL-101 by treating it with chiral L-proline derivatives (Figure. 1.11).⁹³ The functionalization was achieved by dehydration of the chromium trimers followed by the coordination of the L-pyridyl moiety of the ligand. These so-called CMIL materials were found to be active catalysts for asymmetric aldols reactions.⁹⁴

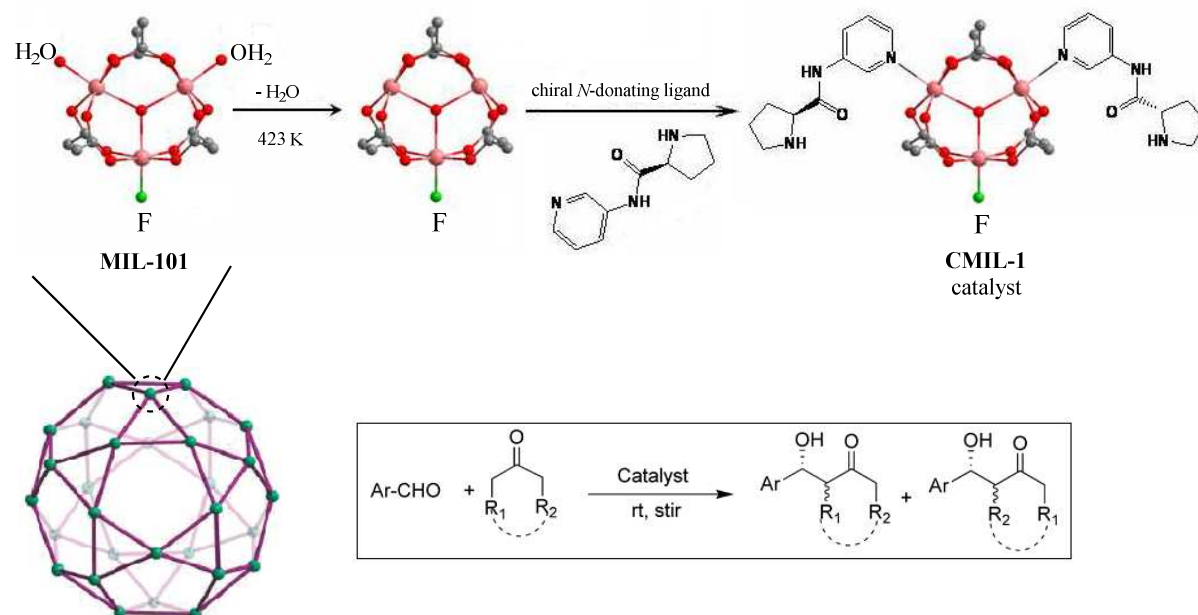


Figure 1.11. Catalytically active homochiral MOF CMIL-1

1.1.5. Nitrile Ligated Chromium Complexes and their Applications

During the last 158 years,⁹⁵ a large number of transition metal organonitrile complexes bearing weakly coordinating counteranions have been synthesized and several useful applications have been found for this compound class. The usefulness of coordinated nitriles (as weak donor ligands) comes from their ease of replacement by more strongly coordinating ligands,^{96,97} other metal cores or substrates which makes them widely employed starting materials for the synthesis of a variety of other materials and complexes.⁹⁸⁻¹⁰¹ Furthermore, some of them are also used as catalysts¹⁰² for organic reactions in both homogeneous and heterogeneous phase such as polymerization reactions. Monomeric and dimeric¹⁰³ organonitrile complexes have the ability to generate molecular wires, therefore they can be used as building blocks in metal-organic frameworks (MOFs). Weakly coordinating anions (WCA)¹⁰⁴⁻¹⁰⁶ as counteranions provide open coordination sites.

Nitrile ligated transition metal complexes with general formulas $[M(RCN)_{2,4,6}][A]_{1,2}$, $[M(RCN)_6][A]_3$, and $[M_2(RCN)_{8-10}][A]_4$ are of interest in synthesis and application. Monomeric complexes bearing weakly coordinating anions include first row transition metals as well as some of the second and third row transition metals have been synthesized and characterized.¹⁰⁷⁻¹¹⁷

Infrared spectra of this type of monomeric complexes in nujol mulls or KBr as matrices display the CN asymmetric stretching vibration in a range between 2266 and 2354 cm^{-1} . Absorption in this spectral region is typical for coordinated acetonitrile.¹¹⁸

$^1\text{H-NMR}$ investigation of these kind of complexes show that because of different donor properties of the metal centres in comparison to the acetonitrile ligands, the $^1\text{H-NMR}$ signals of the diamagnetic compounds corresponding to the methyl group of the acetonitrile ligands have been shifted to slightly higher or lower fields in comparison to uncoordinated MeCN (2.10 ppm in CDCl_3 , 2.00 ppm in CD_3NO_2 , 1.95 ppm in CD_3CN , and 1.93 ppm in CD_2Cl_2). For paramagnetic acetonitrile complexes, $^1\text{H-NMR}$ spectra are different. As an example, for chromium (III) complexes the signals are strongly shifted to high frequencies (162-176 ppm) which is because of inducing considerable spin density on the ligands and consequently transferring the selective spin to the γ protons of acetonitrile.¹¹⁹ In addition, in solid-state $^1\text{H-NMR}$ of $[\text{Cr}(\text{MeCN})_4][\text{BF}_4]_2$ signal appears at 180 ppm. X-ray measurement determines that in $[\text{Cr}(\text{MeCN})_4][\text{BF}_4]_2$, the geometry around Cr^{2+} is highly distorted octahedral with square planar arranged acetonitrile ligands and optical positions depending on used counteranions are occupied by fluorine atom of BF_4^- or oxygen atom of CF_3SO_3^- .⁹⁸ The complexes $[\text{Cr}(\text{RCN})_4][\text{BF}_4]_2$ (Figure 1.12) with $\text{R} = \text{MeCN}$, ^tBu and Ph are active in cyclopentadiene polymerization (Scheme 1.1).^{116,120}

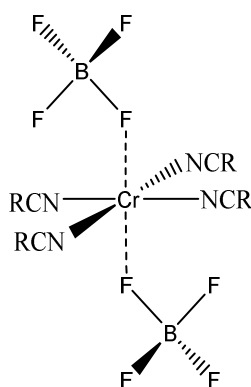
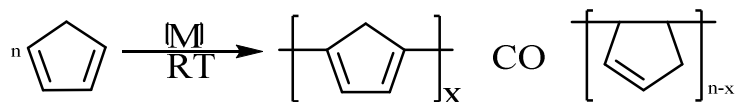


Figure 1.12. $[\text{Cr}(\text{RCN})_4][\text{BF}_4]_2$ complex



Scheme 1.1. Polymerization of cyclopentadiene in the presence of $[\text{M}(\text{MeCN})_n][\text{BF}_4]_2$ complexes ($\text{M} = \text{Pd}^{\text{II}}$ or first row transition metal ions, $n = 4, 6$)

Homoleptic tris(2,2'-bipyridine chelate) metal complexes (Figure 1.13) with general formula $[\text{M}(\text{L-L})_3]^{n+}$ and oxidation states of 3+ to 3- have been synthesized and characterized. The

central metal ion can be a main group element, transition metal, or a lanthanid ion.¹²¹ The highest point symmetry of these chiral homoleptic complexes is D_3 and they have a rigid conformation which can minimize intermolecular disorders and interactions. Their system is also extremely flexible without considerable shape change.¹²²

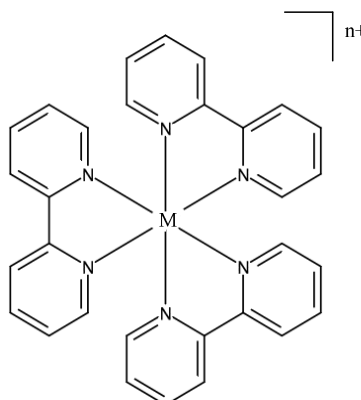


Figure 1.13. Homoleptic tris(2,2'-bipyridine) metal complex

Transition metal complexes containing polypyridyl ligands have been proven to be active in the fields of photo-initiated energy transfer and redox catalysis. Small modifications to the polypyridyl ligand or the metal centre can cause major influences in the properties of the resulting compounds.¹²³ Therefore, a lot of studies in photophysical, photochemical, spectroscopic and electrochemical detail of these kind of complexes have been carried out.¹²⁴⁻
¹³³ Cr³⁺ coordination compounds with nitrogen-containing ligands are amongst the attractive complexes applicable in photochemistry.¹³⁴

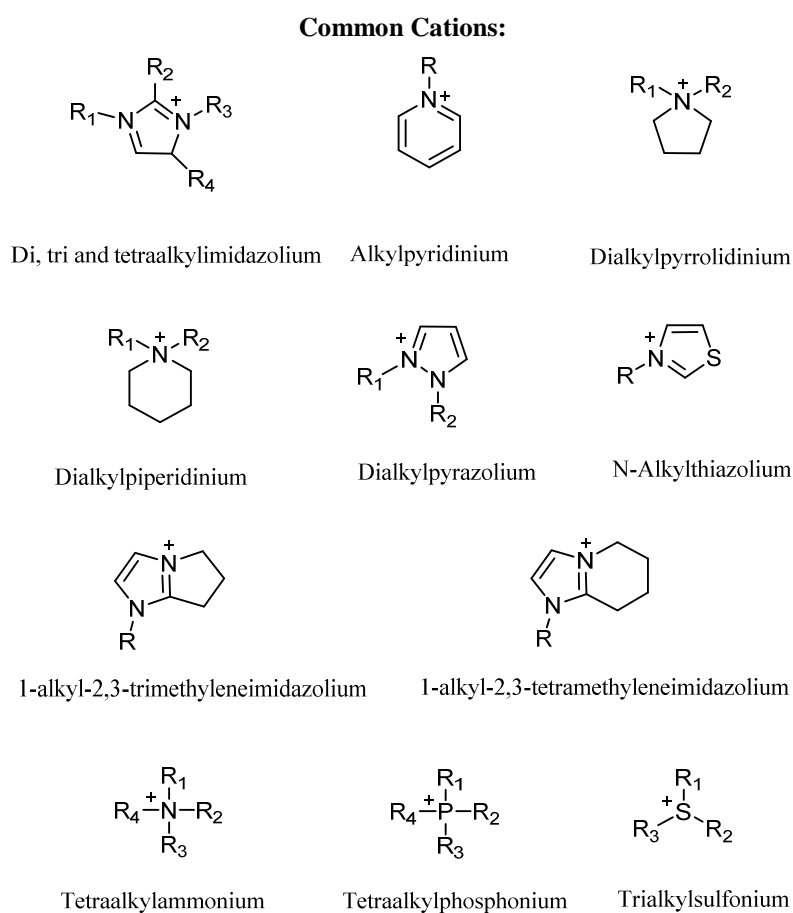
1.2. Ionic Liquids

1.2.1. A Brief History of Ionic Liquids (ILs) and their Applications

Ionic liquids (ILs) are salts with a melting point below 100 °C.¹³⁵ Room temperature ionic liquids (RTILs), have a melting point below room temperature and are of interest in recent years as tuneable “designer solvents”.¹³⁶ ILs have been investigated as ion conductive matrices¹³⁷ as well as reaction solvents¹³⁸ which are electrochemically and thermally stable, have a wide liquid range, high ionic conductivity, wide voltage window, low viscosity, negligible volatility and thus a low flammability.^{139,140,141} The mentioned unique properties as well as their gain in safety make them a promising alternative to conventional organic electrolytes or organic solvent systems in catalytic and synthetic reactions.^{142,143} They can also be used in energy storage applications¹⁴⁴ such as super capacitors, solar cells, fuel cells and batteries.^{140,145-152} In addition to this applications, ILs have attracted much attention in advanced electrochemical applications. Electrochemical reduction of carbon dioxide is one of the examples of this type of utilization.^{153,154} In recent years, ILs have been promoted as “green solvents” because of their low volatility, low flash-point and good thermal stability. Many of them are also considered as non- or low toxic.¹⁵⁵ Nevertheless, toxic ionic liquids are known

as well and the reasons for this toxicity have been examined and established.^{156,157} In contrast to other “green” solvents, ILs have the advantage of dissolving many organometallic complexes and often show a immiscibility with common organic solvents.

As the physical properties of ILs depend strongly on its cations and anions, modifications in the cation structures or changes of anions offer the opportunity to design suitable ILs according to the requirements of a particular purpose.¹³⁶ Figure 1.14 shows typical cations and anions which can be combined in ILs. Up to now, a huge number of ILs have been synthesized for different applications both in academia and industry.¹³⁵



Common Anions:

halides: Cr^- , Br^- , I^- , BF_4^- , PF_6^- , CF_3SO_3^- , $\text{N}(\text{SO}_2\text{CF}_3)_2^-$, $\text{B}(\text{CN})_4^-$, $\text{CH}_2\text{CHBF}_3^-$, CF_3BF_3^- , $\text{C}_2\text{F}_5\text{BF}_3^-$, $\text{nC}_3\text{H}_7\text{BF}_3^-$, $\text{nC}_4\text{H}_9\text{BF}_3^-$, CF_3CO_2^- , $\text{N}(\text{COCF}_3)(\text{SO}_2\text{CF}_3)^-$, $\text{N}(\text{SO}_2\text{F})_2^-$, $\text{N}(\text{CN})_2^-$, $\text{C}(\text{CN})_3^-$, SCN^- , SeCN^- , CuCl_2^- , AlCl_4^- , OH^-

Figure 1.14. Typical cations and anions in ionic liquids

ILs topic's origin is traced back to the second half of nineteenth century when it was observed in liquid form, known as “red oil”, which often appeared as a separate layer during Friedel-

Craft reactions (alkylation and acylation reactions) in 1877.¹⁵⁸ This red oil was later discovered as IL.¹⁵⁹ However, it is generally known that the birth of ILs took place in 1914 with synthesis of room temperature ionic liquid [EtNH₃][NO₃] (m.p. 12 °C) by Paul Walden. However, at that time this compound was not useful for any application due to its high reactivity.¹⁶⁰ In the late 1940s, Frank Hurley and Tom Weir made one of the first major research on the application of RTILs in the electrochemical industry, such as electroplating with aluminium.¹⁶¹⁻¹⁶⁴ The research on ionic liquids was intensified in 1963 by the USA Air Force Academy with the aim of finding a replacement electrolyte for thermal batteries. At that time LiCl-KCl with the melting point 375-550 °C was used as the molten salt electrolyte in thermal batteries. Although it's not a high melting point for an inorganic salt but this temperature cause materials problems inside the battery. Therefore, they tried to find the substances with lower melting points. They began to work with 1-butylpyridinium chloride-aluminum chloride (Figure 1.15). The mixture of AlCl₃ and 1-ethylpyridinium halides (mainly bromides) had been patented in 1948 as ionic conductive mixtures¹⁶¹⁻¹⁶³ and subsequently 1-butylpyridinium chloride-AlCl₃ was found as a better mixed halide system.^{165,166} It was noted that by using butylpyridinium cation and a large asymmetric anions with many degrees of freedom, the products with lower melting points could be obtained. This project was the start of modern era for ILs.¹⁶⁷

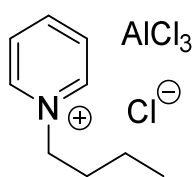


Figure 1.15. 1-butylpyridinium chloride- aluminum chloride

During the time between 1970s-1980s imidazolium salts have been investigated and among them 1-ethyl-3-methylimidazolium [EMIM]Cl mixed with AlCl₃ with a melting point below room temperature found to be a well behaved electrolyte in batteries.¹⁶⁸ It has been also determined that ionic liquids can be used as solvents and catalysts.¹⁶⁹ The first biphasic catalysis described for an IL system in 1972.¹⁷⁰ Since then, using ILs in synthetic chemistry has developed incredibly.^{171,172} In the early 1980s, ILs using chloroaluminate melts (AlCl₃) were used for transition metal complexes studies.¹⁷³⁻¹⁷⁵ As The pyridinium- and the imidazolium-based chloroaluminate ILs are hygroscopic, they must be prepared and stored under inert atmosphere and consequently their applications would be limited. Therefore, the next major step was to find air and water stable ionic liquid analogues.¹⁷⁶ In 1992, Wilkes and Zaworotko with the aim of preparing salts with dialkyl imidazolium cations and water-stable anions, substituted the water sensitive tetrachloroaluminate by weakly coordinating anions such as hexafluorophosphate (PF₆⁻) and tetra fluoroborate (BF₄⁻), allowing a much wider range of applications including battery electrolyte.¹⁷⁷ Recently a new class of air and moisture stable neutral ILs became available. Research has also been moving away from hexafluorophosphate and tetrafluoroborate towards less toxic alternatives such as bistriflimide (N(CF₃SO₂)₂⁻). Less

toxic cations have also been growing, with compounds like ammonium salts (such as choline) proving to be as flexible as imidazolium.¹⁷⁸

1.2.2. Electrochemical Potential of ILs

For electrochemical usage, the most important factors are non-volatility together with high ion conductivity which are the properties of a safe electrolyte solution. Nowadays, safety is a more important issue than performance. By using the RTILs with such properties we can have devices which are safer and have longer operational lives. Table 1.1 shows possible characteristics of organic ionic liquids which are applicable as electrolytes.¹⁴⁰

Low melting point	<ul style="list-style-type: none"> • Threatened as liquid at ambient temperature • Wide usable temperature range
Non-volatility	<ul style="list-style-type: none"> • Thermal stability • Flame retardancy
Composed by ions	<ul style="list-style-type: none"> • High ion density • High ion conductivity
Organic ions	<ul style="list-style-type: none"> • Various kinds of salts • Designable • Unlimited combinations

Table 1.1. Characteristics of organic ionic liquids

Electrochemistry needs electro-conductive and ion conductive materials. ILs open the possibility of improving ion conductive materials. Although aqueous salt solutions are one of the best solutions for electrochemical studies, because of the volatility of water, it is not possible to use them at high temperatures and on a small scale. Polymer electrolytes are non-volatile ion conductors, but they decompose at high temperatures. They also have a low ionic conductivity. In contrast, ILs are proton-conductive at a temperature higher than 100 °C.

Electrolyte solutions are essential for electrochemical devices and among them RTILs have received much attention as new electrolyte materials. Many of ILs show the ionic conductivity of more than 10^2Scm^{-1} at room temperature.^{179,180} Ionic conductivity is generally given by the equation:

$$\sigma_i = \sum n e \mu$$

Where n is the carrier ion number, e is the electric charge, and μ is the mobility of carrier ions. The studies on the electrochemical properties of ILs have been mainly focussed on their ionic conductivity, transference number and potential window. These electrochemical properties differ in accordance with factors such as moisture absorption, experimental atmosphere and electrode species. Electrochemical measurements should be performed in the glove box filled

with inert gas such as argon. Using nitrogen gas when lithium is used as electrode would be problematic due to formation of ion-conductive Li_3N .¹⁸¹

1.2.3. Application of ILs in Batteries

As mentioned in the previous section, the unique physical and chemical properties of ILs make them proper candidates for energy related applications. Different cation-anion combinations with ionic conductivity, low volatility, high electrochemical and thermal stability give us the possibility to design ideal electrolytes for the batteries, thermos-electrochemical cells, fuel cells, dye sensitised solar cells, super-capacitors and actuators.

1.2.4. Application of ILs in Lithium-ion Cells

The large scale application of lithium-ion batteries requires high device safety standards and low impact on human health and environment. The major risks in lithium-ion batteries are related to the current organic electrolyte based on volatile and flammable organic solvents.¹⁸²⁻¹⁸⁴ In the event of short circuits or local overheating there is the possibility to generate undesirable reactions between the batteries components and the liquid organic electrolyte. Exothermic reaction in the batteries can lead to rapid increase in temperature and hence result in fire or explosion. Once a battery is opened in the air, the organic electrolytes can even work as a fuel due to their flammability. If the battery is kept unopened in an elevated temperature, the positive electrode material at the charged state decomposes around 200 °C, providing oxygen inside of the battery with an organic solvent.¹⁸⁵ Hence, ILs come into play to improve the safety levels by replacing the flammable solvents^{186,187} However the stability of ionic liquids at low potentials is problematic particularly in the case of di-substituted imidazolium-based representatives¹⁸⁸ Furthermore, in the presence of lithium salt the electrolyte becomes very water sensitive, and therefore new salts must be designed in order to solve this problem.^{186,189}

IL based electrolytes in Li-ion batteries (LIBs) are ternary mixtures containing Li^+ ions and the anions and cations of the respective IL. The Li salt and the IL usually share the same anion. Therefore, the IL cation becomes the subject of target oriented optimization. Common basic structures are pyridinium,¹⁹⁰ imidazolium,¹⁹¹⁻¹⁹⁴ ammonium,¹⁹³⁻¹⁹⁶ sulfonium, pyrrolidinium,^{193,194,197-199} guanidinium,²⁰⁰⁻²⁰⁶ or piperidinium.^{192-194,207,208}

Early reports of ILs offering sufficient stability for lithium electrochemistry in quaternary ammonium and phosphonium $[\text{NTf}_2]^-$ ILs^{209,210} sparked the interest of battery researchers. Cyclic pyrrolidinium and piperidinium $[\text{NTf}_2]^-$ ILs, which are typically less viscous and slightly more cathodically stable than the aliphatic cations, were then shown to support highly efficient lithium cycling.²¹¹ Subsequently, a large number of research have been conducted with different combinations of IL cation and anion with a range of lithium battery anodes and cathodes.²¹² In 2006 Matsumoto et al.²¹³ reported a high rate cycling of the Li/LiCoO₂ cell using a pyrrolidinium TFSI IL as the electrolyte. This small amide anion demonstrated the ability to

promote higher transport rates. In addition, the used anion avoided the need for additives²¹⁴ to prevent irreversible interaction of the IL cation at the graphitic carbon electrode, indicating a probable chemical role in forming a surface layer on the electrode.²¹⁵ Lane recently reported the assessment of the cation reduction reactions at negative electrodes for most common ILs.²¹⁶ However, despite such extensive studies of the wide applicability of ILs in lithium cells, commercial application of batteries incorporating IL electrolytes has not been well developed. This is mainly due to the high expenses of ILs than the conventional organic solvents.¹⁵² Therefore, the next step is to develop lower cost ILs. The recent study of Li-cells incorporating a pyrrolidinium dicyanamide IL, provide some progress in this direction.²¹⁷ The other factor limiting ILs application relates to the relatively low rate capability displayed by IL based batteries. It is mainly because of increasing in the viscosity of the electrolyte after Li salt addition which contributes to stronger ion association in the electrolyte.²¹³ In order to overcome these two disadvantages of ILs, the number of studies investigating mixed systems of ILs with conventional commercial carbonate-based electrolytes have been growing increasingly.²¹⁸⁻²²⁰

1.2.5. Electrochemical Windows of RTILs

In considering RTILs as an electrolyte for electrochemical applications, we need to know the level of electrochemical stability of the ILs towards a particular electrode. Therefore, the electrochemical potential range, starting from the point where no electrochemical reaction is observed, should be estimated by electrochemical methods. By the term of electrochemical window (EW) of RTILs, we are able to indicate the potential range and the potential difference. EW RTILs can be calculated by subtracting the reduction potential from the oxidation potential.^{221,222} Cyclic voltammetry and linear sweep voltammetry are promising methods for estimating EWs of ILs despite the complication often encountered in comparing the resulting voltammogram with other reported data. These comparison problems resulted not only from technical issues such as “IR drop” but also from the difference in the measurement conditions and factors, including differences between working and reference electrode, potential scanning rate, cut-off current density, etc. In addition, the presence of even small amounts of water, impurity and oxygen in atmosphere cannot be neglected and will affect the measurement results.²²²⁻²²⁴

In addition to electrochemical applications which have been mentioned so far, ILs are used in electrodeposition as well. Electrodeposition is a technique where an electric current reduces dissolved deposited metal cations. It is used in several industries such as optical, sensorial, automotive and aerospace. The already aqueous existing solutions provide a narrow EW (+/- 4 V), preventing the deposition of metals with large negative reduction potentials.²²⁵ As some ILs provide wide electrochemical windows up to 6 V or even more, they can be good candidates for the electrodeposition of metals and semiconductors, and displays great potential in electroplating. Among ILs, the one with TFSI, BF₄ and PF₆ anions are known to be stable below the Li/Li⁺ reductive region, enabling its deposition.^{226,227}

2. Objective

2.1. Chromium-based Building Blocks for Metal-Organic Frameworks

The first part of this work was largely focused on synthesis of chromium based building blocks for metal-organic frameworks. Organometallic networks or metal organic frameworks (MOFs) have very interesting applications ranging from storage of gases up to self-assembled catalysts. At first, the focus was on paddle wheel structures and as chromium has the ability to form compounds with quadruple bonds based on Cr_2^{4+} moieties with a paddle wheel structure, dichromium tetracarboxylate was chosen as the starting material. Subsequently, it has been attempted to replace the acetate group in chrome acetate with ferrocene monocarboxylic acid (FCA). Different other methodologies were also tried in order to synthesize dichromium tetraferrocenemonocarboxylate ($\text{Cr}_2(\text{O}_2\text{C-Fc})_4$).

In the next step of the research, it has been tried to increase the solubility of the system. Therefore, nitrile complex of $[\text{Cr}(\text{NCR})_4][\text{BF}_4]_2$ ($\text{R} = \text{Ph}, \text{Me}$) was used as the starting material and reacted with different carboxylic acids, phosphorous and nitrogen bidentate and multi dentate ligands.

2.2. Ionic Liquids in Li-ion Batteries

The second part of the research was focused on Ionic liquids (ILs). ILs have attracted much attention as a promising alternative to the conventional organic electrolyte and the organic solvent systems for capacitors, solar cells, fuel cells and batteries. Although many applications have already been found for ionic liquids, their applications' potential in future technologies is still unlimited.

Electrochemistry has become a big field covering several key ideas such as energy, environment, and nanotechnology. Ionic Liquids are considered as potential candidates for use in advanced electrochemical applications. The studies of ionic liquids in this work have been narrowed to the application of ionic liquids in Li-ion batteries. Therefore, several imidazolium and pyrrolidinium based ILs with different cation and anion types were synthesized and after achieving a high level of purity, their electrochemical properties examined by CV and LSV measurements. For this purpose, they were added to the commercially available Li-ion batteries' electrolytes in order to find the best mixtures with high electrochemical windows.

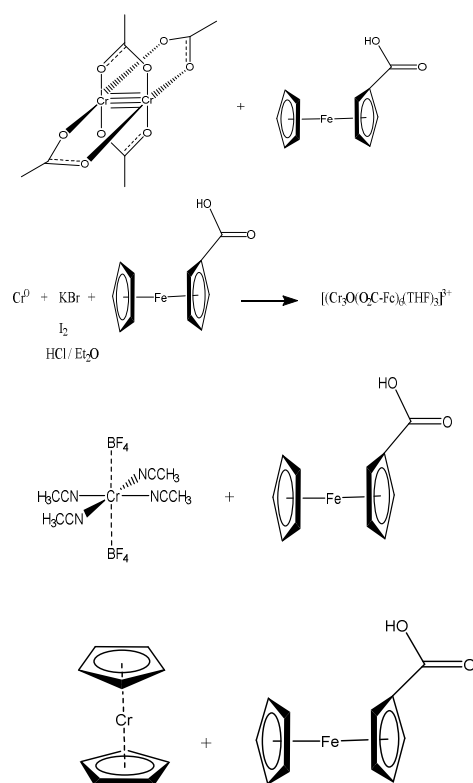
A part of the synthesized ILs were sent to the Nanyang Technological University (NTU) in Singapore in order to be used as electrolytes and electrolyte additives in a LiFePO_4 battery half-cell. It is planned that the achieved results at two different temperature levels will be compared to the behavior of the same cell using a commercial electrolyte. Furthermore, These ILs will be used in electrochemical reduction of carbon dioxide under two scenarios of: 1- using as electrolyte, 2- using as catalyst-promoter.

3. Results and Discussion

3.1. Chromium Complexes

3.1.1. A Review of the Performed Research on Chromium Complexes

During the first year of the research, the main research conducted was dedicated to chromium (II) complexes. As chromium has the ability to form compounds with quadruple bonds based on Cr_2^{4+} moieties with a paddlewheel structure, different ways were tried in order to synthesize dichromium tetraferrocenemonocarboxylate ($\text{Cr}_2(\text{O}_2\text{C-Fc})_4$). At first, dichromium tetracarboxylate was chosen as the starting material and it was attempted to replace the acetate group in chrome acetate with ferrocene monocarboxylic acid (FCA), as it had been achieved before in molybdenum chemistry.²²⁸ Chromium metal and tetrakis(nitrile)chromium(II) complex were the other starting materials used for such a purpose. The performed reactions are summarized in the scheme 3.1.

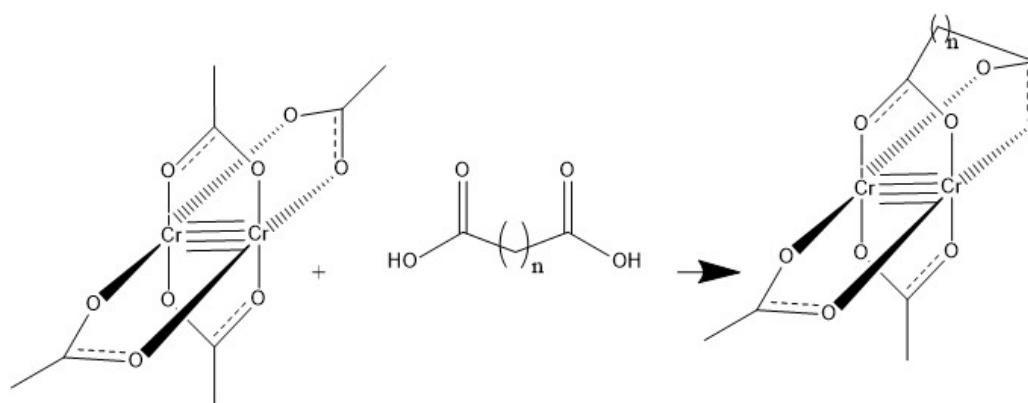


Scheme 3.1. Performed reactions in order to synthesize $\text{Cr}_2(\text{O}_2\text{C-Fc})_4$ complex

In the second reaction of scheme 3.1 when HCl and iodine were used for the oxidation of the chromium metal, Cr^{III} complex $[\text{Cr}_3\text{O}(\text{O}_2\text{C-Fc})_6(\text{THF})_3][\text{CrCl}_4(\text{THF})_2]$ and $[\text{Cr}_3\text{O}(\text{O}_2\text{C-Fc})_6(\text{THF})_3]\text{I}_3$ were resulted respectively. In spite of multiple efforts, although the results of IR, UV-Vis and NMR spectroscopy show that ferrocene carboxylic acid had been coordinated to the chromium metal in all of the performed reactions, we could not obtain a suitable crystal of a paddle wheel chromium (II) complex with ferrocene mono-carboxylate.

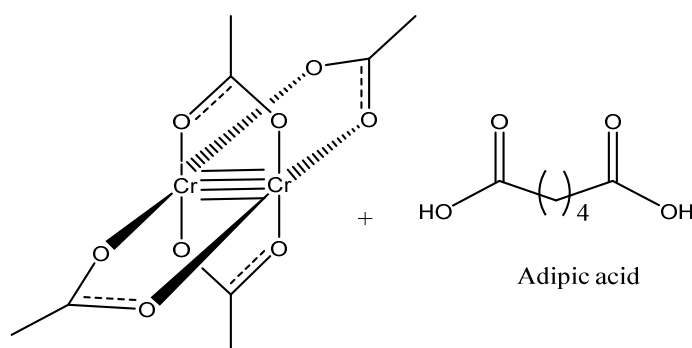
Furthermore, the paramagnetism of the products made the characterization with NMR difficult and none of the chromium complexes could be characterized using mass spectroscopy. Moreover, excluding the second reaction of scheme 3.1, The lack of an adequate level of solubility also made the purification and crystallization of the products difficult.

The other reaction was performed on dichromium tetracarboxylic acid with the aim of replacing two neighboring carboxylate groups of a $\text{Cr}_2(\text{O}_2\text{CCH}_3)_4$ complex with a proper dicarboxylic acid which has an appropriate carbon chain. It has been attempted to find such a dicarboxylic acid. The desired reaction has been sketched in scheme 3.2.

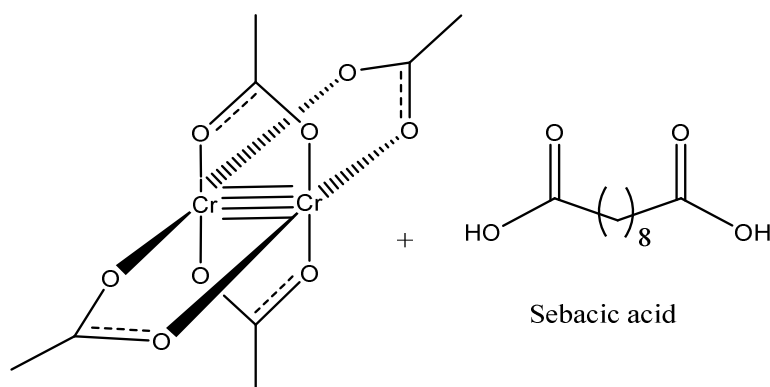


Scheme 3.2. Desired reaction for replacing two neighboring carboxylate groups of $\text{Cr}_2(\text{O}_2\text{CCH}_3)_4$ with a proper dicarboxylic acid

Dicarboxylic acids with $n = 4$ and more were considered as good choices for such a reaction as it was assumed that they may be bent and get the proper angle to seat on a dichromium paddle wheel complex. Otherwise depending on the used dicarboxylic acid dimer, triangle, square or other types of improper structures would have been formed. The two performed reactions are shown in scheme 3.3 and 3.4.



Scheme 3.3. Reaction of dichromium tetraacetate complex with adipic acid



Scheme 3.4. Reaction of dichromium tetraacetate complex with sebacic acid

These reactions led to a green-blue product starting from a brown chromium complex. According to the respective IR spectra, dicarboxylic acids have been linked to the chromium complex, but the products could not be solved in any of the various solvents used. Therefore, it was difficult to characterize the products and recognize the position of the used dicarboxylic acid in the chromium complex. Nevertheless, according to the X-ray powder diffraction conducted on the product of the reaction specified in scheme 3.3, it may be possible that the product was forming a polymeric structure (a MOF).

The experimental work conducted on the first year of the research, led to the conclusion that the chromium complexes of the mentioned types are significantly more sensitive to moisture, air and temperature than their molybdenum derivatives that could be isolated. Paramagnetism of the products made the NMR characterization difficult and in addition, the lack of an adequate level of solubility also contributed significantly to the encountered problems in purification and crystallization of the materials. In the next steps of the research, it was attempted to find a way to increase the solubility of the system.

During the second year of the research, based on the decision to start the reactions with a compound which has a good level of solubility, chromium nitrile complexes with the general formula $[\text{Cr}(\text{NCR})_4][\text{BF}_4]_2$ ($\text{R} = \text{Ph}$ and in a few cases $\text{R} = \text{Me}$)⁹⁸ were selected as the starting material to react with different carboxylic acids such as FCA, *p*-toluic acid, bidentate and multidentate ligands. Performed reactions have been summarized in scheme 3.5. The usefulness of coordinated nitriles (as weak donor ligands) comes from their ease of replacement, which makes them a widely employed starting material for the synthesis of other complexes, inorganic materials and catalysts.⁹⁸⁻¹⁰² Therefore, since 158 years ago, a large number of transition-metal organonitrile complexes have been prepared and several useful applications have been found for this compound class.

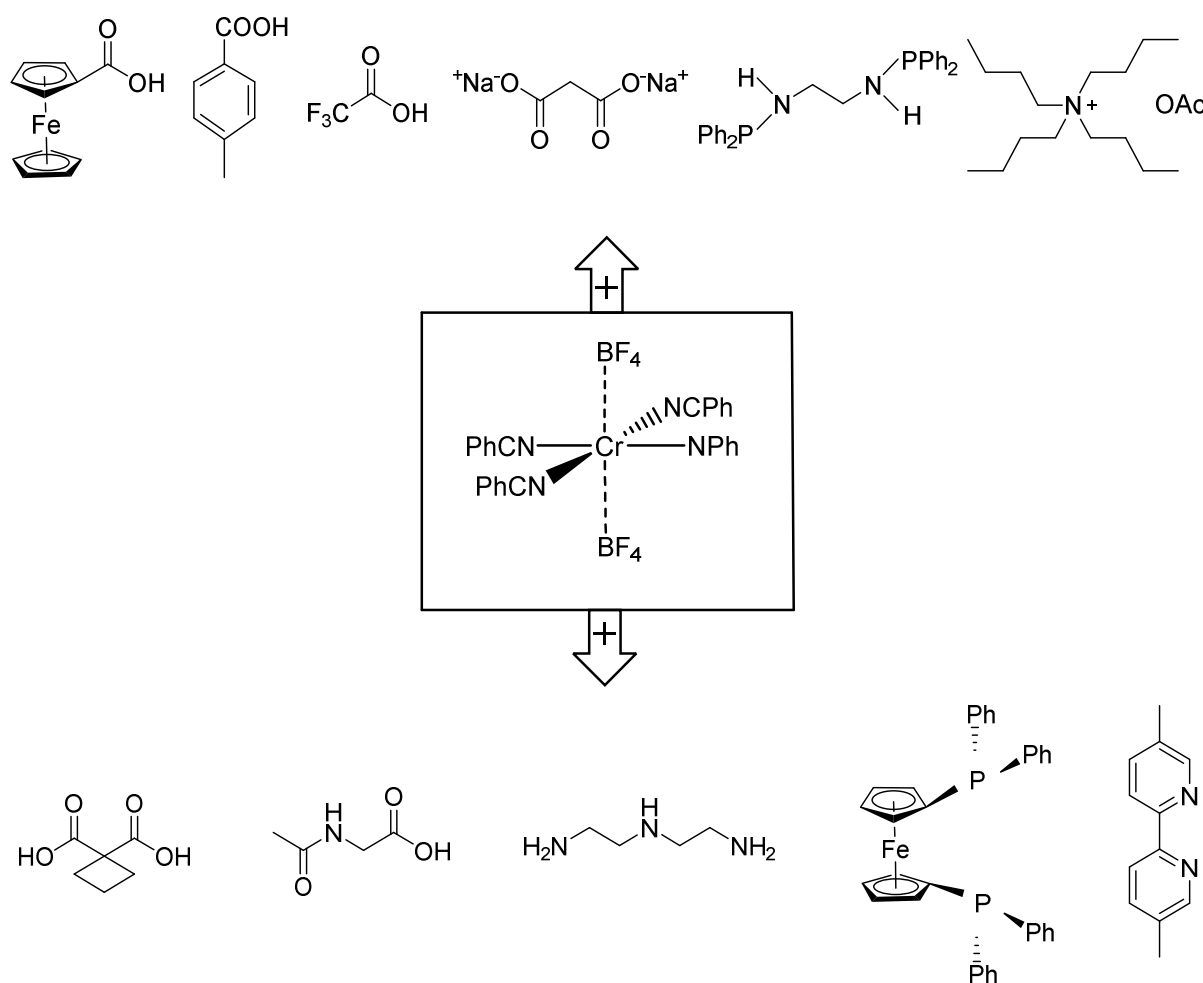
Under a varying set of reaction condition (long reaction time, elevated temperature, salt metathesis, addition of activators and promoters, etc.), carboxylic acids did not react with the applied chromium nitrile complexes.

During the third year of the work, additional research on chromium and molybdenum complexes were conducted in order to complete the last two years' research leading to

obtaining a few crystal structures. But the main focus at this time was shifted to the ILs project described in more detail at the end of this chapter.

3.1.2. Chromium (III) Complexes

Chromium, as a group VI transition metal exhibits a wide range of accessible oxidation states, with the most common being 0, I, II, III, IV and VI. In contrast to its heavier congeners Mo and W, however the highest oxidation states are less stable, +III is the most common oxidation state for chromium.



Scheme 3.5. Performed reactions of $[Cr(NCR)_4][BF_4]_2$ with carboxylic acids and multidentate ligands

3.1.2.1. $[Cr(mbpy)_3][BF_4]_3$

Compound $[Cr(NCPh)_4][BF_4]_2$ (3a) was synthesized according to the literature procedure published by Henriques et al.⁹⁸ At first the brown anhydrous acetate was obtained by heating the red-brown $Cr_2(O_2CCH_3)_4(H_2O)_2$ at 100-110 °C overnight. $Cr_2(O_2CCH_3)_4$ was then suspended in a mixture of benzonitrile and dichloromethane. $HBF_4 \cdot Et_2O$ was dropwise added

to this mixture with vigorous stirring. The reaction mixture turned deep blue immediately which shows the existence of Cr^{II} complex. After stirring for 3 hours the solvents were removed under vacuum. Diethyl ether was added to the remaining blue oil and crystallisation induced by scratching the wall of the flask. After filtration, the greenish blue precipitate was washed with diethyl ether and n-pentane and then dried under vacuum.

Despite the paramagnetism of compound 3a by making a diluted NMR sample in CD_3CN , a rather good ^1H -NMR spectrum could be obtained. However, if the solution of the NMR sample gets concentrated, the peaks of the product could not be observed. Figure 3.6 shows the difference between ^1H -NMR of diluted and concentrated NMR sample.

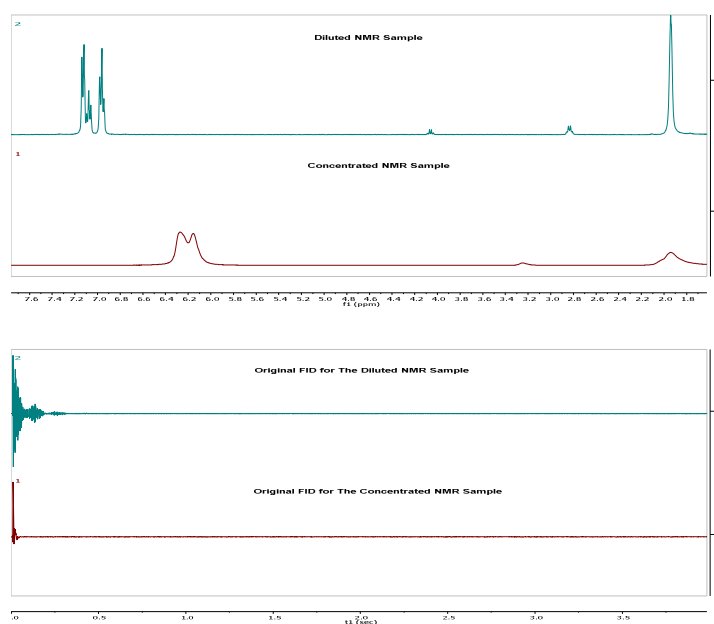


Figure 3.6. Comparison of the resulting ^1H -NMR spectra for diluted and concentrated solutions of compound 3a in CD_3CN

In the next step synthesized Cr^{II} complex of $[\text{Cr}(\text{NCPH})_4][\text{BF}_4]_2$ (1 equiv.) was solved in dichloromethane to make a blue solution and then was reacted with 2 equiv. 5,5'-Dimethyl-2,2'-bipyridine (mbpy). The mixture immediately turned to dark violet which shows the existence of Cr^{II} product. After a reaction time of around 1 hour, formation of Cr^{III} complex could be observed due to the witnessed change in the color of the solution to brown as well as appearance of some yellow precipitate. The amount of the precipitate increased as the reaction developed further. The reaction was left overnight at room temperature. The yellow precipitate which was collected after filtration, was washed with dichloromethane. Crystallization from acetonitrile and pentane/diethyl ether gave yellow shiny, paramagnetic crystals with $[\text{Cr}(\text{mbpy})_3][\text{BF}_4]_3$ formula (3b). Electrochemical studies of the product showed three reversible waves. The product has been characterized by NMR spectroscopy, elemental analysis, UV-Vis, IR, CV, magnetic susceptibility measurement and SC-XRD. The resulted data are available in the experimental part.

Figure 3.7 shows the crystal structure of the yellow fragment-like specimen of the Compound 3b with $C_{36}H_{36}B_3CrF_{12}N_6$ formula and approximate dimensions $0.349 \times 0.362 \times 0.627$, crystallized in the P -1 space group. The full data of single crystal X-ray diffraction (SC-XRD) measurement is shown in the Appendix to this report.

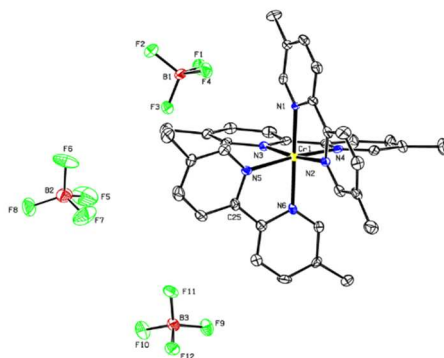


Figure 3.7. Crystal structure of complex 3b

Crystallization from the brown solution reaction was performed by DCM/pentane and resulted into brown crystals, most probably with $[Cr(mbpy)_2][BF_4]_2$ formula (3c). As can be seen in Figure 3.8, chromium is coordinated to two 5,5'-Dimethyl-2,2'-bipyridine ligands and possibly two fluorine atoms of two BF_4 anions, although only one BF_4 could be observed in the SC-XRD result. There is also the possibility of having coordinated chloride to the chromium centre which could come from the used solvent. The structure could not be obtained at the sufficient quality level but the general structure has been proven.



Figure 3.8. Crystal structure of complex 3c (Cr: blue, C: grey, N: yellow, F: light green, B: pink)

It is noteworthy to mention that with changing the ratio of 5,5'-Dimethyl-2,2'-bipyridine to 3 equiv., the reaction was stopped in the first stage of the formation of deep violet color and even with increasing the reaction time the color did not change. This shows we have a complex with

an oxidation state of 2+ inside the reaction flask. It seems that the amount of the bipyridine derivative ligand affects the oxidation state of the final product.

Table 3.1 shows the color difference and the proposed electronic structure for complexes with general formula of $[\text{Cr}(\text{bpy})_3]^n$ ($n = 3+, 2+, 1+, 0$). Different oxidation states of this kind of chromium complexes arise from the fact that bipyridine ligands are redox-active or redox-non-innocent and may exist in three different oxidation levels, namely as neutral (bpy^0), π -radical monoanionic (bpy^\bullet)¹⁻ and diamagnetic dianionic (bpy^{2-})²⁻.²²⁹

Complex	Color	Electronic Structure	Reference
$[\text{Cr}(\text{bpy})_3]^{3+}$	yellow	$\text{Cr}^{\text{III}} (\text{d}^3)$	230,231
$[\text{Cr}(\text{bpy})_3]^{2+}$	deep violet	$\text{Cr}^{\text{II}} (\text{low-spin } \text{d}^4)$	232
$[\text{Cr}(\text{bpy})_3]^{1+}$	deep blue	$\text{Cr}^{\text{I}} (\text{low-spin } \text{d}^5)$	232
$[\text{Cr}(\text{bpy})_3]^0$	red-brown solution, black crystals	$\text{Cr}^0 (\text{low-spin } \text{d}^6)$	233-235

Table 3.1. $[\text{Chromium}(2,2'\text{-bipyridine})_3]^n$ Complexes

3.1.2.2. $[\text{Cr}_3\text{O}(\text{O}_2\text{C-Fc})_6(\text{THF})_3]^{+1}$ Complexes

At first our aim was synthesis of a paddle wheel dichromium teraacetate complex of $\text{Cr}_2(\text{O}_2\text{C-Fc})_4$ with the procedure published by Levy et al. for synthesizing of anhydrous chromium acetate.⁷³ In order to do this, chromium powder was reacted with ferrocene dicarboxylic acid inside a THF solution in the presence of an oxidant (Iodine, HCl or KBr). Although the expected product was not achieved, paramagnetic Cr^{III} complexes of $[\text{Cr}_3\text{O}(\text{O}_2\text{C-Fc})_6(\text{THF})_3][\text{CrCl}_4(\text{THF})_2]$ (3d) and $[\text{Cr}_3\text{O}(\text{O}_2\text{C-Fc})_6(\text{THF})_3]\text{I}_3$ (3e) were obtained by using HCl and iodine respectively as the reaction oxidant. The products were characterized by NMR, X-ray diffraction, IR, UV-Vis and elemental analysis. Paramagnetism of the products, makes the NMR spectra not clear enough for investigation. As can be seen in the Figures 3.9 and 3.10, three nuclear chromium cores have a central oxygen atom. Three chromium (III) atoms form vertices of a nearly equilateral triangle. Each of the six acetate groups of ferrocene monocarboxylates, bridges a Cr-O-Cr fragment. One THF solvent molecule has been connected to each chromium core. The counteranion beside the cation fragment of Complex 3d is $[\text{CrCl}_4(\text{THF})_2]^-$ and that of Complex 3e is I_3^- . In order to prevent excessive accumulation, Ferrocene fragments with different styles have been shown in the Figures 3.9 and 3.10. Due to the size of the compounds and the associated solvent molecule, the structures sketched below could not be obtained at the sufficient quality level. They provide nevertheless a structural proof of the respective compounds' composition.

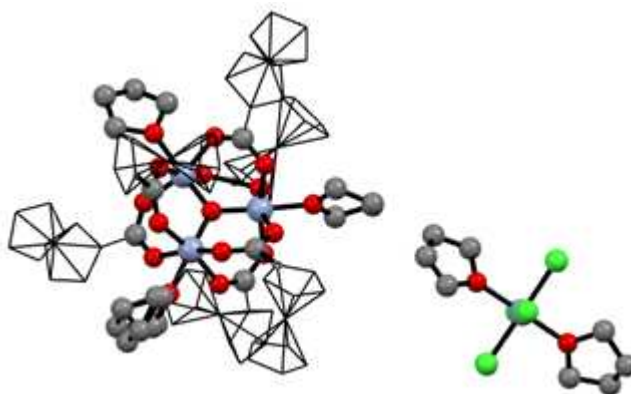


Figure 3.9. Crystal structure of complex 3d (Cr: blue, O: red, C: grey, Cl: green)

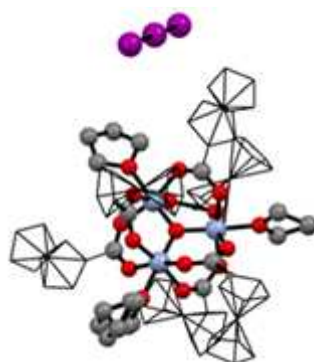


Figure 3.10. Crystal structure of complex 3e (Cr: blue, O: red, C: grey, I: violet)

In this reaction the free halogens probably oxidize chromium to some extent forming HX that serves as the main oxidant. It is believed that the oxidation of chromium metal in the presence of a strong acid is accomplished by H^+ ions according to $Cr^0 + 2H^+ \rightarrow Cr^{+2} + H_2$ ⁷³ and subsequently formation of Cr^{+3} . The chromous ions then react with ferrocene monocarboxylic acid. It was assumed that using KBr salt like HBr and HCl could be also effective as the interaction of the salt with FCA can produce HBr and subsequently dissolves the metal. Although using KBr turned out not to be a good choice and could not oxidize chromium (probably because of the weak solubility of KBr), the reaction took place using iodine and HCl each.

3.1.3. Chromium (II) Complex of $CrCl_2(DPPF)$

The reaction of 1 equiv. $[Cr(NCPh)_4][BF_4]_2$ with 2 equiv. 1,1'-bis(diphenylphosphino)ferrocene (DPPF) in DCM resulted in a green solution. Orange crystals were obtained in a month, after layering the reaction solution with pentane. Figure 3.11 shows the crystal structure of $CrCl_2(DPPF)$ (3f) in which Cr^{II} ion is coordinated to DPPF and two chlorine atoms. Although the resulted general structure proves, the respective compound composition, the structure could not be obtained at the sufficient quality level. ¹H-NMR reveals

a low field shift for DPPF peaks in this complex. Unfortunately, the crystal could not be achieved again making further investigation impossible.

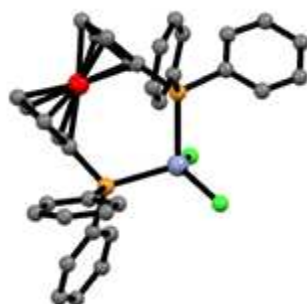


Figure 3.11. Crystal structure of complex 3f (Cr: blue, Fe: red, C: grey, P: orange, Cl: green)

3.2. Ionic Liquids

3.2.1. Synthesis

3.2.1.1. Preparation of the Ionic Liquid Halide Salts

The full List of all synthesized cations for desired ionic liquids is given in Figure 3.12. They were combined later with BF_4 , OTf , PF_6 and TFSI anions.

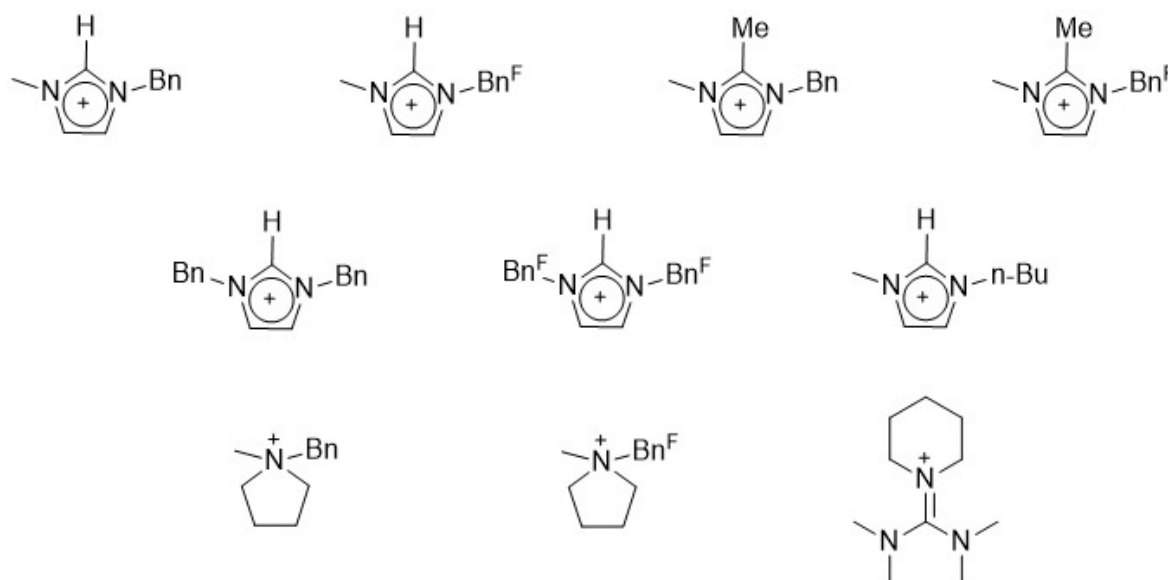
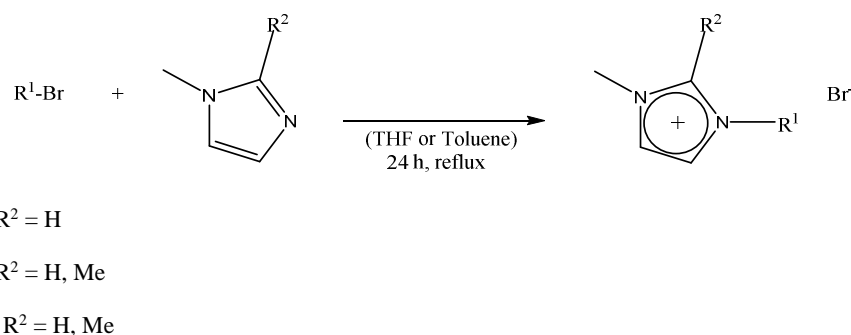


Figure 3.12. Synthesized imidazolium, pyrrolidinium and guanidinium-piperidinium cations

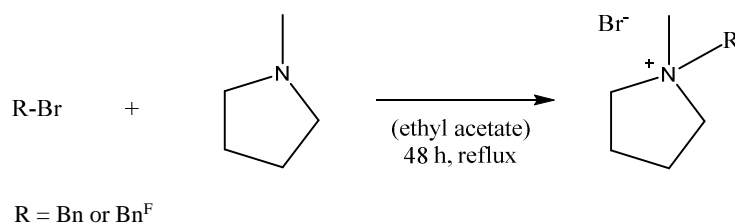
Synthesis procedure for imidazolium and pyrrolidinium bromides have been previously reported. They were synthesized through quaternization reaction of imidazole or pyrrolidine with alkylhalides, although some differences in the synthesis path were applied as different

derivatives were intended. Scheme 3.6 shows the general procedure used for synthesis of the imidazolium bromides with proton or methyl group in C2 position. 1- methyl or 1,2-dimethylimidazole was dissolved in tetrahydrofuran (THF) or toluene and a slight excess of the respective alkyl bromide was added. After a reaction time of 24 hours the remaining solvents were evaporated. The crude product was washed with hexane, diethyl ether and ethyl acetate.



Scheme 3.6. General procedure for synthesis of imidazolium bromides

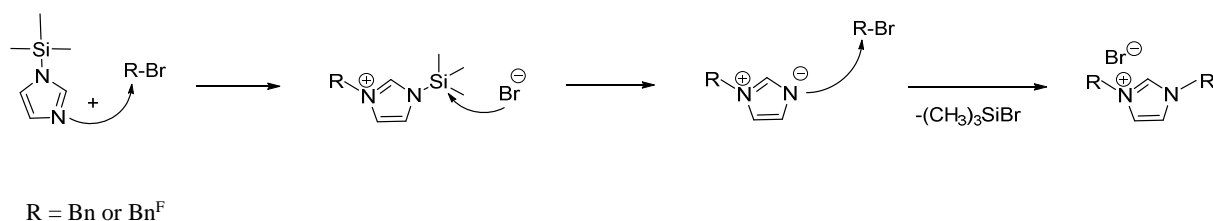
For synthesizing the pyrrolidinium bromides, benzyl bromide or pentafluorobenzyl bromide was slowly added to a solution of 1-methylpyrrolidine in ethyl acetate under argon atmosphere while the reaction was vigorously stirring. The reaction was stirred under reflux for 48 hours and then filtered to remove the solvent. The white solid product was washed with ethyl acetate. Scheme 3.7 shows the general procedure:



Scheme 3.7. General procedure for synthesis of pyrrolidinium bromides

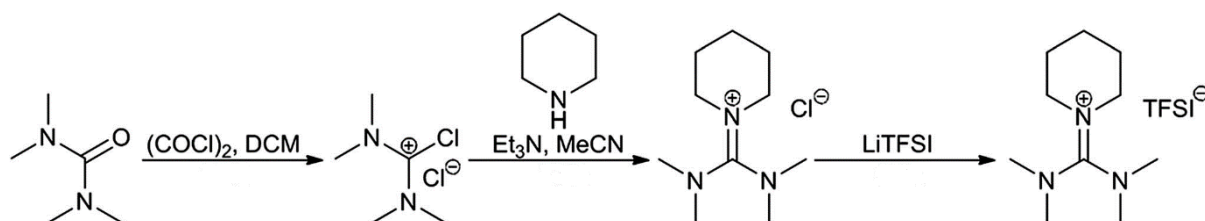
1,3-Bis-(2',3',4',5',6'-pentafluorobenzyl) imidazolium bromide and 1,3-dibenzyl imidazolium bromide were synthesized as shown in scheme 3.8 by quaternization reaction of 1-(trimethylsilyl)-1H-imidazole with dropwise addition of the excess of pentafluorobenzyl bromide and benzyl bromide respectively in dry THF. The reaction mixtures were stirred under reflux for 24 hours. Pentafluorobenzyl derivative was formed during the reaction time as a white precipitate, which was collected by filtration and washed with THF and diethyl ether.

After finalizing the reaction time of benzyl derivative, a brown viscous oil which was denser than the reaction solvent and immiscible with the solvent was formed. The solvent was evaporated and the light-yellow residue was dissolved in a minimal amount of acetonitrile. Subsequently, crystallization was induced by adding ethyl acetate and diethyl ether and scratching the wall of the flask inside an ice bath. The product was filtered and the obtained yellow white powder was washed a few times with diethyl ether to result a white powder.



Scheme 3.8 Synthesis of imidazolium bromide by quaternization reaction of 1-(trimethylsilyl)-1H-imidazole

The guanidinium-piperidinium based ionic liquid of N, N, N', N'-tetramethyl-N'', N''-pentamethyleneguanidinium chloride (PipGuan-Cl) and consequently its bis(tetrafluoromethylsulfonyl)imide (PipGuan-TFSI) derivative were synthesized from tetramethylurea according the procedure reported by Bucher et al.¹⁵¹ (Scheme 3.9)



Scheme 3.9. Synthesis procedure for PipGuan-based ionic liquid

3.2.1.2. Anion Exchange

3.2.1.2.1. ILs with BF₄, OTf, PF₆ and TFSI counter anions

It has been tried to synthesize the appropriate anion-cation combination to obtain suitable ILs with thermal, moisture and electrochemical stability in order to find the best aprotic media with a wide electrochemical window.

ILs containing smaller anions like Cl⁻ and Br⁻ have relatively higher cation-anion interactions compared to ILs containing larger anions like OTf⁻ and TFSI (NTf₂⁻). In ILs, the spatial distribution of anions is closer to the acidic hydrogen atom of the cation compared to the two

nonacidic hydrogen atoms of the cation. The diffusion coefficients of cations and anions (ionic conductivity) increase with anionic size. In other words, a decrease in ion-pair interaction cause an increase in conductivity of ILs. Therefore, the cationic and anionic diffusion and ionic conductivity are lowest in ILs containing anions like Cl^- and Br^- and highest in ILs containing anions like BF_4^- , OTf^- , and NTf_2^- . It has been assumed that ILs with an intermediate size BF_4^- anion show the highest cationic and anionic diffusion (ionic conductivity).²³⁶

Tetrafluoroborate ILs are considerably more stable against moisture. The hexafluorophosphate ionic liquids are similar to tetrafluoroborate ionic liquids, but the former is not completely miscible with water. Thus, the PF_6^- ionic liquids sometimes are regarded as hydrophobic. However, it should be noted that the PF_6^- anion can undergo hydrolysis when it comes into contact with an acidic aqueous solution. Ionic liquids (ILs) with the triflate anion ($[\text{CF}_3\text{SO}_3]^-$; OTf) are of interest for practical applications in various fields.^{171,237-240}

Triflate ionic liquids are hydrolytically more stable than ILs with PF_6^- and BF_4^- anions²³⁵ Bis(trifluorosulfonyl)imide ($\text{N}(\text{CF}_3\text{SO}_2)_2^-$; TFSI) ionic liquids are not only stable against moisture but also are immiscible with water, whereas a certain amount of water dissolves in the $\text{N}(\text{CF}_3\text{SO}_2)_2^-$ ionic liquids. Therefore, these kind of ILs are promising candidates as supporting electrolytes for practical electrodeposition processes.²³⁷

In general, a certain kind of fluorinated anion formed ILs with a melting point lower than room temperature and sufficient anodic stability. Moreover, the sensitivity against water decreased.²⁴¹ The imide anion greatly improved the chemical stability in the air, which enable the easy handling of ILs.¹⁸⁵

3.2.1.2.2. Preparation of BF_4 , OTf , PF_6 and TFSI Salts of ILs

In this part of the work, 29 anion substituted ILs were successfully synthesized and purified. All products were purified very carefully as pure products are of high importance due to the fact that impurities can spoil the electrochemical experiments and cause unwanted side-reactions. The previously synthesized Imidazolium and pyrrolidinium bromides were transformed to the corresponding BF_4 , OTf , PF_6 and TFSI analogues through anion metathesis reactions.

An excess amount of silver tetrafluoroborate (AgBF_4), silver trifluoromethanesulfonate (AgOTf) and Silver hexafluorophosphate (AgPF_6) were separately added to the solutions of ionic liquid bromides in order to replace the bromide with weakly coordinating BF_4 , PF_6 and OTf anions. Because Silver salts are known as photosensitive and hygroscopic substances, they were handled in glove box and protected from light. The reactions were carried out in dark as well. In these reactions, the substitution of the bromide was driven by the precipitation of silver bromide. This process was conducted in a solution of acetonitrile which is a perfect solvent for these reactions, because it dissolves the starting silver salts as well as ILs but not the byproduct of silver halide which can be removed easily by filtration. Methanol was used as the reaction solvent only when $[\text{MMBn}][\text{Br}]$ was the starting ionic liquid, because its solubility was not good in acetonitrile.

Although Ag^+ salts are expensive, they give much lower levels of residual Br^- and allow isolation of the ionic liquids in high yields and purities. Using Na^+ salts, results in high residual concentrations of Br^- .²⁴²

After filtration of the resulting reaction solutions, the solvent was evaporated and the resulting products were purified by DCM / H_2O (3:1 v/v) extraction for the products which are liquid and crystallisation from acetonitrile/diethyl ether or ethylene acetate for solid products. Minimum amount of water should be used for extraction due to the fact that the products were also partially soluble in water.

In a few cases even after purification process, although elemental analysis and NMR results didn't show the presence of any impurity, the color of the product turned from white to grey after some days. It is assumed that the trace of silver salt impurity had been causing such a color change after exposing the ionic liquid product to the light for a while. This effect was observed when AgBF_4 was used with 1.1 equivalent for the anion exchange reaction. In the beginning, it was assumed that the product might be heat sensitive and the applying heat during the drying process caused the decomposition of the product and subsequently such a color change. Thus, drying of the product was done under vacuum without applying additional heat to check the influence of temperature. But after a few days, the compound turned from white to grey again. Hence, it was concluded that heating of the product may not be the reason of the color change. In order to determine the cause of this phenomenon, the grey product was dissolved in acetonitrile and the undissolved grey particles were collected by filtration. These grey particles were examined using atom absorption spectroscopy and the presence of silver was proven.

AgOTf and AgPF_6 have a good solubility in diethyl ether. Hence, we assumed that AgBF_4 also has a good solubility in this solvent as well. Therefore, diethyl ether was used to wash the final ionic liquid product in order to remove the remained AgBF_4 . However, the product turned grey even after multiple recrystallization, filtration and washing processes in attempt to remove the silver impurities. By dissolving AgBF_4 in diethyl ether, we then found out that AgBF_4 has a lower rate of solubility than AgOTf and AgPF_6 . Therefore, an alternative washing solvent is needed. Solubility of AgBF_4 was tested in acetonitrile, diethyl ether, ethyl acetate and water in order to find a proper solvent for purification. Ethyl acetate was considered as a substitute washing solvent of diethyl ether to wash products that used AgBF_4 as the providing anion salt. Nevertheless, this brought up a next issue that the IL products are partially soluble in ethyl acetate because when too much ethyl acetate was used to wash the product, most of the product was lost during the purification process and the final product resulted in a low yield. Hence, reactions of ILs- BF_4 had to be repeated. In order to prevent the loss of the product and on the other hand to ensure a clean product, a small amount of ethyl acetate was mixed with a bulk amount of diethyl ether for washing the final product. The product remained white after drying under vacuum with 40 °C.

The providing TFSI salt for the substitution of bromide and synthesis of $[\text{BMIm}][\text{TFSI}]$, $[\text{BnMIm}][\text{TFSI}]$ and $[\text{Bn}^{\text{F}}\text{MIm}][\text{TFSI}]$ was lithium bis(trifluoromethanesulfonyl)imide (LiTFSI). Corresponding ionic liquid bromides were reacted with the excess of LiTFSI in deionised

water. After the reaction time, the products were extracted with DCM. Subsequently, the products were stirred over charcoal. Using activated carbon has already been reported as a successful method for removing impurities from ILs.²⁴³ However this treatment with adsorbents launched some controversy due to the possibility of adding extra impurities, even harder to extract.²⁴⁴ A color change from light yellow to white was observed in $[\text{Bn}^{\text{F}}\text{MIm}][\text{TFSI}]$ after purification with charcoal. It has been already reported by Nockermann et al. that ILs tend to be contaminated by colored impurities that can be removed by treatment with active charcoal.²⁴⁵ $[\text{BMIm}][\text{TFSI}]$ and $[\text{BnMIm}][\text{TFSI}]$ in liquid and $[\text{Bn}^{\text{F}}\text{MIm}][\text{TFSI}]$ in solid form were resulted. The solid product was washed a few times with diethyl ether for more purification.

3.2.2. Characterization

All synthesized ionic liquids were characterized and their levels of purity were proven by nuclear magnetic resonance (^1H , ^{13}C , ^{19}F , ^{31}P , ^{11}B NMR) and elemental analysis. The full list of the characterization results for all synthesized compounds can be found in the experimental part.

^1H -NMR of a imidazolium and a pyrrolidinium synthesized ionic liquid bromide have been shown in Figure 3.13 and 3.14 in order to illustrate the range of other products' peaks. Furthermore, the results of the spectroscopic methods are discussed exemplarily for $[\text{BMIm}]^+$ in this part.

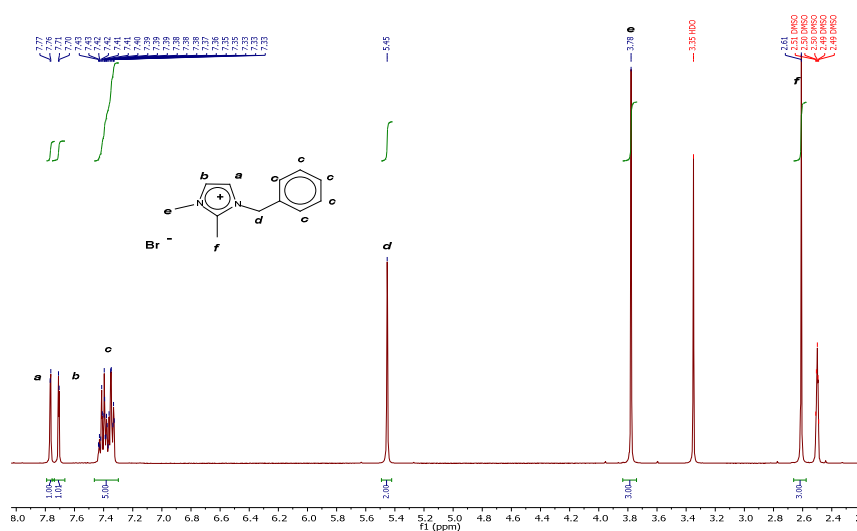
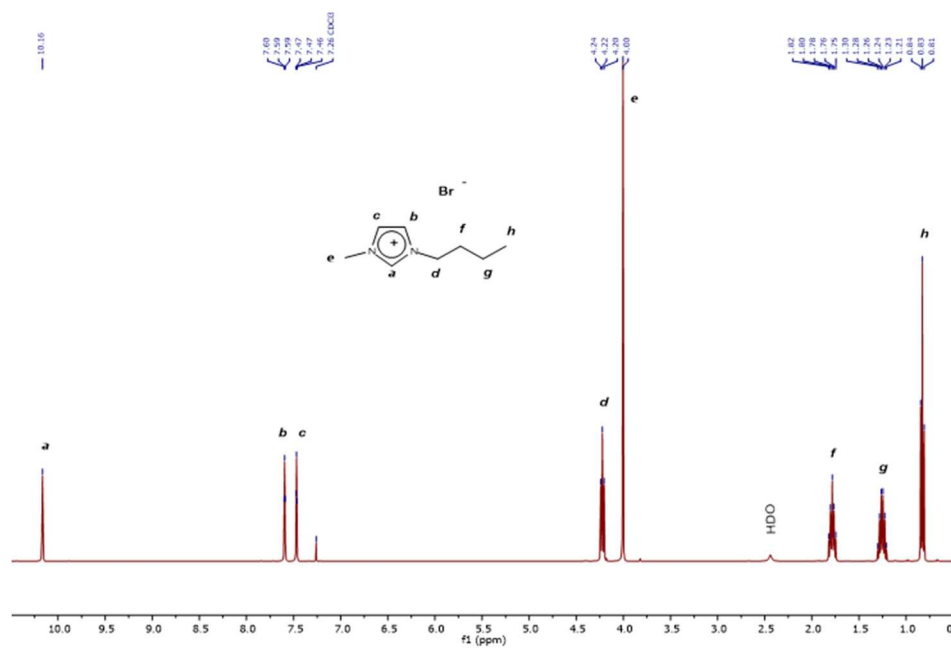
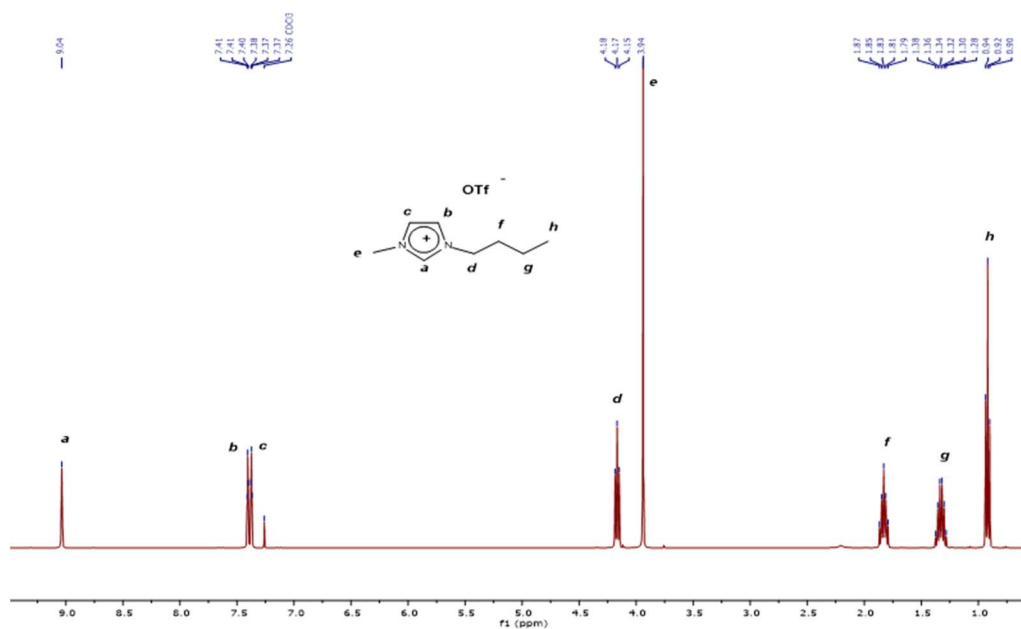


Figure 3.13. ^1H -NMR spectrum of $[\text{MMBnIm}][\text{Br}]$

Figure 3.15. $^1\text{H-NMR}$ spectrum of $[\text{BMIm}][\text{Br}]$ Figure 3.16. $^1\text{H-NMR}$ spectrum of $[\text{BMIm}][\text{OTf}]$

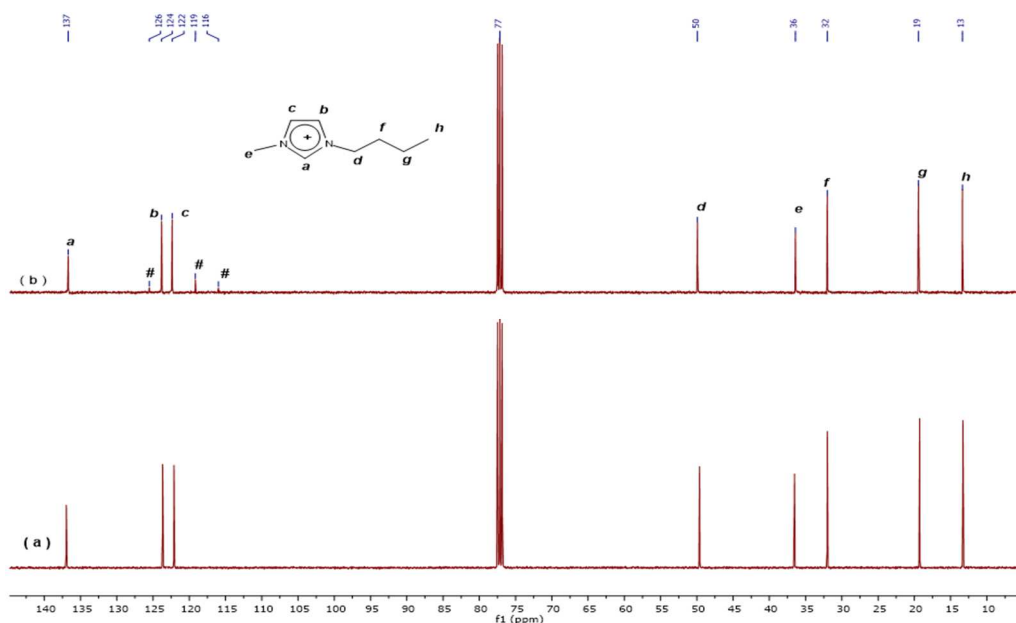


Figure 3.17. ^{13}C -NMR spectra of $[\text{BMIm}][\text{Br}]$ (a) and $[\text{BMIm}][\text{OTf}]$ (b) (# peaks belong to OTf anion)

3.2.3. Electrochemical Tests

3.2.3.1. Preparation

Since it is known that the size of the EW is inversely proportional to the water content in the ionic liquids,²²² all the products were dried over 16 hours under reduced pressure in order to remove any vestigial water. The products were then kept under argon. On the other hand, the soluble oxygen is electrochemically active. Therefore, its reduction can be a problem for accurate electrochemical window measurements.²⁴⁶ To make sure that the electrochemical tests were carried out under inert atmosphere, all solutions for CV and LSV tests were prepared in a glove box operating with argon. Each of the IL solutions (0.1 M and 0.25 M) were prepared in the blank electrolyte (“1 M LiPF_6 in EC/DEC” and “1 M LiPF_6 in DEC”) inside electrochemical cells. Ideally CV and LSV tests should be done inside the glove box to make sure that no oxygen or water would affect the measurement, however in the present work that was not possible as there was no measurement device inside the glove box. Therefore, the electrochemical cells were sealed with parafilm and transported to the electrochemical measurement room inside a bigger flask which was in turn sealed with parafilm. This movement did not take longer than 5 minutes.

The electrochemical tests were performed with a Reference 600 Potentiostat ZRA controlled by the Gamry Framework software. All measurements were performed at room temperature by cyclic voltammetry and linear sweep voltammetry (scan rate: 10 mV s^{-1}), electrochemical windows were calculated between -4 and 4 V for the cut-off current density 0.5 mA cm^{-2} . Thus the potential area 0 to 4 V for the anodic limit and 0 to -4 V for cathodic limit had been swept. The used electrodes were Glassy carbon as the working electrode, Ag/AgCl as the reference electrode, and Pt/Ti as the counter electrode.

3.2.3.2. Electrochemical Window Results

In order to improve the electrochemical window (EW) of the commercial electrolytes (“1 M LiPF₆” in EC/DEC” and “1 M LiPF₆ in DEC”), the synthesized BF₄, OTf, PF₆ and TFSI ionic liquids were used as the electrolyte additives to these available electrolytes. Afterwards, the electrochemical windows of these new electrolytes were measured by linear sweep voltammetry (LSV) and the obtained results were compared to the primary electrolytes (blank electrolytes).

It was concluded that when “1 M LiPF₆ in EC/DEC” was used as the blank electrolyte, the electrochemical window was increased whenever imidazolium analogues excluding [MBnIm][BF₄] were added. Among them [BMIm][PF₆] and [MBn^FIm][TFSI] with respective 0.6 and 0.5 V difference in comparison with the neat blank electrolyte resulted in the biggest electrochemical windows. Results of the tested pyrrolidinium based ionic liquids show that increasing the electrochemical window with the addition of MBn^FPyr-ILs leads to a [MBn^FPyr][PF₆] > [MBn^FPyr][BF₄] > [MBn^FPyr][OTf] pattern with a respective increase of 0.5, 0.3 and 0.1 V compared to the neat blank electrolyte. Among the MBn^FPyr-ILs just [MBn^FPyr][PF₆] increased the electrochemical window 0.04 V which is so small.

In order to test the influence of the ionic liquids' concentration on the electrochemical window, 0.5 M [MBn^Fpyr][PF₆] in the blank electrolyte “1 M LiPF₆ in EC/DEC” was prepared and tested. It was resulted in a 0.1 V increase of EW which is 0.4 V less than the same sample with 0.1 M IL concentration. Therefore, it is concluded that increasing the concentration of the additive ILs does not have a direct relation with the increase in electrochemical window.

In the next step “1 M LiPF₆ in DEC” was used as the blank electrolyte. This electrolyte with EW = 5.89 V has the higher EW in comparison with the previous used electrolyte which has EW = 5.07 V. Excluding [MBn^FPyr][PF₆] and [MBn^FPyr][BF₄] with 0.1 and 0.2 V respectively increasing in EW and [BnBnIm][PF₆], which did not make a considerable change, all other imidazolium and pyrrolidinium based ILs made the electrochemical window of the blank electrolyte smaller.

Increasing the concentration of [MBn^FPyr][PF₆] from 0.1 to 0.5 M resulted in decreasing the electrochemical window from 5.99 to 5.81 V that can confirm the previous conclusion about the relevance of the concentration of additive ionic liquids and electrochemical window change.

Continuing the research, we assumed that the addition of IL-TFSI to a blank electrolyte containing LiTFSI may make a mixture with a large electrochemical window as on the one hand TFSI anion is considered to have a good electrochemical stability and on the other hand the existence of the same anion may have an influence in increasing EW. Therefore, LiTFSI with two different concentration of 0.1 M and 0.25 M was added to both used commercial electrolytes. Subsequently, ILs containing TFSI were added to these new mixtures and the electrochemical windows were examined. We have divided the results into two sections mentioned in the following:

1. LiTFSI + “1 M LiPF₆ in EC/DEC”: Addition of LiTFSI to the blank electrolyte led to an increase in EW. By increasing the concentration of LiTFSI from 0.1 M to 0.25 M, the electrochemical window was increased by 0.1 V. Nevertheless, when [MBn^FIm][TFSI] was added to the electrolyte containing 0.1 M LiTFSI, the resulting EW decreased and the amount was almost equal to the primary blank electrolyte.

2. LiTFSI + “1 M LiPF₆ in DEC”: The results show that although adding 0.1 M LiTFSI to the electrolyte could result in a 0.4 V increase in the electrochemical window, after adding imidazolium based ionic liquids with TFSI counter anion, EWs were decreased. Furthermore, after adding ILs-TFSI, addition of LiTFSI to the blank electrolyte does not have any effect on the electrochemical window.

In general, it is concluded that when we use ILs as the electrolyte additives, the primary mentioned electrolytes of “1 M LiPF₆ in EC/DEC” and “1 M LiPF₆ in DEC” without any other added salt may be a proper combination for being blank electrolytes.

4. Conclusion and Summary

Chromium Complexes

In the first part of this research work, the main focus has been on synthesis of chromium complexes as building blocks for metal-organic frameworks (MOFs), as their molybdenum derivatives have been successfully applied for the synthesis of MOFs.

During the first part of the research, as chromium has the ability to form compounds with quadruple bonds based on Cr_2^{4+} moieties with a paddlewheel structure, different ways were tried in order to synthesize dichromium tetraferrocenemonocarboxylate ($\text{Cr}_2(\text{O}_2\text{C-Fc})_4$). In this part, dichromium tetracarboxylate ($\text{Cr}_2(\text{O}_2\text{CCH}_3)_4$) was selected as the starting material and it was attempted to replace the acetate group in chromium acetate with ferrocene monocarboxylic acid (FCA), as it had been achieved before in molybdenum chemistry.²²⁸ Chromium metal and tetrakis(nitrile)chromium(II) complex were the other starting materials used.

When chromium metal was used as starting material and HCl and iodine were used for the oxidation of the chromium metal, two paramagnetic Cr^{III} complexes, namely $[\text{Cr}_3\text{O}(\text{O}_2\text{C-Fc})_6(\text{THF})_3][\text{CrCl}_4(\text{THF})_2]$ and $[\text{Cr}_3\text{O}(\text{O}_2\text{C-Fc})_6(\text{THF})_3]\text{I}_3$ were obtained. The products were characterized by NMR, X-ray diffraction, IR, UV-Vis and elemental analysis.

Due to high reactivity of the chromium compounds, not all reactions yielded the intended products. In any case, the resulting compounds were collected and characterized. In spite of multiple efforts, although the results of IR, UV-Vis and NMR spectroscopy show that ferrocene carboxylic acid had been coordinated to the chromium metal in all of the performed reactions, a suitable crystal of a paddle wheel chromium (II) complex with ferrocene mono-carboxylate could not be obtained.

Another reaction was performed with dichromium tetracarboxylic acid, aiming to the replacement of two neighboring carboxylate groups of a $\text{Cr}_2(\text{O}_2\text{CCH}_3)_4$ complex with a proper dicarboxylic acid with an appropriate carbon chain. Dicarboxylic acids with $n = 4$ and more were considered for such a reaction.

By using adipic and sebacic acid as dicarboxylic acid the reactions led to a green-blue product starting from a brown chromium complex. According to the respective IR spectra, dicarboxylic acids have been linked to the chromium complex but the products could not be solved in any of the various solvents used. Therefore, it was difficult to characterize the products and recognize the position of the used dicarboxylic acids in the chromium complex. Nevertheless, according to the X-ray powder diffraction conducted on the product of the reaction of dichromium tetra acetate complex with adipic acid, it may be possible that the product was already forming a polymeric structure (a MOF).

The experimental work described above, led to the conclusion that the chromium complexes of the mentioned types are significantly more sensitive to moisture, air and temperature than their molybdenum derivatives that could be isolated. Furthermore, the paramagnetism of the products made the characterization with NMR difficult and none of the chromium complexes could be characterized using mass spectroscopy. Moreover, the lack of an adequate level of solubility also contributed significantly to the difficulties faced in purification and crystallization of the materials. In the next steps of the research, it was attempted to find a way

to increase the solubility of the system.

The next major step of the project was based on the decision to start the reactions with a compound with higher solubility. Chromium nitrile complexes of the general formula $[\text{Cr}(\text{NCR})_4][\text{BF}_4]_2$ ($\text{R} = \text{Ph}$ and in a few cases $\text{R} = \text{Me}$) were selected as the starting material to react with different carboxylic acids such as FCA, p-toluic acid and bidentate ligands. The usefulness of coordinated nitriles (as weak donor ligands) comes from their ease of replacement, which makes them a widely employed starting material for the synthesis of other complexes.⁹⁸

Under a varying set of reaction conditions (long reaction time, elevated temperature, salt metathesis, addition of activators and promoters, etc.), however, the carboxylic acids did not react with the applied chromium nitrile complexes.

From the reaction of Cr^{II} nitrile complex of $[\text{Cr}(\text{NCPH})_4][\text{BF}_4]_2$ with 5,5'-Dimethyl-2,2'-bipyridine (mbipy) with the ratio of 1:2 equiv. a yellow precipitate and brown solution was achieved. Crystallization from the yellow precipitate resulted in yellow shiny, paramagnetic crystals of the composition $[\text{Cr}(\text{mbpy})_3][\text{BF}_4]_3$. Electrochemical studies of the product showed three reversible waves. The product has been characterized by NMR spectroscopy, elemental analysis, UV-Vis, IR, CV, squid measurement and SC-XRD. Crystallization from the brown solution reaction resulted into brown crystals of $[\text{Cr}(\text{mbpy})_2][\text{BF}_4]_2$.

It is noteworthy to mention that by changing the ratio of the starting chromium nitrile complex and 5,5'-Dimethyl-2,2'-bipyridine to 1:3 equiv., the reaction was stopped in the first stage forming a compound of deep violet color and even with increasing the reaction time the color did not change. Based on this observation, it may be concluded that a complex with an oxidation state of 2+ has been obtained. It appears that the amount of the bipyridine derivative ligand as redox-active or redox-non-innocent ligand affects the oxidation state of the final product.

The reaction of $[\text{Cr}(\text{NCPH})_4][\text{BF}_4]_2$ with 1,1'-bis(diphenylphosphino)ferrocene (DPPF) resulted in the formation of $\text{CrCl}_2(\text{DPPF})$. $^1\text{H-NMR}$ reveals a low field shift for DPPF peaks in this complex.

During the final of the work, different ways and new starting materials were tried in order to synthesize the intended $(\text{Cr}_2(\text{O}_2\text{C-Fc})_4)$ complex but the main focus at this time was shifted to a cooperation project dealing with the synthesis and purification of ionic liquids (ILs) as additives to electrolytes for batteries.

In general, the research on chromium complexes led to obtaining five crystal structures, not all of them of sufficient quality for a full discussion, however. Nevertheless, the structural proof of the respective compounds' composition has been achieved in all cases.

Ionic Liquids

In this part of the research, differently substituted imidazolium and pyrrolidinium ionic liquids with bromides as counter ions and in one case guanidinium-piperidinium chloride were synthesized. They were combined later with BF_4 , OTf, PF_6 and TFSI anions using anion exchange reactions in order to synthesize the appropriate anion-cation combination to obtain suitable ILs with thermal, moisture and electrochemical stability, which can provide the best aprotic media with a wide electrochemical window. All synthesized ionic liquids were characterized and their levels of purity were proven by nuclear magnetic resonance (^1H , ^{13}C , ^{19}F , ^{31}P , ^{11}B NMR) and elemental analysis. After obtaining a sufficiently high level of purity of the products, they were dried and then electrochemical properties of the synthesized ILs were examined by CV and LSV measurements under argon atmosphere in order to use them later as electrolytes or electrolyte additives of Li-ion or Na based batteries. For the electrochemical examinations, a certain amount of each of the ILs was dissolved in selected electrolytes (“1 M LiPF_6 in EC/DEC” and “1 M LiPF_6 in DEC”) with the aim of improving the electrochemical window (EW) of these commercial electrolytes. The resulting EWs were compared to commercial electrolytes.

It was concluded that when “1 M LiPF_6 in EC/DEC” was used as the blank electrolyte, the electrochemical window was increased when imidazolium analogues excluding $[\text{MBnIm}][\text{BF}_4]$ were added. Among them $[\text{BMIm}][\text{PF}_6]$ and $[\text{MBn}^{\text{F}}\text{Im}][\text{TFSI}]$ with respective 0.6 and 0.5 V difference in comparison with the neat blank electrolyte resulted in the biggest electrochemical windows. Results of the tested pyrrolidinium based ionic liquids show that increasing the electrochemical window with the addition of $\text{MBn}^{\text{F}}\text{Pyr}$ -ILs leads to a $[\text{MBn}^{\text{F}}\text{Pyr}][\text{PF}_6] > [\text{MBn}^{\text{F}}\text{Pyr}][\text{BF}_4] > [\text{MBn}^{\text{F}}\text{Pyr}][\text{OTf}]$ pattern with a respective increase of 0.5, 0.3 and 0.1 V compared to the neat blank electrolyte. Among the $\text{MBn}^{\text{F}}\text{Pyr}$ -ILs just $[\text{MBn}^{\text{F}}\text{Pyr}][\text{PF}_6]$ increased the electrochemical window with a mere 0.04 V.

In order to test the influence of the ionic liquids' concentration on the electrochemical window, 0.5 M $[\text{MBn}^{\text{F}}\text{pyr}][\text{PF}_6]$ in the blank electrolyte “1 M LiPF_6 in EC/DEC” was prepared and tested. It was resulted in a 0.1 V increase of EW, which is 0.4 V less than the same sample with 0.1 M IL concentration. Therefore, it may be concluded that increasing the concentration of the additive ILs does not have a direct relation with the increase in electrochemical window.

In the next step “1 M LiPF_6 in DEC” was used as the blank electrolyte. Excluding $[\text{MBn}^{\text{F}}\text{Pyr}][\text{PF}_6]$ and $[\text{MBn}^{\text{F}}\text{Pyr}][\text{BF}_4]$ with 0.1 and 0.2 V respectively increasing in EW and $[\text{BnBnIm}][\text{PF}_6]$, which did not result in a considerable change, all other imidazolium and pyrrolidinium based ILs made the electrochemical window of the blank electrolyte smaller.

Increasing the concentration of $[\text{MBn}^{\text{F}}\text{Pyr}][\text{PF}_6]$ from 0.1 to 0.5 M resulted in decreasing the electrochemical window from 5.99 to 5.81 V confirming the previous conclusion about the relevance of the concentration of additive ionic liquids and electrochemical window change.

Continuing the research, it was assumed that the addition of IL-TFSI to a blank electrolyte containing LiTFSI may lead to a mixture with a large electrochemical window as on the one hand the TFSI anion is considered to have a good electrochemical stability and on the other

hand the existence of the same anion may have an influence in increasing EW. Therefore, LiTFSI in two different concentrations was added to both used commercial electrolytes. Subsequently, ILs containing TFSI were added to these new mixtures and the electrochemical windows were examined.

Addition of LiTFSI to the blank electrolyte “1 M LiPF₆ in EC/DEC” led to an increase in EW. By increasing the concentration of LiTFSI from 0.1 M to 0.25 M, the electrochemical window was increased by 0.1 V. Nevertheless, when [MBn^FIm][TFSI] was added to the electrolyte containing 0.1 M LiTFSI, the resulting EW decreased and the amount was almost equal to the primary blank electrolyte.

The results show that although the addition of 0.1 M LiTFSI to the electrolyte “1 M LiPF₆ in DEC” could result in a 0.4 V increase of the electrochemical window, after adding imidazolium based ionic liquids with TFSI counter anion, the EWs were decreased. Furthermore, after adding ILs-TFSI, addition of LiTFSI to the blank electrolyte does not have any effect on the electrochemical window.

In general, it is concluded that when ILs are used as the electrolyte additives, the primary mentioned electrolytes of “1 M LiPF₆ in EC/DEC” and “1 M LiPF₆ in DEC”, themselves, without any other added salt may be a proper combination for being blank electrolytes.

The IL research was conducted in cooperation with a battery research group at the Nanyang Technological University (NTU) in Singapore. A part of the synthesized ILs were sent to the NTU in order to be used as electrolytes and electrolyte additives in a LiFePO₄ battery half-cell. It is planned that the achieved results at two different temperature levels will be compared to the behavior of the same cell using a commercial electrolyte. Furthermore, the ILs will be used in electrochemical reduction of carbon dioxide under two scenarios of: 1- using as electrolyte, 2- using as catalyst-promoter. Unfortunately, most of the research conducted at NTU was not finished when this thesis was written.

5. Experimental Details

5.1. General Procedure

For chromium investigations all preparations and reactions were carried out under argon atmosphere using standard *Schlenk* techniques. The solvents were dried according to conventional procedures and stored over molecular sieves (3 Å, 4 Å). For the ionic liquids part, synthesis of [BnBnIm][Br], [Bn^FBn^FIm][Br], [MBnPyr][Br] and [MBn^FPyr][Br] as well as all preparations for electrochemical tests were performed under argon. Anion exchange reactions with silver salts were carried out in the dark environment.

The Chemicals were purchased from Alfa Aesar, abcr, Sigma-Aldrich and Acros Organics and were used without further purification.

NMR measurements were performed on Bruker AVANCE-DPX-400 and AVANCE-DRX-400 MHz spectrometers (¹H, 400.13 MHz; ¹¹B, 128.38 MHz; ¹³C, 100.62 MHz; ¹⁵N, 40.55 MHz; ¹⁹F, 376.46 MHz; ³¹P, 161.97 MHz). Chemical shifts were reported in ppm and referenced to the solvent as internal standard.

Solid-state NMR spectra were recorded on a Bruker Avance 300, spectrometer equipped with a 4 mm BBMAS probe head and referenced to adamantane as an external standard at 300 K.

IR spectra were recorded on a Varian FTIR-670 spectrometer. The shifts of the signals were given in cm⁻¹.

UV-Vis spectra were recorded with a Jasco V-550 spectrometer using a quartz cell with a path length of 1 cm vs the solvent.

Elemental analysis were carried out at the microanalytical laboratory of technical university of Munich.

Thermogravimetric analysis coupled with mass spectrometry for fragment detection (TGA-MS) were conducted using a Netzsch-STA 409PC/PG machine. Around 3 mg of the samples were heated from 30 to 1000 °C with a heating rate of 10 °C min⁻¹.

X-ray single crystal diffraction data were collected on a Bruker Kappa APEX II CCD system equipped with a graphite monochromator and a Mo fine focus tube ($\lambda = 0.71073 \text{ \AA}$).

X-ray powder diffraction was carried out using a Stoe Stadi P diffractometer operated with CuK α_1 radiation ($\lambda = 1.5406 \text{ \AA}$) and a Ge (111) monochromator.

Magnetic susceptibility measurements were performed in the range of 2-300 K with a 5 T superconducting magnet.

Cyclic voltammetry (CV) and linear sweep voltammetry (LSV) were performed with a Reference 600 Potentiostat ZRA controlled by the Gamry Framework software. All measurements were performed at room temperature and with a scan rate = 10 mV s⁻¹. Glassy carbon with 1 mm diameter as the working electrode, Pt/Ti as the counter electrode and Ag/AgCl as the reference electrode were used. The Ag/AgCl electrode was stored inside the solution of 3.5 M KCl in distilled water.

5.2. Chromium Complexes

5.2.1. Synthesis of $\text{Cr}_2(\text{O}_2\text{C-Fc})_4$ Complex

5.2.1.1. Substitution of the Acetate Group in $\text{Cr}_2(\text{O}_2\text{CCH}_3)_4$ Complex

It has been attempted to replace the acetate group in dichromium tetraacetate with ferrocene substituted mono carboxylic acid (FCA). The performed reactions are summarized in the following:

$\text{Cr}_2(\text{O}_2\text{CCH}_3)_4 + \text{FCA}$

By heating the red-brown $\text{Cr}_2(\text{O}_2\text{CCH}_3)_4(\text{H}_2\text{O})_2$ at 100-110 °C overnight, the brown anhydrous chromium (II) acetate could be obtained. Subsequently, to a suspension of $\text{Cr}_2(\text{O}_2\text{CCH}_3)_4$ (1 equiv.) in THF, a solution of ferrocene monocarboxylic acid (FCA) in THF was added. Different ratios of 1:4, 1:5 and 1:10 for starting materials were tried. The solution's color started to change from medium to dark brown after 30 minutes. The mixture was stirred for 48 hours under reflux at 70 °C (different temperature levels was tried. Starting from RT to the reflux temperature). After filtration, the obtained yellow solid was washed with Et_2O and dried under vacuum. Attempts for crystallization were unsuccessful.

$^1\text{H-NMR}$ (DMSO- d_6 , 400.13 MHz, ppm): $\delta = 4.50, 4.14, 3.83$. (broad peaks because of paramagnetism)

selected IR (cm^{-1}): $\nu_a(\text{COO}) 1474 \text{ s}$; $\nu_s(\text{COO}) 1391 \text{ s}$.

5 mL hexane was added to the filtrate of the reaction in order to remove the extra unreacted FCA. The obtained dark brown solid was separated and the solvent was evaporated under reduced pressure. The yellow solid was washed a few times with diethyl ether and dried under vacuum.

selected IR (cm^{-1}): $\nu_a(\text{COO}) 1476 \text{ s}$; $\nu_s(\text{COO}) 1393 \text{ s}$.

$\text{Cr}_2(\text{O}_2\text{CCH}_3)_4 + \text{FCA} + n\text{-butyllithium}$

To a mixture of 1 equiv. $\text{Cr}_2(\text{O}_2\text{CCH}_3)_4$ (0.1 g, 0.29 mmol) and 4 equiv. ferrocene monocarboxylic acid (0.27 g, 1.17 mmol) in THF, 2.38 mL *n*-butyllithium (2.5 M in hexane) was added. After being stirred for one day, a red-brown gelly compound appeared inside the reaction flask which made the filtration difficult. In order to make it easier, during the filtration THF was added frequently to the reaction flask. The solvent of the filtrate was evaporated and the red brown solid was washed a few times with hexane and left to dry under reduced pressure. The product had paramagnetic properties. Nevertheless, according to solvent and solid state NMR spectra, the trace of ferrocene carboxylate in the product could be observed. It was attempted several times to obtain the pure product by crystallization none of which was successful.

Solid-state NMR: **$^1\text{H-NMR}$** (ppm): $\delta = 4$. **$^{13}\text{C-NMR}$** (ppm): $\delta = 70.3, 180.4$.

In $^1\text{H-NMR}$ (DMSO- d_6) different peaks could be observed in the ferrocene carboxylate area (between 4 - 5 ppm) but because of paramagnetism of the product, the peaks could not be specified clearly.

Cr₂(O₂CCH₃)₄(H₂O)₂ + FCA + NaOMe

To the suspension of 4 equiv. ferrocene monocarboxylic acid (0.24 g, 1.06 mmol) in dry and degassed ethanol, sodium methoxide (0.2 mL) was added. Then a suspension of 1 equiv. Cr₂(O₂CCH₃)₄(H₂O)₂ (0.1 g, 0.26 mmol) in ethanol was added to the reaction mixture. The reaction was stirred overnight, resulting to a yellow solution together with some green precipitate. The precipitate was filtered off and the yellow solution was evaporated under reduced pressure. Crystallisation was not successful.

¹H-NMR (C₆D₆, 400.13 MHz, ppm): δ = 5.51, 3.29. (broad peaks)

selected IR (cm⁻¹): ν_a(COO) 1549 s; ν_s(COO) 1412 s.

UV-Vis (CH₃CN): λ_{max} (nm) 212, 260.

5.2.1.2. Using Chromium Metal as the Starting Material

Chromium powder was used as the starting material and was reacted with ferrocene monocarboxylic acid in the presence of an oxidant. Performed reactions have been summarized in below:

1. Cr⁰ + KBr + FCA
2. Cr⁰ + I₂ + FCA
3. Cr⁰ + HCl / Et₂O + FCA

[Cr₃O(O₂C-Fc)₆(THF)₃]⁺¹ complex was obtained as the result of pathways 2 and 3. Therefore, the reaction experimental details will be described in a separate part (section 5.2.2).

5.2.1.3. Using Tetrakis(nitrile)chromium(II) Complex as the Starting Material**[Cr(CH₃CN)₄][BF₄]₂ + FCA**

Blue complex [Cr(CH₃CN)₄][BF₄]₂ was prepared as described in literature.⁹⁸

A suspension of 1 equiv. [Cr(CH₃CN)₄][BF₄]₂ (0.1 g, 0.25 mmol) and 2 equiv. ferrocene monocarboxylic acid (0.118 g, 0.51 mmol) in a solvent mixture of DCM (10 mL) and THF (5 mL) was stirred for 48 hours at 40 °C. Adding solvents, the color of the suspension became orange after 3 minutes. In 30 minutes it became darker and after 2 days we had a brown solution. The solution was filtered off and the green-grey solid was separated. Solvent was evaporated under reduced pressure and the obtained brown-yellow solid was washed a few times with diethyl ether and pentane. Despite multiple, repetitive and continuous efforts the crystal could not be obtained.

It is noteworthy that different ratios of starting material and different temperature levels had been tried for this reaction.

¹H-NMR (DMSO-d₆, 400.13 MHz, ppm): δ = 4.58, 4.28, 4.15. (broad peaks because of paramagnetism)

selected IR (cm⁻¹): ν_a(COO) 1478 s; ν_s(COO) 1395 s.

5.2.1.4. Using Chromocene as the Starting Material

Cr(C₅H₅)₂ + FCA

A mixture of 1 equiv. chromocene (0.1 g, 0.55 mmol) and 4 equiv. ferrocene monocarboxylic acid (0.5 g, 2.2 mmol) in dry and degassed THF was stirred for 24 hours at RT. The dark brown precipitate was filtered off and the brown-red solution was evaporated. The obtained solid was washed a few times with diethyl ether and pentane to yield a brown paramagnetic solid. Crystallisation was not successful.

selected IR (cm⁻¹): $\nu_a(\text{COO})$ 1477 s; $\nu_s(\text{COO})$ 1394 s.

UV-Vis (CH₃CN): λ_{max} (nm) 211, 265.

5.2.2. Synthesis of [Cr₃O(O₂C-Fc)₆(THF)₃]⁺¹ Complexes

5.2.2.1. [Cr₃O(O₂C-Fc)₆(THF)₃][CrCl₄(THF)₂]

To a suspension of 1 equiv. chromium powder (0.1 g, 1.92 mmol) and 2 equiv. ferrocene monocarboxylic acid (0.88 g, 3.84 mmol) in THF, hydrogen chloride solution; 2 M in diethyl ether (2.89 mL) was added. The mixture was stirred under 45 °C overnight. During the course of the reaction, chromium was solved in the solution and a brown solution together with some orange precipitate was obtained. The reaction was let to cool down. 2/3 of the brown solution obtained by filtration was evaporated. Then diethyl ether (20 mL) was added to the solution and the resulting yellow precipitate was collected and washed a few times with diethyl ether and pentane and dried under reduced pressure.

In order to grow crystals, the concentrated brown THF solution was carefully layered with pentane and a small amount of diethyl ether. Brown crystals were obtained after two weeks.

¹H-NMR (CD₃CN, 400.13 MHz, ppm): δ = 4.86, 4.39, 4.09.

selected IR (cm⁻¹): 3098 vw, 2973 vw, 1576 s, 14.89 vs, 14.02 s, 1364 s, 1202 w, 1105 w, 1025 s, 922 w, 823 s, 797 s, 704 s, 556 vs, 482 s.

UV-Vis (CH₃CN): λ_{max} (nm) 211, 265.

elemental analysis (%): C₇₄H₇₀C₁₄Cr₄Fe₆O₁₅ requires C, 47.17; H, 3.74; Fe, 17.78; found: C, 46.09; H, 3.9; Fe; 17.77.

The orange precipitate obtained from the first filtration of the reaction was washed a few times with THF, diethyl ether and pentane then dried under vacuum.

¹H-NMR (CD₃CN, 400.13 MHz, ppm): δ = 4.85, 4.40, 4.08.

CV in acetonitrile (0.1 M [N(*n*Bu)₄]BF₄) and the potential range from 0 to 1.5 V vs Fc/Fc⁺: two reversible waves at 0.81 and 1.47 V were observed.

5.2.2.2. [Cr₃O(O₂C-Fc)₆(THF)₃]I₃

To a suspension of 1 equiv. chromium powder (0.05 g, 0.96 mmol) and 2 equiv. ferrocene monocarboxylic acid (0.244 g, 1.92 mmol) in THF, iodine (0.244 g) was added. The dark brown mixture was stirred for 24 hours at 70 °C under reflux. The mixture was allowed to cool

down and then was cooled in an ice bath for 30 minutes. The precipitate was filtered off and the solvent of the solution was evaporated under reduced pressure. The obtained dark solid was washed a few times with diethyl ether and hexane and dried under vacuum.

$^1\text{H-NMR}$ (DMSO- d_6 , 400.13 MHz, ppm.): $\delta = 4.79, 4.56, 4.25$.

Note: Because of paramagnetism of the compound, the two last peaks could not be recognized easily. Therefore, NMR spectrum needs to be scaled up in order to observe them.

The precipitate achieved from the first filtration of the reaction was washed with hexane and then solved in DCM. The DCM solution was filtered in order to remove the remaining chromium powder and then layered carefully with hexane. Within a few days, yellow paramagnetic crystals were formed.

$^1\text{H-NMR}$ (DMSO- d_6 , 400.13 MHz, ppm): $\delta = 4.74, 4.38, 4.11$. (The two last peaks could not be recognized easily.)

selected IR (cm^{-1}): 3092 vw, 2959 vw, 1589 s, 14.77 s, 13.92 s, 1359 s, 1197 w, 1105 w, 1023 w, 920 w, 820 w, 777 w, 667 s, 541 vs, 479 s.

elemental analysis (%): $\text{C}_{78}\text{H}_{84}\text{Cr}_3\text{Fe}_6\text{I}_3\text{O}_{16}$ requires: C, 43.59; H, 3.94; Cr, 7.26; found: C, 43.72; H, 4.01; Cr, 7.38.

UV-Vis (CH_3CN): λ_{max} (nm) 234, 312.

5.2.3. Reactions of $\text{Cr}_2(\text{O}_2\text{CCH}_3)_4$ with Long Carbon Chain Dicarboxylic Acids

Experiments aimed at finding a proper dicarboxylic acid which can be replaced with the acetate groups of a dichromium teraacetate complex.

5.2.3.1. $\text{Cr}_2(\text{O}_2\text{CCH}_3)_4$ + Adipic acid

A colorless THF solution of 1 equiv. adipic acid (0.043 g, 0.29 mmol) was dropwise added to a brown suspension of 1 equiv. $\text{Cr}_2(\text{O}_2\text{CCH}_3)_4$ (0.1 g, 0.29 mmol) in THF. The reaction was stirred for 24 hours at 60 °C to yield a dark green solution. Light green solid was obtained by filtration and dried under reduced pressure. The product could not be solved in any of the various solvents used.

selected IR (cm^{-1}): $\nu_{\text{a}}(\text{COO})$ 1545 s, $\nu_{\text{s}}(\text{COO})$ 1448 s.

5.2.3.2. $\text{Cr}_2(\text{O}_2\text{CCH}_3)_4$ + Sebacic acid

To a suspension of 1 equiv. $\text{Cr}_2(\text{O}_2\text{CCH}_3)_4$ (0.1 g, 0.29 mmol) in dry and degassed THF, a THF solution of 1 equiv. sebacic acid (0.059 g, 0.29 mmol) was slowly added. The mixture was stirred for 48 hours at RT to yield some green precipitate inside a dark solution. The green precipitate was collected by filtration and dried under vacuum. The product could not be solved in any of the various solvents used.

selected IR (cm^{-1}): $\nu_{\text{a}}(\text{COO})$ 1539 s, $\nu_{\text{s}}(\text{COO})$ 1447 s.

5.2.4. Reactions of Tetrakis(nitrile)chromium(II) tetrafluoroborate Complex of $[\text{Cr}(\text{NCPh})_4][\text{BF}_4]_2$

5.2.4.1. Reaction of $[\text{Cr}(\text{NCPh})_4][\text{BF}_4]_2$ with 5,5'-Dimethyl-2,2'-bipyridine

Synthesis of Compound $[\text{Cr}(\text{mbpy})_3][\text{BF}_4]_3$

The compound $[\text{Cr}(\text{NCPh})_4][\text{BF}_4]_2$ was synthesized according to the related literature.⁹⁸ colorless solution of 2 equiv. 5,5'-Dimethyl-2,2'-bipyridine (0.058 g, 0.313 mmol) in dichloromethane was added to a blue solution of 1 equiv. $[\text{Cr}(\text{NCPh})_4][\text{BF}_4]_2$ (0.1 g, 0.156 mmol) in dichloromethane. The reaction mixture turned immediately into dark violet. After one hour, the color changed to brown and some yellow precipitate started to appear. The reaction was stirred overnight at room temperature. In the meantime, the amount of yellow precipitate was increased. The yellow precipitate was filtered and washed a few times with dichloromethane and consequently dried under reduced pressure. Crystallisation from acetonitrile and pentane/diethyl ether gave yellow air stable paramagnetic crystals (80% yield). Note: By changing the ratios of educts to 3:1, the yellow product could not be achieved.

elemental analysis (%): $\text{C}_{36}\text{H}_{36}\text{B}_3\text{CrF}_{12}\text{N}_6$ requires C, 49.98; H, 4.19; N, 9.71; found: C, 50; H, 4.20; N, 9.73.

selected IR (cm^{-1}): 3033 w, 2964 w, 2924 w, 1607 m, 1508 m, 1476 s, 1393 m, 1322 m, 1252 m, 1083 vs, 1059 vs, 831 m, 724 m, 667 m, 552 m.

UV-Vis (CH_3CN): λ_{max} (nm): 241, 320.

CV in acetonitrile (0.1 M $[\text{N}(n\text{Bu})_4][\text{BF}_4]$) and the potential range from 0 to -2 V vs Fc/Fc^+ , three reversible waves at -0.71, -1.17 and -1.91 V were observed.

Magnetic susceptibility measurement: From the field-dependent magnetization at 300 K, magnetic moment of $3.8 \mu_{\text{B}}$ was determined, indicating an $S = 3/2$ ground state

Compound $[\text{Cr}(\text{mbpy})_2][\text{BF}_4]_2$

Crystallization of the previous reaction solution from DCM/ Et_2O resulted into the air sensitive brown crystals of $[\text{Cr}(\text{mbpy})_2][\text{BF}_4]_2$

$^1\text{H-NMR}$ (CD_3CN , 400.13 MHz, ppm): $\delta = 8.65, 8.32, 8.01, 2.52$.

selected IR (cm^{-1}): 3603 w, 3448 w, 3050 w, 2157 w, 2036 w, 1604 m, 1508 w, 1477 s, 1391 m, 1317 m, 1236 m, 1055 vs, 831 m, 728 m, 665 m, 567 s.

UV-Vis (CH_3CN): λ_{max} (nm): 260, 315.

5.2.4.2. Reaction of $[\text{Cr}(\text{NCPh})_4][\text{BF}_4]_2$ with Diethylenetriamine

To a blue solution of $[\text{Cr}(\text{NCPh})_4][\text{BF}_4]_2$ (0.1 g, 0.16 mmol) in DCM, diethylenetriamine (0.017 mL) was added. The color of the mixture changed to red-pink immediately. The mixture was stirred for 24 hours at RT. The solvent was evaporated and the obtained solid was washed a few times with pentane and then solved in CH_3CN to yield a pink solution together with some grey-green precipitate. The precipitate was filtered off and the solvent of the filtrate was evaporated under reduced pressure. Crystallisation was not successful.

¹H-NMR (CD₃CN, 400.13 MHz, ppm): δ = 3.06, 2.88, 1.96.

5.2.4.3. Reaction of [Cr(NCPh)₄][BF₄]₂ with N,N,N',N'-Tetrakis(di-phenylphosphanyl)ethane-1,2-diamine

To a solution of 1 equiv. [Cr(NCPh)₄][BF₄]₂ (0.1 g, 0.16 mmol) in DCM, a solution of 2 equiv. N,N,N',N'-terakis(di-phenylphosphanyl)ethane-1,2-diamine (0.13 g, 0.31 mmol) in DCM was added. The color of the reaction was changed from blue to green after 5 minutes. The mixture was stirred at RT for 48 hours to yield a grey precipitate inside a colorless solution. The suspension was filtrated and the precipitate was washed a few times with DCM to yield a white-grey solid. The paramagnetic solid was dried under reduced pressure. Crystallisation was not successful.

¹H-NMR (CD₃CN, 400.13 MHz, ppm): δ = 7.60, 3.43. (broad peaks)

¹⁵N-NMR (CD₃CN, 40.55 MHz, ppm): δ = -244.83.

5.2.4.4. Reaction of [Cr(NCPh)₄][BF₄]₂ with 1,1'-Bis(diphenylphosphino)ferrocene (DPPF)

To a blue solution of 1 equiv. [Cr(NCPh)₄][BF₄]₂ (0.1 g, 0.16 mmol) in DCM, 2 equiv. DPPF (0.17 g, 0.31 mmol) was added. The reaction mixture was stirred for 48 hours to yield a green solution. The solution was then filtrated and layered with pentane. After one month orange crystals formed.

¹H-NMR (CD₃CN, 400.13 MHz, ppm): δ = 7.41, 4.52, 4.26. (The first two peaks are broad.)

³¹P-NMR (CD₃CN, 161.97 MHz, ppm): δ = -16.89, -50.

Note: The crystal of the product could not be obtained again by repeating the reaction. Therefore, more analytical data is not available.

5.3. Ionic liquids

5.3.1. Synthesis and General Procedure

The imidazolium and pyrrolidinium bromides of [BMIm][Br], [MBnIm][Br], [MMBnIm][Br], [MMBn^FIm][Br], [BnBnIm][Br], [Bn^FBn^FIm][Br], [MBnPyr][Br], [MBn^FPyr][Br] were synthesized through the quaternization reaction of imidazole or pyrrolidine with alkylhalides. Some differences in the synthesis path were applied as different derivatives were intended. Furthermore, N,N,N',N'-tetramethyl-N'',N''-pentamethyleneguanidinium chloride (PipGuan-Cl) was prepared according to the procedure known from literature.¹⁵¹

In the next step, thermally and kinetically more stable cation-anion combinations were obtained via salt metathesis reactions. All products were purified very carefully as pure products are of high importance due to the fact that impurities can spoil the electrochemical experiments and cause unwanted side reactions.

The previously synthesized imidazolium and pyrrolidinium bromides were transformed to the corresponding OTf, PF₆ and BF₄ analogues through anion exchange reactions as described below:

To a solution of ionic liquid bromide (1 equiv.) in acetonitrile or methanol, a solution of corresponding silver salt (1.1 equiv.) in acetonitrile was added. The resulting mixture was stirred in dark at RT over a period of 1.5 to 3 hours and then was filtered to remove the yellow precipitate. The solvent of the filtrate was rotary evaporated under vacuum at 45 °C and then while stirring was cooled down and dried under reduced pressure. Afterwards, the resulting residue was purified. The purification method was different depending on the obtained product:

Liquid residues were extracted with DCM / H₂O (3:1 v/v). The solvent of the organic phase was rotary evaporated and the product was dried under vacuum.

The crude solid products were purified by crystallization from acetonitrile solution with diethyl ether or ethyl acetate (depending on the solubility of the compound). subsequently, the product was washed a few times with diethyl ether and then dried under vacuum.

For synthesis of [BMIm][TFSI], [BnMIm][TFSI] and [Bn^FMIm][TFSI], corresponding imidazolium bromide (1 equiv.) was dissolved in deionised water. Subsequently, LiTFSI (1.1 equiv.) was added slowly to the solution. The reaction was stirred at room temperature for 16 hours and the product was extracted with DCM. The organic phase was separated and washed with several portions of deionised water to remove the excess of LiTFSI salt present in the solution. Consequently, the solution was dried with Na₂SO₄, stirred over charcoal for 30 minutes, and filtered. Afterwards, the solvent was removed at 40 °C with a rotary evaporator resulting in a liquid product for [BMIm][TFSI] and [BnMIm][TFSI] and a solid product for [Bn^FMIm][TFSI] which was washed a few times with diethyl ether as well. All products were dried for 8 hours at 50 °C. Furthermore, PipGuan-Cl was transformed to PipGuan-TFSI according to the procedure reported in literature.¹⁵¹

The synthesized compounds were characterized and their levels of purity was proven by (¹H, ¹³C, ¹⁹F, ³¹P, ¹¹B)-NMR and elemental analysis. Finally, the obtained ILs were used as electrolyte additives of the commercial electrolytes (“1 M LiPF₆ in EC/DEC” and “1 M LipF₆ in DEC”) and the electrochemical properties were examined by cyclic voltammetry (CV) and linear sweep voltammetry (LSV). Subsequently, the results were compared to the electrochemical windows of the used commercial electrolytes.

5.3.2. Analysis

5.3.2.1. Imidazolium-based ILs

1-Butyl-3-methylimidazolium tetrafluoroborate ([BMIm][BF₄])



$C_8H_{15}BF_4N_2$ (226.03g/mol); colorless oil; yield: 83%

1H -NMR ($CDCl_3$, 400.13 MHz, RT, ppm): 8.88 (s, 1H, NCHN), 7.31 (t, $^3J = 2$ Hz, 1H, NCH), 7.26 (t, $^3J = 2$ Hz, 1H, NCH), 4.19 (t, $^3J = 7$ Hz, 2H, NCH₂), 3.96 (s, 3H, NCH₃), 1.90 - 1.83 (m, 2H, CH₂), 1.42 - 1.32 (m, 2H, CH₂), 0.96 (t, $^3J = 7$ Hz, 3H, CH₂CH₃).

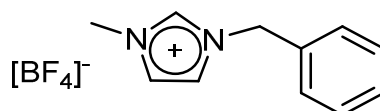
^{13}C -NMR ($CDCl_3$, 100.62 MHz, RT, ppm): $\delta = 136.89, 123.62, 122.04, 50.07, 36.53, 32.04, 19.55, 13.46$.

^{19}F -NMR ($CDCl_3$, 376.46 MHz, RT, ppm): $\delta = -151.50$ ($^{11}B-F, BF_4$), -151.55 ($^{10}B-F, BF_4$).

^{11}B -NMR ($CDCl_3$, 128.38 MHz, RT, ppm): $\delta = -0.98$.

elemental analysis (%): $C_8H_{15}BF_4N_2$ requires: C, 42.51; H, 6.69; N, 12.39 F, 33.62. found: C, 42.37; H, 6.91; N, 12.75; F, 32.8.

1-Benzyl-3-methylimidazolium tetrafluoroborate ([MBnIm][BF₄])



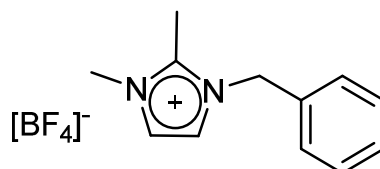
$C_{11}H_{13}BF_4N_2$ (260.04 g/mol); white solid; yield: 91%

1H -NMR (DMSO-*d*₆, 400.13 MHz, RT, ppm) $\delta = 9.12$ (s, 1H, NCHN), 7.71 (t, $^3J = 2$ Hz, 1H, NCH), 7.64 (t, $^3J = 2$ Hz, 1H, NCH), 7.44 - 7.36 (m, 5H, CH_{ar}), 5.38 (s, 2H, NCH₂), 3.83 (s, 3H, NCH₃).

^{13}C -NMR (DMSO-*d*₆, 100.62 MHz, RT, ppm) $\delta = 136.79, 134.97, 129.38, 129.17, 128.59, 124.29, 122.58, 52.26, 36.16$.

elemental analysis (%): $C_{11}H_{13}BF_4N_2$ requires: C, 50.81; H, 5.04; N, 10.77; F 29.22; found: C, 50.87; H, 5.25; N, 10.68; F, 28.82.

1-Benzyl-2,3-dimethylimidazolium tetrafluoroborate ([MMBnIm][BF₄])



$C_{12}H_{15}N_2BF_4$ (274.07 g/mol); white solid; yield: 88%

1H -NMR (DMSO-*d*₆, 400.13 MHz, RT, ppm): $\delta = 7.71$ (d, $^3J = 2$ Hz, 1H, NCH), 7.66 (d, $^3J = 2$ Hz, 1H, NCH), 7.44 - 7.31 (m, 5H, CH_{ar}), 5.41 (s, 2H, NCH₂), 3.76 (s, 3H, NCH₃), 2.99 (s, 3H, NCH₃).

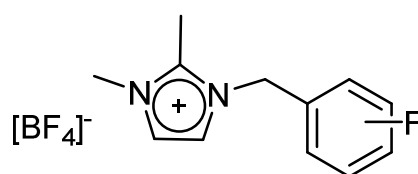
¹³C-NMR (DMSO-d₆, 100.62 MHz, RT, ppm): 144.66, 134.66, 129.01, 128.49, 127.71, 122.71, 121.25, 50.57, 34.84, 9.45.

¹⁹F-NMR (DMSO-d₆, 376.46 MHz, RT, ppm): δ = -148.22 (¹¹B-F, BF₄), -148.27 (¹⁰B-F, BF₄).

¹¹B-NMR (DMSO-d₆, 128.38 MHz, RT, ppm): δ = -1.29.

elemental analysis (%): C₁₂H₁₅BF₄N₂ requires: C, 52.59; H, 5.52; N, 10.22; F, 27.73; found: C, 51; H, 5.6; N, 10.24; F, 28.

1,2-Dimethyl-3-(2', 3', 4', 5', 6'-pentafluorobenzyl)imidazolium tetrafluoroborate ([MMBn^FIm][BF₄])



C₁₂H₁₀BF₉N₂ (364.02 g/mol); white solid; yield: 80%

¹H-NMR (CDCl₃, 400.13 MHz, RT, ppm): δ = 7.49 (d, ³J = 2 Hz, 1H, NCH), 7.23 (d, ³J = 2 Hz, 1H, NCH), 5.42 (s, 2H, NCH₂), 3.83 (s, 3H, NCH₃), 2.75 (s, 3H, NCCCH₃).

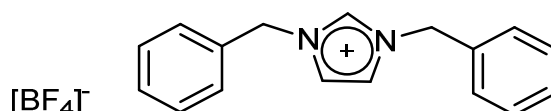
¹³C-NMR (DMSO-d₆, 100.62 MHz, RT, ppm): δ = 145.35, 122.70, 121.27, 34.91, 9.29.

¹⁹F-NMR (DMSO-d₆, 376.46 MHz, RT, ppm): δ = -140.99 (dd, ³J = 24, 8 Hz, 2F, CF_{ortho}), -148.28 (¹¹B-F, BF₄), -148.34 (¹⁰B-F, BF₄), -152.98 (t, ³J = 22 Hz, 1F, CF_{para}), -161.67 (m, 2F, CF_{meta}).

¹¹B-NMR (DMSO-d₆, 128.38 MHz, RT, ppm): δ = -1.31.

elemental analysis (%): C₁₂H₁₀BF₉N₂ requires: C, 39.59; H, 2.77; N, 7.70; F, 46.97; found: C, 39.44; H, 2.84; N, 7.62; F, 46.47.

1,3-Dibenzylimidazolium tetrafluoroborate ([BnBnIm][BF₄])



C₁₇H₁₇BF₄N₂ (336.14 g/mol); white solid; yield: 86%

¹H-NMR (400.13 MHz, DMSO-d₆, RT, ppm): δ = 9.38 (s, 1H, NCH), 7.82 (d, ³J = 2 Hz, 2H, NCH), 7.46 - 7.38 (m, 10H, CH_{ar}), 5.42 (s, 4H, NCH₂).

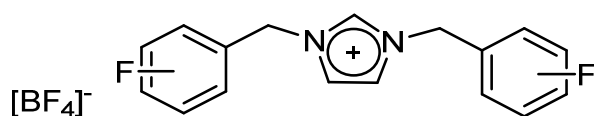
^{13}C -NMR (100.62 MHz, DMSO- d_6 , RT, ppm): $\delta = 136.29, 134.76, 129.07, 128.83, 128.35, 122.95, 52.11$.

^{19}F -NMR (376.46 MHz, DMSO- d_6 , RT, ppm): $\delta = -148.15$ ($^{11}\text{B-F}$, BF_4), -148.20 ($^{10}\text{B-F}$, BF_4).

^{11}B -NMR (128.38 MHz, DMSO- d_6 , RT, ppm): $\delta = -1.28$.

elemental analysis (%): $\text{C}_{17}\text{H}_{17}\text{BF}_4\text{N}_2$ requires: C, 60.74; H, 5.10; N, 8.33; F, 22.61; found: C, 60.64; H, 5.18; N, 8.34; F, 22.9.

1,3-Bis-(2', 3', 4', 5', 6'-pentafluorobenzyl)imidazolium tetrafluoroborate ([Bn^FBn^FIm][BF₄])



$\text{C}_{17}\text{H}_7\text{BF}_{14}\text{N}_2$ (516.04 g/mol); white solid; yield: 77%

^1H -NMR (DMSO- d_6 , 400.13 MHz, RT, ppm): $\delta = 9.45$ (s, 1H, NCH), 7.82 (d, $^3J = 2$ Hz, 2H, NCH), 5.64 (s, 4H, NCH₂).

^{13}C -NMR (DMSO- d_6 , 100.62 MHz, RT, ppm): $\delta = 137.60, 123.10, 40.20$.

^{19}F -NMR (DMSO- d_6 , 376.46 MHz, RT, ppm): $\delta = -141.19$ (dd, $^3J = 24, 8$ Hz, 2F, CF_{ortho}), -148.32 ($^{11}\text{B-F}$, BF_4), -148.37 ($^{10}\text{B-F}$, BF_4), -152.66 (t, $^3J = 22$ Hz, 1F, CF_{para}), -161.71 (m, 2F, CF_{meta}).

elemental analysis (%): $\text{C}_{17}\text{H}_7\text{BF}_{14}\text{N}_2$ requires: C, 39.57; H, 1.37; N, 5.43; F, 51.54; found: C, 39.33; H, 1.32; N, 5.49; F, 51.3.

1-Butyl-3-methylimidazolium trifluoromethanesulfonate ([BMIm][OTf])



$\text{C}_9\text{H}_{15}\text{N}_2\text{F}_3\text{O}_3\text{S}$ (288.29 g/mol); colorless oil; yield: 97%

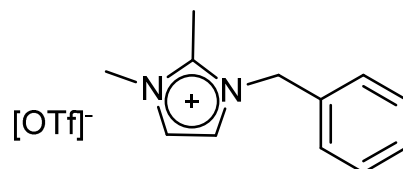
^1H -NMR (CDCl_3 , 400.13 MHz, ppm): $\delta = 9.04$ (s, 1H, NCHN), 7.41 (t, $^3J = 2$ Hz, 1H, NCH), 7.37 (t, $^3J = 2$ Hz, 1H, NCH), 4.17 (t, $^3J = 7$ Hz, 2H, NCH₂), 3.94 (s, 3H, NCH₃), 1.87 - 1.79 (m, 2H, CH₂), 1.38 - 1.28 (m, 2H, CH₂), 0.92 (t, $^3J = 7$ Hz, 3H, CH₂CH₃).

^{13}C -NMR (CDCl_3 , 100.62 MHz, ppm): $\delta = 136.69, 125.52, 123.81, 122.36, 122.34, 119.16, 116, 49.91, 36.40, 32.01, 19.43, 13.37$.

^{19}F -NMR (CDCl_3 , 376.46 MHz, ppm): $\delta = -78.69$.

elemental analysis (%): C₉H₁₅F₃N₂O₃S requires: C, 37.50; H, 5.24; N, 9.72; F, 19.77; S, 11.12; found: C, 37.17; H, 5.28; N, 9.99; F, 18.7; S, 10.36.

1-Benzyl-2,3-dimethylimidazolium trifluoromethanesulfonate ([MMBnIm][OTf])



C₁₃H₁₅ F₃N₂O₃S (336.33 g/mol); white solid; yield: 89%

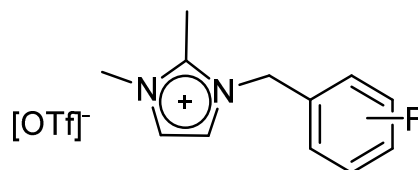
¹H-NMR (DMSO-d₆, 400.13 MHz, ppm): δ = 7.70 (d, ³J = 2 Hz, 1H, NCH), 7.66 (d, ³J = 2 Hz, 1H, NCH), 7.44-7.31 (m, 5H, CH_{ar}), 5.41 (s, 2H, NCH₂), 3.76 (s, 3H, NCH₃), 2.99 (s, 3H, NCC₃H₃).

¹³C-NMR (DMSO-d₆, 100.62 MHz, ppm): δ = 144.66, 134.63, 129, 128.48, 127.71, 122.70, 122.29, 121.24, 119.09, 50.60, 34.83, 9.45.

¹⁹F-NMR (CDCl₃, 376.46 MHz, ppm): δ = -78.47.

elemental analysis (%): C₁₃H₁₅N₂F₃O₃S requires: C, 46.43; H, 4.50; N, 8.33; F, 16.95; S, 9.53; found: C, 46.39; H, 4.49; N, 8.28; F, 16.3; S, 8.13.

1,2-Dimethyl-3-(2', 3', 4', 5', 6'-pentafluorobenzyl)imidazolium trifluoromethanesulfonate ([MMBn^FIm][OTf])



C₁₃H₁₀ F₈N₂O₃S (426.28 g/mol); white solid; yield: 85%

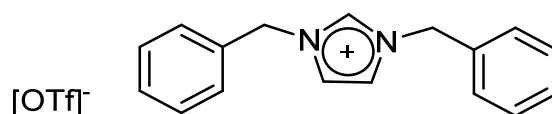
¹H-NMR (CDCl₃, 400.13 MHz, ppm): δ = 7.29 (d, ³J = 2 Hz, 1H, NCH), 7.28 (d, ³J = 2 Hz, 1H, NCH), 5.44 (s, 2H, NCH₂), 3.84 (s, 3H, NCH₃), 2.75 (s, 3H, NCC₃H₃).

¹³C-NMR (DMSO-d₆, 100.62 MHz, ppm): δ = 145.33, 122.67, 122.26, 121.24, 34.88, 9.26.

¹⁹F-NMR (CDCl₃, 376.46 MHz, ppm): δ = -78.49, -140.84 (dd, ³J = 24, 8 Hz, 2F, CF_{ortho}), -149.22 (t, ³J = 22 Hz, 1F, CF_{para}), -158.95 (m, 2F, CF_{meta}).

elemental analysis (%): C₁₃H₁₀N₂F₈O₃S requires: C, 36.63; H, 2.36; N, 6.57; F, 35.65; S, 7.52; found: C, 36.61; H, 2.38; N, 6.58; F, 35.8; S, 7.37.

1,3-Dibenzylimidazolium trifluoromethanesulfonate ([BnBnIm][OTf])



$C_{18}H_{17}N_2F_3O_3S$ (398.40 g/mol); white solid; yield: 89%

1H -NMR (400.13 MHz, DMSO- d_6 , RT, ppm): δ = 9.38 (s, 1H, NCH), 7.83 (d, 3J = 2 Hz, 2H, NCH), 7.46 - 7.37 (m, 10H, CH_{ar}), 5.43 (s, 4H, NCH_2).

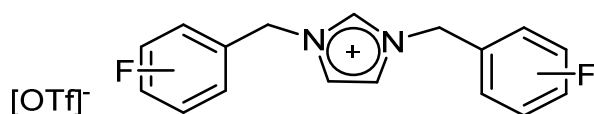
^{13}C -NMR (100.62 MHz, DMSO- d_6 , RT, ppm): δ = 136.30, 134.76, 129.07, 128.84, 128.36, 122.96, 122.30, 119.12, 52.12.

^{19}F -NMR (376.46 MHz, DMSO- d_6 , RT, ppm): δ = -77.77.

elemental analysis (%): $C_{18}H_{17}N_2F_3O_3S$ requires: C, 54.27; H, 4.30; N, 7.03; F, 14.31; S, 8.05; found: C, 54.02; H, 4.21; N, 7.04; F, 15.0; S, 8.20.

1,3-Bis-(2', 3', 4', 5', 6'-pentafluorobenzyl)imidazolium trifluoromethanesulfonate

([Bn^FBn^FIm][OTf])



$C_{18}H_7F_{13}N_2O_3S$ (578.30 g/mol); white solid; yield: 95%

1H -NMR (DMSO- d_6 , 400.13 MHz, RT, ppm): δ = 9.46 (s, 1H, NCH), 7.82 (d, 3J = 2 Hz, 2H, NCH), 5.66 (s, 4H, NCH_2).

^{13}C -NMR (DMSO- d_6 , 100.62 MHz, RT, ppm): δ = 137.65, 125.45, 123.12, 122.25, 119.05, 115.85, 40.28.

^{19}F -NMR (DMSO- d_6 , 376.46 MHz, RT, ppm): δ = -77.82, -141.18 (dd, 3J = 24, 8 Hz, 2F, CF_{ortho}), -152.62 (t, 3J = 22 Hz, 1F, CF_{para}), -161.68 (m, 2F, CF_{meta}).

elemental analysis (%): $C_{18}H_7F_{13}N_2O_3S$ requires: C, 37.38; H, 1.22; N, 4.84; F, 42.71; S, 5.54; found: C, 37.06; H, 1.13; N, 4.83; F, 43.2; S, 5.76.

1-Butyl-3-methylimidazolium hexafluorophosphate ([BMIm][PF₆])



$C_8H_{15}F_6N_2P$ (284.19 g/mol); colorless oil; yield: 99%

1H -NMR (CD_3CN , 400.13 MHz, RT, ppm): $\delta = 8.37$ (s, 1H, NCHN), 7.36 (t, $^3J = 2$ Hz, 1H, NCH), 7.32 (t, $^3J = 2$ Hz, 1H, NCH), 4.11 (t, $^3J = 7$ Hz, 1H, NCH₂), 3.81 (s, 3H, NCH₃), 1.84 - 1.76 (m, 2H, CH₂), 1.37 - 1.27 (m, 2H, CH₂), 0.94 (t, $^3J = 7$ Hz, 3H, CH₂CH₃).

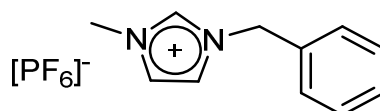
^{13}C -NMR (CD_3CN , 100.62 MHz, RT, ppm): $\delta = 136.80, 124.64, 123.25, 50.26, 36.83, 32.55, 19.93, 13.63$.

^{19}F -NMR ($CDCl_3$, 376.46 MHz, RT, ppm): $\delta = -70.91, -71.60$.

^{31}P -NMR (CD_3CN , 161.97 MHz, RT, ppm): $\delta = -144.62$ (sep, $J = 706$ Hz, 6P, PF₆)

elemental analysis (%): $C_8H_{15}F_6N_2P$ requires: C, 33.81; H, 5.32; N, 9.86; F, 40.11; P, 10.90; found: C, 33.66; H, 5.48; N, 10.06; F, 40.6; P, 9.85.

1-Benzyl-3-methylimidazolium hexafluorophosphate ([MBnIm][PF₆])



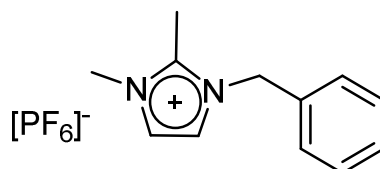
$C_{11}H_{13}F_6N_2P$ (318.20 g/mol); white solid; yield: 96%

1H -NMR ($DMSO-d_6$, 400.13 MHz, RT, ppm) $\delta = 9.12$ (s, 1H, NCHN), 7.71 (t, $^3J = 2$ Hz, 1H, NCH), 7.64 (t, $^3J = 2$ Hz, 1H, NCH), 7.44 - 7.36 (m, 5H, CH_{ar}), 5.38 (s, 2H, NCH₂), 3.83 (s, 3H, NCH₃).

^{13}C -NMR ($DMSO-d_6$, 100.62 MHz, RT, ppm) $\delta = 136.80, 134.96, 129.36, 129.14, 128.57, 124.28, 122.57, 52.24, 36.15$.

elemental analysis (%): $C_{11}H_{13}F_6N_2P$ requires: C, 41.52; H, 4.12; N, 8.80; F, 35.82; P, 9.73; found: C, 41.18; H, 4.18; N, 8.69; F, 35.4; P, 9.26.

1-Benzyl-2,3-dimethylimidazolium hexafluorophosphate ([MMBnIm][PF₆])



$C_{12}H_{15}F_6N_2P$ (332.23 g/mol); white solid; yield: 92%

1H -NMR ($DMSO-d_6$, 400.13 MHz, RT, ppm): $\delta = 7.71$ (d, $^3J = 2$ Hz, 1H, NCH), 7.65 (d, $^3J = 2$ Hz, 1H, NCH), 7.44 - 7.31 (m, 5H, CH_{ar}), 5.41 (s, 2H, NCH₂), 3.76 (s, 3H, NCH₃), 2.59 (s, 3H, NCC₃).

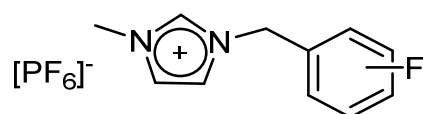
^{13}C -NMR (DMSO- d_6 , 100.62 MHz, RT, ppm): $\delta = 144.66, 134.66, 129.01, 128.49, 127.71, 122.71, 121.26, 50.57, 34.85, 9.46$.

^{19}F -NMR (DMSO- d_6 , 376.46 MHz, RT, ppm): $\delta = -69.19, -71.08$.

^{31}P -NMR (DMSO- d_6 , 161.97 MHz, RT, ppm): -144.21 (sep, $J = 706$ Hz, 6P, PF_6)

elemental analysis (%): $\text{C}_{12}\text{H}_{15}\text{F}_6\text{N}_2\text{P}$ requires: C, 43.38; H, 4.55; N, 8.43; F, 34.31; P, 9.32; found: C, 43.22; H, 4.54; N, 8.35; F, 34.4; P, 9.32.

1-Methyl-3-(2', 3', 4', 5', 6'-pentafluorobenzyl)imidazolium hexafluorophosphate ([MBn^FIm][PF₆])



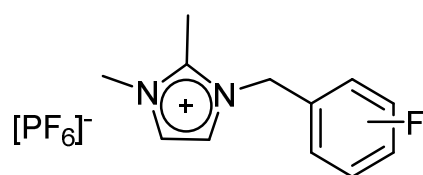
$\text{C}_{11}\text{H}_8\text{F}_{11}\text{N}_2\text{P}$ (408.16 g/mol); white solid; yield: 93%

^1H -NMR (CD_3CN , 400.13 MHz, RT, ppm) $\delta = 8.51$ (s, 1H, NCHN), 7.40 (t, $^3J = 2$ Hz, 1H, NCH), 7.36 (t, $^3J = 2$ Hz, 1H, NCH), 5.45 (s, 2H, NCH_2), 3.81 (s, 3H, NCH_3).

^{13}C -NMR (100.62 MHz, CD_3CN , RT, ppm) $\delta = 137.59, 125.15, 123.46, 41.23, 37.09$.

elemental analysis (%): $\text{C}_{11}\text{H}_8\text{F}_{11}\text{N}_2\text{P}$ requires: C, 32.37; H, 1.98; N, 6.86; F, 51.20; P, 7.59; found: C, 32.38; H, 2.01; N, 6.80; F, 50.7; P, 7.91.

1,2-Dimethyl-3-(2', 3', 4', 5', 6'-pentafluorobenzyl)imidazolium hexafluorophosphate ([MMBn^FIm][PF₆])



$\text{C}_{12}\text{H}_{10}\text{F}_{11}\text{N}_2\text{P}$ (422.18 g/mol); white solid; yield: 99%

^1H -NMR (DMSO- d_6 , 400.13 MHz, RT, ppm): $\delta = 7.65$ (d, $^3J = 2$ Hz, 1H, NCH), 7.63 (d, $^3J = 2$ Hz, 1H, NCH), 5.60 (s, 2H, NCH_2), 3.75 (s, 3H, NCH_3), 2.60 (s, 3H, NCCCH_3).

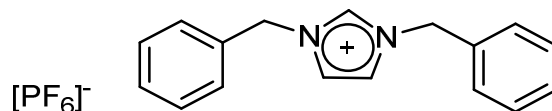
^{13}C -NMR (DMSO- d_6 , 100.62 MHz, RT, ppm): $145.35, 122.70, 121.28, 34.90, 30.71, 9.28$.

^{19}F -NMR (DMSO- d_6 , 376.46 MHz, RT, ppm): $-69.20, -71.09, -140.98$ (dd, $^3J = 24, 8$ Hz, 2F, CF_{ortho}), -152.93 (t, $^3J = 22$ Hz, 1F, CF_{para}), -163.63 (m, 2F, CF_{meta}).

^{31}P -NMR (DMSO- d_6 , 161.97 MHz, RT, ppm): -144.24 (sep, $J = 706$ Hz, 6P, PF_6).

elemental analysis (%): C₁₂H₁₀F₁₁N₂P requires: C, 34.14; H, 2.39; N, 6.64; F, 49.50; P, 7.34; found: C, 34.08; H, 2.16; N, 6.54; F, 50.5; P, 7.04.

1,3-Dibenzylimidazolium hexafluorophosphate ([BnBnIm][PF₆])



C₁₇H₁₇F₆N₂P (394.30 g/mol); white solid; yield: 98%

¹H-NMR (DMSO-*d*₆, 400.13 MHz, RT, ppm): δ = 9.38 (s, 1H, NCH), 7.82 (d, ³J = 2 Hz, 2H, NCH), 7.46 - 7.37 (m, 10H, CH_{ar}), 5.42 (s, 4H, NCH₂).

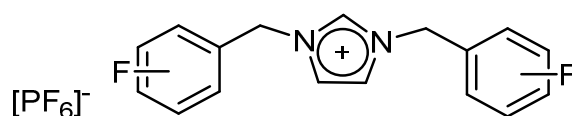
¹³C-NMR (DMSO-*d*₆, 100.62 MHz, RT, ppm): δ = 136.30, 134.76, 129.07, 128.84, 128.35, 122.96, 52.11.

¹⁹F-NMR (DMSO-*d*₆, 376.46 MHz, RT, ppm): 69.18, 71.07.

³¹P-NMR (DMSO-*d*₆, 161.97 MHz, RT, ppm): δ = 141.19 (sep, J = 706 Hz, 6P, PF₆).

elemental analysis (%): C₁₇H₁₇F₆N₂P requires: C, 51.78; H, 4.35; N, 7.10; F, 28.91; P, 7.86; found: C, 50.97; H, 4.41; N, 6.95; F, 28.5; P, 7.52.

1,3-Bis-(2', 3', 4', 5', 6'-pentafluorobenzyl)imidazolium hexafluorophosphate ([Bn^FBn^FIm][PF₆])



C₁₇H₇F₁₆N₂P (574.21 g/mol); white solid; yield: 94%

¹H-NMR (DMSO-*d*₆, 400.13 MHz, RT, ppm): δ = 9.45 (s, 1H, NCH), 7.82 (d, ³J = 2 Hz, 2H, NCH), 5.64 (s, 4H, NCH₂).

¹³C-NMR (DMSO-*d*₆, 100.62 MHz, RT, ppm): δ = 137.61, 123.10, 40.20.

¹⁹F-NMR (DMSO-*d*₆, 376.46 MHz, RT, ppm): -69.32, -71.20, -141.21 (dd, ³J = 24, 8 Hz, 2F, CF_{ortho}), -152.67 (t, ³J = 22 Hz, 1F, CF_{para}), -161.71 (m, 2F, CF_{meta}).

³¹P-NMR (DMSO-*d*₆, 161.97 MHz, RT, ppm): δ = -144.25 (sep, J = 706 Hz, 6P, PF₆).

elemental analysis (%): C₁₇H₇F₁₆N₂P requires: C, 35.56; H, 1.23; N, 4.88; F, 52.94; P, 5.39; found: C, 35.37; H, 1; N, 5.05; F, 53; P, 5.07.

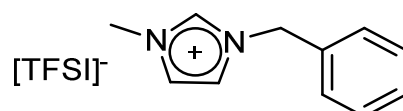
1-Butyl-3-methylimidazolium bistriflimide ([BMIm][TFSI])

$C_{10}H_{15}F_6N_3O_4S_2$ (419.36 g/mol); colorless liquid; yield: 86%

1H -NMR ($CDCl_3$, 400.13 MHz, RT, ppm) δ = 8.75 (s, 1H, NCHN), 7.31 (d, 3J = 2 Hz, 1H, NCH), 7.29 (d, 3J = 2 Hz, 1H, NCH), 4.16 (t, 3J = 7 Hz, 1H, NCH₂), 3.93 (s, 3H, NCH₃), 1.88 - 1.80 (m, 2H, CH₂), 1.40 - 1.31 (m, 2H, CH₂), 0.95 (t, 3J = 7 Hz, 3H, CH₂CH₃).

^{13}C -NMR ($CDCl_3$, 100.62 MHz, RT, ppm) δ = 136.23, 123.79, 122.36, 121.51, 118.32, 50.09, 36.47, 32.05, 19.46, 13.33.

elemental analysis (%): $C_{10}H_{15}F_6N_3O_4S_2$ requires: C, 28.64; H, 3.61; N, 10.02; F, 27.18; S, 15.29; found: C, 28.41; H, 3.82; N, 9.88; F, 27.3; S, 15.06.

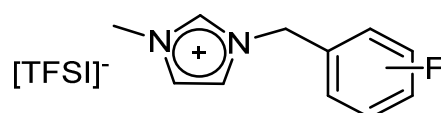
1-Benzyl-3-methylimidazolium bistriflimide ([MBnIm][TFSI])

$C_{13}H_{13}F_6N_3O_4S_2$ (453.37 g/mol); colorless liquid; yield: 83%

1H -NMR ($CDCl_3$, 400MHz, RT, ppm) δ = 8.77 (s, 1H, NCHN), 7.42 - 7.34 (m, 5H, CH_{ar}), 7.26 (t, 3J = 2 Hz, 1H, NCH), 7.19 (t, 3J = 2 Hz, 1H, NCH), 5.29 (s, 2H, NCH₂), 3.90 (s, 3H, NCH₃).

^{13}C -NMR ($CDCl_3$, 100.62 MHz, RT, ppm) δ = 136.18, 132.36, 129.91, 129.72, 129, 123.93, 122.23, 121.52, 118.32, 53.74, 36.53.

elemental analysis (%): requires: C, 34.44; H, 2.89; N, 9.27; F, 25.14; S, 14.14; found: C, 34.65; H, 2.88; N, 9.11; F, 25.7; S, 14.05.

1-Methyl-3-(2', 3', 4', 5', 6'-pentafluorobenzyl)imidazolium bistriflimide ([MBn^FIm][TFSI])

$C_{13}H_8F_{11}N_3O_4S_2$ (543.33 g/mol); white solid; yield: 94 %

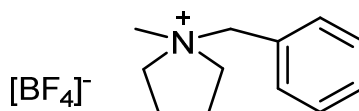
1H -NMR (CD_3CN , 400.13 MHz, RT, ppm) δ = 8.52 (s, 1H, NCHN), 7.39 (t, 3J = 2 Hz, 1H, NCH), 7.36 (t, 3J = 2 Hz, 1H, NCH), 5.44 (s, 2H, NCH₂), 3.81 (s, 3H, NCH₃).

$^{13}\text{C-NMR}$ (CD_3CN , 100.62 MHz, RT, ppm) $\delta = 137.58, 125.15, 123.46, 41.23, 37.10$.

elemental analysis (%): $\text{C}_{13}\text{H}_8\text{F}_{11}\text{N}_3\text{O}_4\text{S}_2$ requires: C, 28.74; H, 1.48; N, 7.73; F 38.46; S, 11.80; found: C, 28.71; H, 1.45; N, 7.73; F, 39; S, 11.73.

5.3.2.2. Pyrrolidinium-based ILs

1-Benzyl-1-methylpyrrolidinium tetrafluoroborate ([MBnPyr][BF₄])



$\text{C}_{12}\text{H}_{18}\text{BF}_4\text{N}$ (263.09 g/mol); white solid; yield: 82%

$^1\text{H-NMR}$ (CD_3CN , 400.13 MHz, RT, ppm): $\delta = 7.58 - 7.51$ (m, 5H, CH_{ar}), 4.41 (s, 2H, NCH_2C), 3.57 - 3.49 (m, 2H, NCH_2), 3.37 - 3.31 (m, 2H, NCH_2), 2.87 (s, 3H, NCH_3), 2.24 - 2.17 (m, 4H, NCH_2CH_2).

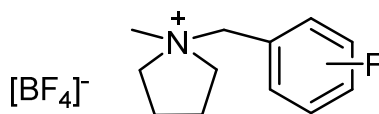
$^{13}\text{C-NMR}$ (CD_3CN , 100.62 MHz, RT, ppm): $\delta = 133.43, 131.56, 130.18, 129.31, 67.37, 64.31, 48.68, 21.82$.

$^{19}\text{F-NMR}$ (CD_3CN , 376.46 MHz, RT, ppm): $\delta = -151.54$ ($^{11}\text{B-F}$, BF_4), -151.59 ($^{10}\text{B-F}$, BF_4).

$^{11}\text{B-NMR}$ (CD_3CN , 128.38 MHz, RT, ppm): $\delta = -1.16$.

elemental analysis (%): $\text{C}_{12}\text{H}_{18}\text{BF}_4\text{N}$ requires: C, 54.78; H, 6.90; N, 5.32; F, 28.89; found: C, 54.53, H, 6.92; N 5.32; F, 29.

1-Methyl-1-(2', 3', 4', 5', 6'-pentafluorobenzyl)pyrrolidinium tetrafluoroborate ([MBn^FPyr][BF₄])



$\text{C}_{12}\text{H}_{13}\text{BF}_9\text{N}$ (353.04 g/mol); white solid; yield: 86%

$^1\text{H-NMR}$ (CD_3CN , 400.13 MHz, RT, ppm): $\delta = 4.59$ (s, 2H, NCH_2C), 3.57 - 3.47 (m, 4H, NCH_2), 2.97 (s, 3H, NCH_3), 2.29 - 2.18 (m, 4H, NCH_2CH_2).

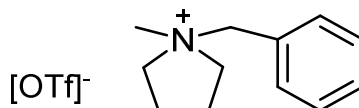
$^{13}\text{C-NMR}$ (CD_3CN , 100.62 MHz, RT, ppm): $\delta = 65, 54.66, 48.60, 21.77$.

$^{19}\text{F-NMR}$ (CD_3CN , 376.46 MHz, RT, ppm): $\delta = -137.95$ (m, 2F, CF_{ortho}), -151.08 (tt, $^3J = 20$, 4 Hz, 1F, CF_{para}), -151.71 ($^{11}\text{B-F}$, BF_4), -151.77 ($^{10}\text{B-F}$, BF_4), -162.21 (m, 2F, CF_{meta}).

$^{11}\text{B-NMR}$ (CD_3CN , 128.38 MHz, RT, ppm): $\delta = -1.22$.

elemental analysis (%): $C_{12}H_{13}BF_9N$ requires: C, 40.83; H, 3.71; N, 3.97; F, 48.43; found: C, 40.52; H, 3.71; N 3.97; F, 48.4.

1-Benzyl-1-methylpyrrolidinium trifluoromethanesulfonate ([MBnPyr][OTf])



$C_{13}H_{18}F_3NO_3S$ (325.35 g/mol); white solid; yield: 92%

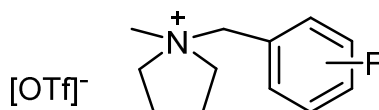
1H -NMR (400.13 MHz, D_2O , RT, ppm): $\delta = 7.56 - 7.48$ (m, 5H, CH_{ar}), 4.47 (s, 2H, NCH_2C), 3.62 - 3.56 (m, 2H, NCH_2), 3.42 - 3.36 (m, 2H, NCH_2), 2.92 (s, 3H, NCH_3), 2.23 - 2.17 (m, 4H, NCH_2CH_2).

^{13}C -NMR (D_2O , 100.62 MHz, RT, ppm): $\delta = 132.30, 130.52, 129.09, 128.06, 124.28, 121.13, 117.97, 114.82, 66.51, 63.19, 47.45, 20.72$.

^{19}F -NMR (D_2O , 376.46 MHz, RT, ppm): $\delta = -78.95$.

elemental analysis (%): $C_{13}H_{18}F_3NO_3S$ requires: C, 47.99; H, 5.58; N, 4.31; F, 17.52; S, 9.85; found: C, 47.52; H, 5.70; N, 4.32; F, 17.86; S, 9.03.

1-Methyl-1-(2',3',4',5',6'-pentafluorobenzyl)pyrrolidinium trifluoromethanesulfonate ([MBn^FPyr][OTf])



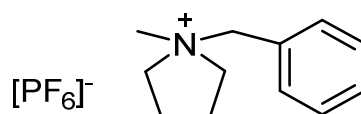
$C_{13}H_{13}F_8NO_3S$ (415.30 g/mol); white solid; yield: 92%

1H -NMR (D_2O , 400.13 MHz, RT, ppm): $\delta = 4.73$ (s, 2H, NCH_2C), 3.66 - 3.53 (m, 4H, NCH_2), 3.04 (s, 3H, NCH_3), 2.31-2.19 (m, 4H, NCH_2CH_2).

^{13}C -NMR (D_2O , 100.62 MHz, RT, ppm): $\delta = 124.27, 121.12, 117.96, 114.81, 63.89, 53.55, 47.35, 20.69$.

^{19}F -NMR (D_2O , 376.46 MHz, RT, ppm): $\delta = -79, -137.58$ (m, 2F, CF_{ortho}), -148.91 (tt, $^3J = 21, 4$ Hz, 1F, CF_{para}), -160.57 (m, 2F, CF_{meta}).

elemental analysis (%): $C_{13}H_{13}F_8NO_3S$ requires: C, 37.60; H, 3.16; N, 3.37; F, 36.60; S 7.72; found: C, 37.66; H, 3.11; N, 3.44; F, 37.1; S, 7.32.

1-Benzyl-1-methylpyrrolidinium hexafluorophosphate ([MBnPyr][PF₆])

C₁₂H₁₈F₆NP (321.25 g/mol); white solid; yield: 97%

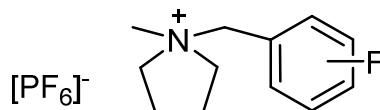
¹H-NMR (CD₃CN, 400.13 MHz, RT, ppm): δ = 7.57 - 7.49 (m, 5H, CH_{ar}), 4.40 (s, 2H, NCH₂C), 3.56 - 3.49 (m, 2H, NCH₂), 3.37 - 3.31 (m, 2H, NCH₂), 2.86 (s, 3H, NCH₃), 2.23 - 2.17 (m, 4H, NCH₂CH₂).

¹³C-NMR (CD₃CN, 100.62 MHz, RT, ppm): δ = 133.42, 131.58, 130.19, 129.26, 67.41, 64.34, 48.71, 21.82.

¹⁹F-NMR (CD₃CN, 376.46 MHz, RT, ppm): δ = -71.92, -73.83.

³¹P-NMR (161.97 MHz, CD₃CN, RT, ppm): δ = -144.63 (sep, *J* = 706 Hz, 6P, PF₆).

elemental analysis (%): C₁₂H₁₈F₆NP requires: C, 44.87; H, 5.65; N, 4.36; F, 35.48; P, 9.64; found: C, 44.77; H, 5.61; N, 4.44; F, 35; P, 9.32.

1-Methyl-1-(2', 3', 4', 5', 6'-pentafluorobenzyl)pyrrolidinium hexafluorophosphate ([MBn^FPyr][PF₆])

C₁₂H₁₃F₁₁NP (411.20 g/mol); white solid; yield: 91%

¹H-NMR (CD₃CN, 400.13 MHz, RT, ppm): δ = 4.58 (s, 2H, NCH₂C), 3.56 - 3.46 (m, 4H, NCH₂), 2.96 (s, 3H, NCH₃), 2.29 - 2.17 (m, 4H, NCH₂CH₂).

¹³C-NMR (CD₃CN, 100.62 MHz, RT, ppm): δ = 65.01, 54.69, 48.63, 21.77.

¹⁹F-NMR (CD₃CN, 376.46 MHz, RT, ppm): δ = -72, -73.87, -137.95 (m, 2F, CF_{ortho}), -151.03 (tt, ³*J* = 20, 4 Hz, 1F, CF_{para}), -162.17 (m, 2F, CF_{meta}).

³¹P-NMR (CD₃CN, 161.97 MHz, RT, ppm): δ = -144.68 (sep, *J* = 706 Hz, 6P, PF₆).

elemental analysis (%): C₁₂H₁₃F₁₁NP requires: C, 35.05; H, 3.19; N, 3.41; F, 50.82; P, 7.53; found: C, 34.87; H, 3.17; N, 3.41; F, 51.2; P, 7.30.

5.3.3. Electrochemical Measurements

All preparations were carried out under argon atmosphere. In order to prepare the samples for electrochemical analysis, a solution from each IL (0.1 M/0.25 M) in two blank electrolytes of “1 M LiPF₆ in EC/DEC” and “1 M LiPF₆ in DEC” was prepared. The electrochemical windows were calculated for the cut-off current density of 0.5 mA cm⁻². The performed electrochemical experiments and the obtained data are summarized as follows:

1- ILs (0.1 M/0.5 M) were added to “1 M LiPF₆ in EC/DEC” (Blank A):

	E_{AL} (V) vs. Fe/Fe⁺	E_{CL} (V) vs. Fe/Fe⁺	Electrochemical Window
Blank A	2.12	-2.95	5.07
[BMIm][PF ₆] 0.1 M	2.15	-3.49	5.64
[BMIm][TFSI] 0.1 M	2.25	-3.06	5.31
[MBnIm][BF ₄] 0.1 M	1.87	-3.09	4.96
[MBnIm][PF ₆] 0.1 M	1.89	-3.28	5.17
[MBnIm][TFSI] 0.1 M	1.99	-3.14	5.13
[MBn ^F Im][PF ₆] 0.1 M	2.21	-3.05	5.26
[MBn ^F Im][TFSI] 0.1 M	2.20	-3.34	5.54
[MBnPyr][BF ₄] 0.1 M	2.02	-3.02	5.04
[MBnPyr][OTF] 0.1 M	2.03	-2.93	4.96
[MBnPyr][PF ₆] 0.1 M	2.07	-3.03	5.1
[MBn ^F Pyr][BF ₄] 0.1 M	2.30	-3.05	5.35
[MBn ^F Pyr][OTF] 0.1 M	2.35	-2.82	5.17
[MBn ^F Pyr][PF ₆] 0.1 M	2.30	-3.28	5.58
[MBn ^F Pyr][PF ₆] 0.5 M	2.40	-2.78	5.18

Table 5.1. Resulted EWs after addition of the ILs into blank A

2- ILs (0.1 M/0.5 M) were added to “1 M LiPF₆ in DEC” (Blank B):

	E_{AL} (V) vs. Fe/Fe⁺	E_{CL} (V) vs. Fe/Fe⁺	Electrochemical Window
Blank B	2.23	-3.66	5.89
[BMIm][PF ₆] 0.1 M	2.1	-3.63	5.73
[BMIm][TFSI] 0.1 M	2.11	-3.67	5.78
[MBnIm][BF ₄] 0.1 M	1.85	-3.31	5.16
[MBnIm][PF ₆] 0.1 M	1.87	-3.67	5.54
[MBnIm][TFSI] 0.1 M	1.85	-3.70	5.55
[MBn ^F Im][PF ₆] 0.1 M	2.18	-3.66	5.84
[MBn ^F Im][TFSI] 0.1 M	2.14	-3.70	5.84
[BnBnIm][BF ₄] 0.1 M	1.87	-3.54	5.41
[BnBnIm][OTF] 0.1 M	1.85	-3.63	5.48
[BnBnIm][PF ₆] 0.1 M	1.92	-4.01	5.93
[Bn ^F Bn ^F Im][BF ₄] 0.1 M	2.16	-3.52	5.68
[MBnPyr][BF ₄] 0.1 M	2.08	-3.53	5.61
[MBnPyr][OTF] 0.1 M	2.07	-3.53	5.6
[MBnPyr][PF ₆] 0.1 M	2.05	-3.71	5.76
[MBn ^F Pyr][BF ₄] 0.1 M	2.42	-3.72	6.14
[MBn ^F Pyr][OTF] 0.1 M	2.17	-3.62	5.79
[MBn ^F Pyr][PF ₆] 0.1 M	2.28	-3.71	5.99
[MBn ^F Pyr][PF ₆] 0.5 M	2.11	-3.70	5.81

Table 5.2. Resulted EWs after addition of the ILs into blank B

- 3- LiTFSI (0.1 M and 0.25 M) was added to Blank A in order to make new blank electrolytes (A' and A''). Afterwards, an ionic liquid with TFSI counter anion (0.1 M) was added to Blank A and the selected blank electrolyte (A''):

	E_{AL} (V) vs. Fe/Fe ⁺	E_{CL} (V) vs. Fe/Fe ⁺	Electrochemical Window
Blank A	2.12	-2.95	5.07
Blank A + 0.1 M LiTFSI (A')	2.38	-3.44	5.82
Blank A + 0.25 M LiTFSI (A'')	2.47	-3.47	5.94
0.1 M [MBn ^F Im][TFSI] + Blank A	2.20	-3.34	5.54
0.1 M [MBn ^F Im][TFSI] + A'	2.21	-2.85	5.06

Table 5.3. Comparison of the resulted EWs with and without addition of LiTFSI into blank A

- 4- LiTFSI (0.1 M and 0.25 M) was added to Blank B in order to make new blank electrolytes (B' and B''). Subsequently, ionic liquids with TFSI counter anion (0.1 M) were added to Blank B and B'':

	E_{AL} (V) vs. Fe/Fe ⁺	E_{CL} (V) vs. Fe/Fe ⁺	Electrochemical Window
Blank B	2.23	-3.66	5.89
Blank B + 0.1 M LiTFSI (B')	2.34	-3.91	6.25
Blank B + 0.25 M LiTFSI (B'')	2.17	-3.73	5.9
0.1 M [MBnIm][TFSI] + Blank B	1.85	-3.70	5.55
0.1 M [MBnIm][TFSI] + B'	1.92	-3.62	5.54
0.1 M [MBn ^F Im][TFSI] + Blank B	2.14	-3.70	5.84
0.1 M [MBn ^F Im][TFSI] + B'	2.18	-3.68	5.86

Table 5.4. Comparison of the resulted EWs with and without addition of LiTFSI into blank B

6. References

- [1] S. Horike, S. Kitagawa, "Design of Porous Coordination Polymers/Metal-Organic Frameworks: Past, Present and Future", in *Metal-Organic Frameworks: Application from Catalysis to Gas Storage*, ed. D. Farrusseng, Wiley-VCH, Weinheim, Germany, 2011, pp. 3 - 21.
- [2] Y. Kinoshita, I. Matsubara, T. Higuchi and Y. Saito, *Bull. Chem. Soc. Jpn.*, 1959, 32, 1221 - 1226.
- [3] A. A. Berlin, N. G. Matveeva, *Russ. Chem. Rev.*, 1960, 29, 119 - 128.
- [4] D. B. Sowerby, L. F. Audrieth, *J. Chem. Educ.*, 1960, 37, 134.
- [5] E. A. Tomic, *J. Appl. Polym. Sci.*, 1965, 9, 3745 - 3752.
- [6] J. E. Bailar, *Preparative Inorganic Reactions*, ed. W. Jolly, Interscience, New York, 1964, vol. 1, pp. 1 - 27.
- [7] B. F. Hoskins, R. Robson, *J. Am. Chem. Soc.*, 1990, 112, 1546 - 1554.
- [8] R. Robson, B. F. Abrahams, S.R. Batten, R. W. Gable, Hoskins, B. F. Hoskins, J. P. Liu, *ACS Symp. Ser.*, 1992, 499, 256 - 273.
- [9] S. R. Batten, R. Robson, *Angew. Chem. Int. Ed. Engl.*, 1998, 37, 1460 - 1494.
- [10] S. R. Batten, N. R. Champness, X. M. Chen, J. Garcia-Martinez, S. Kitagawa, L. Öhrström, M. O'Keefe, M. P. Suh, J. Reedijk, *CrystEngComm*, 2012, 14, 3001 - 3004.
- [11] C. Janiak, J.K. Vieth, *New J. Chem.*, 2010, 34, 2366 - 2388.
- [12] X. Lin, N. R. Champness, M. Schröder, *Top. Curr. Chem.*, 2010, 293, 35 - 76.
- [13] L. J. Murray, M. Dincă, J. Long, *Chem. Soc. Rev.*, 2009, 38, 1294 - 1314.
- [14] A. R. Millward, O. M. Yaghi, *J. Am. Chem. Soc.*, 2005, 127, 17998 - 17999.
- [15] S. Bourrelly, P. L. Llewellyn, C. Serre, F. Millange, T. Loiseau, G. Férey, *J. Am. Chem. Soc.* 2005, 127, 13519 - 13521.
- [16] M. Eddaoudi, J. Kim, N. Rosi, D. Vodak, J. Wachter, M. O'Keefe, O. M. Yaghi, *Science*, 2002, 295, 469 - 472.
- [17] A. U. Czaja, N. Trukhan, U. Müller, *Chem. Soc. Rev.*, 2009, 38, 1284 - 1293.
- [18] T. Düren, Y. S. Bae, R. Q. Snurr, *Chem. Soc. Rev.*, 2009, 38, 1237 - 1247.
- [19] R. Matsuda, R. Kitaura, S. Kitagawa, Y. Kubota, R. V. Belosludov, T. C. Kobayashi, H. Sakanoto, T. Chiba, M. Takata, Y. Kawasoe, Y. Mita, *Nature*, 2005, 436, 238 - 241.
- [20] S. Ma, D. Sun, X.-S. Wang, H.-C. Zhou, *Angew. Chem. Int. Ed.* 2007, 46, 2458 - 2462.
- [21] L. Ma and W. Lin, *Top. Curr. Chem.*, 2010, 293, 175 - 205.
- [22] D. Farrusseng, S. Aguado, C. Pinel, *Angew. Chem., Int. Ed.*, 2009, 48, 7502 - 7513.

- [23] A. Hu, H. L. Ngo, W. Lin, *J. Am. Chem. Soc.*, 2003, 125, 11490 - 11491.
- [24] J. S. Seo, D. Whang, H. Lee, S. I. Jun, J. Oh, Y. J. Jeon, K. A. Kim, *Nature*, 2000, 404, 982 - 986.
- [25] S. Kitagawa, M. Kondo, *Bull. Chem. Soc. Jpn.*, 1998, 71, 1739 - 1753.
- [26] A. U. Czaja, N. Trukhan, U. Müller, *Chem. Soc. Rev.*, 2009, 38, 1284 - 1293.
- [27] D. J. Collins, S. Ma, H.-C. Zhou, "Hydrogen and Methane Storage in Metal-Organic Frameworks", in *Metal-Organic Frameworks: Design and Application*, ed. L. R. MacGillivaray, Wiley, Hoboken, New Jersey, 2010, pp. 249 - 266.
- [28] K. Konstas, T. Osl, Y. Yang, M. Battern, N. Burke, A. J. Hill, M. R. Hill, *J. Mater. Chem.*, 2012, 22, 16698 - 16708.
- [29] L. H. Wee, L. Alaerts, J. A. Martens, D. De Vos, "Metal-Organic Frameworks as Catalysts for Organic Reactions" in *Metal-Organic Frameworks: Application from Catalysis to Gas Storage*, ed. D. Farrusseng, Wiley-VCH, Weinheim, Germany, 2011, pp. 191 - 212.
- [30] P. Horcajada, C. Serre, A. C. McKinlay, R. E. Morris, "Biomedical Applications of Metal-Organic Frameworks, in *Metal-Organic Frameworks: Application from Catalysis to Gas Storage*, ed. D. Farrusseng, Wiley-VCH, Weinheim, Germany, 2011, pp. 215 - 246.
- [31] G. Férey, C. Serre, *Chem. Soc. Rev.*, 2009, 38, 1380 - 1399.
- [32] A. J. Fletcher, K. M. Thomas, M. J. Rosseinsky, *J. Solid state Chem.*, 2005, 178, 2491 - 2510.
- [33] S. Kitagawa, R. Kitaura, S. Noro, *Angew. Chem, Int. Ed.*, 2004, 43, 2334 - 2375.
- [34] M. Eddaoudi, D. B. Moler, H. L. Li, B. L. Chen, T. M. Reineke, M. O'Keeffe, O. M. Yaghi, *Acc. Chem. Res.*, 2001, 34, 319 - 330.
- [35] N. R. Champness, N. S. Oxtoby, *Encyclopaedia of Nanoscience and Nanotechnology*, 2004, 845.
- [36] M. W. Hosseini, *Acc. Chem. Res.*, 2005, 38, 313 - 323.
- [37] N.W. Ockwig, O. Delgado-Friedrichs, M. O'Keeffe, O. M. Yaghi, *Acc. Chem. Res.*, 2005, 38, 176 - 182.
- [38] R. J. Hill, D.-L. Long, N. R. Champness, P. Hubberstey, M. Schröder, *Acc. Chem. Res.*, 2005, 38, 335 - 348.
- [39] N. L. Rosi, J. Eckert, M. Eddaoudi, D. T. Vodak, J. Kim, M. O'Keeffe, O. M. Yaghi, *Science*, 2003, 300, 1127 - 1129.
- [40] X. B. Zhao, B. Xiao, A. J. Fletcher, K. M. Thomas, D. Bradshaw, M. J. Rosseinsky, *Science*, 2004, 306, 1012 - 1015.

- [41] R. Kitaura, S. Kitagawa, Y. Kubota, T. C. Kobayashi, K. Kindo, Y. Mita, A. Matsuo, M. Kobayashi, H. C. Chang, T. C. Ozawa, M. Suzuki, M. Sakata, M. Takata, *Science*, 2002, 298, 2358 - 2361.
- [42] D. Maspoch, D. Ruiz-Molina, K. Wurst, N. Domingo, M. Cavallini, F. Biscarini, J. Tejada, C. Rovira, J. Veciana, *Nat. Mater.*, 2003, 2, 190 - 195.
- [43] E. Coronado, J. R. Galan-Mascaros, C. J. Gomez-Garcia, V. Laukhin, *Nature*, 2000, 408, 447 - 449.
- [44] A. R. Millward, O. M. Yaghi, *J. Am. Chem. Soc.*, 2005, 127, 17998 - 17999.
- [45] P. Hubberstey, X. Lin, N. R. Champness, M. Schröder, "Highly Connected Metal-Organic Frameworks", in *Metal-Organic Frameworks: Design and Application*, ed. L. R. MacGillivray, Wiley, Hoboken, New Jersey, 2010, pp. 131 - 163.
- [46] M. Köberl, M. Cokoja, W. A. Herrmann, F. E. Kühn, *Dalton Trans.*, 2011, 40, 6834 - 6859.
- [47] S. S.-Y. Chui, S. M.-F. Lo, J. P. H. Charmant, A. G. Orpen, I. D. Williams, *Science*, 1999, 283, 1148 - 1150.
- [48] B. Chen, M. Eddaoudi, T. M. Reineke, J. W. Kampf, M. O'Keeffe, O. M. Yaghi, *J. Am. Chem. Soc.*, 2000, 122, 11559 - 11560.
- [49] D. N. Dybtsev, H. Chun, K. Kim, *Angew. Chem., Int. Ed.*, 2004, 43, 5033 - 5036.
- [50] B.-Q. Ma, K. L. Mulfort, J. T. Hupp, *Inorg. Chem.*, 2005, 44, 4912 - 4914.
- [51] M. Kramer, U. Schwarz, S. Kaskel, *J. Mater. Chem.*, 2006, 16, 2245 - 2248.
- [52] M. Köberl, M. Cokoja, W. A. Herrmann, F. E. Kühn, *Dalton Trans.*, 2011, 40, 6834 - 6859.
- [53] N. Stock, S. Biswas, *Chem. Rev.*, 2012, 112, 933 - 969.
- [54] X.-M. Cai, D. Höhne, M. Köberl, M. Cokoja, A. Pöthig, E. Herdtweck, S. Haslinger, W. A. Herrmann, F. E. Kühn, *Organometallics*, 2013, 32, 6004 - 6011.
- [55] D. Höhne, E. Herdtweck, A. Pöthig, F. E. Kühn, *Dalton Trans.*, 2014, 43, 15367 - 15374.
- [56] D. Höhne, E. Herdtweck, A. Pöthig, F. E. Kühn, *Inorg. Chim. Acta*, 2015, 424, 210 - 215.
- [57] F. A. Cotton, C. A. Murillo, R. A. Walton, *Multiple Bonds Between Metal Atoms*, 3rd ed., Springer Science and Business Media, Inc., New York, 2005.
- [58] E. Pligot, *C. R. Acad. Sci.*, 1844, 19, 609 - 611.
- [59] E. Pligot, *Ann. Chim. Phys.*, 1844, 12, 528.
- [60] W. Traube, E. Burmeister, R. Stahn, *Z. Anorg. Allg. Chem.*, 1925, 147, 50 - 67.
- [61] W. R. King Jr, C. S. Garner, *J. Chem. Phys.*, 1950, 18, 689 - 691.

- [62] J. N. Van Niekerk, F. R. L. Schoening, J. F. De Wet, *Acta Crystallogr.*, 1953, 6, 501 - 504.
- [63] B. N. Figgis, R. L. Martin, *J. Chem. Soc.*, 1956, 3837 - 3846.
- [64] S. Herzog, W. Kalies, *Z. Chem.*, 1964, 4, 183 - 184.
- [65] S. Herzog, W. Kalies, *Z. Anorg. Allg. Chem.*, 1964, 329, 83 - 91.
- [66] S. Herzog, W. Kalies, *Z. Chem.*, 1965, 5, 273 - 274.
- [67] S. Herzog, W. Kalies, *Z. Chem.*, 1966, 6, 344 - 345.
- [68] S. Herzog, W. Kalies, *Z. Anorg. Allg. Chem.*, 1967, 351, 237 - 250.
- [69] S. Herzog, W. Kalies, *Z. Chem.*, 1968, 8, 81 - 92.
- [70] F. A. Cotton, B. G. DeBoer, M. D. LaPrade, J. R. Pipal, D. A. Ucko, *J. Am. Chem. Soc.*, 1970, 92, 2926 - 2927.
- [71] F. A. Cotton, B. G. DeBoer, M. D. LaPrade, J. R. Pipal, D. A. Ucko, *Acta Crystallogr.*, 1971, 27, 1664 - 1671.
- [72] F. A. Cotton, E. A. Hillard, C. A. Murillo, H.-C. Zhou, *J. Am. Chem. Soc.*, 2000, 122, 416 - 417.
- [73] O. Levy, B. Bogoslavsky, A. Bino, *Inorg. Chim. Acta*, 2012, 391, 179 - 181.
- [74] F. A. Cotton, M. W. Extine, G. W. Rice, *Inorg. Chem.*, 1978, 17, 176 - 186.
- [75] L. Benne, J. Kalousova, and J. Votinsky, *J. Organomet. Chem.*, 1985, 290, 147 - 151.
- [76] F. A. Cotton, J. L. Thompson, *Inorg. Chem.*, 1981, 20, 1292 - 1296.
- [77] F. A. Cotton, X. Feng, P. A. Kibala, M. Matusz, *J. Am. Chem. Soc.*, 1988, 110, 2807 - 2815.
- [78] P. D. Ford, L. F. Larkworthy, D. C. Povey, A. J. Roberts, *Polyhedron*, 1983, 2, 1317 - 1322.
- [79] C. J. Bilgrien, R. S. Drago, C. J. O'Connor, N. Wong, *Inorg. Chem.*, 1988, 27, 1410 - 1417.
- [80] F. A. Cotton, H. Chen, L. M. Daniels, X. Feng, *J. Am. Chem. Soc.*, 1992, 114, 8980 - 8983.
- [81] C. Serre, F. Millange, S. Surblé, G. Férey, *Angew. Chem. Int. Ed.*, 2004, 43, 6285 - 6289.
- [82] G.-Q. Jiang, J.-H. Li, M. Wang, Y.-J. Shi, *Acta Cryst.*, 2011, E67, m1483.
- [83] A. Earnshaw, B. N. Figgis, J. Lewis, *J. Chem. Soc. A*, 1966, 1656 - 1663.
- [84] A. K. Dutta, S. K. Maji, S. Dutta, *J. Mol. Struct.*, 2012, 1027, 87 - 91.
- [85] R. D. Cannon, R. P. White, *Chemical and Physical Properties of Trinuclear Bridged Metal Complexes*, Vol. 36, London, 1987.

- [86] B. J. Hataway, *Comprehensive Coordination Chemistry*, ed. G. Wilkinson, Pergamon, Oxford, 1987, Vol. 2, pp. 439 - 441.
- [87] S. Surblé, F. Millange, C. Serre, G. Férey, R. I. Walton, *Chem. Commun.*, 2006, 1518 - 1520.
- [88] G. Férey, *Chem. Soc. Rev.*, 2008, 37, 191 - 214.
- [89] G. Férey, C. Serre, C. Mellot-Draznieks, F. Millange, S. Surblé, J. Dutour, I. Margiolaki, *Angew. Chem. Int. Ed.*, 2004, 43, 6296 - 6301.
- [90] G. Férey, C. Mellot-Draznieks, C. Serre, F. Millange, J. Dutour, S. Surblé, I. Margiolaki, *Science*, 2005, 309, 2040 - 2042.
- [91] A. Vimont, J. M. Goupil, J. C. Lavalley, M. Daturi, S. Surblé, C. Serre, F. Millange, G. Férey, N. Audebrand, *J. Am. Chem. Soc.*, 2006, 128, 3218 - 3227.
- [92] Y. K. Hwang, D. Y. Hong, J. S. Chang, S. H. Jung, Y. K. Seo, J. Kim, A. Vimont, M. Daturi, C. Serre, G. Férey, *Angew. Chem. Int. Ed.*, 2008, 47, 4144 - 4148.
- [93] M. Banerjee, S. Das, M. Yoon, H. J. Choi, M. H. Hyun, S. M. Park, G. Seo, K. Kim, *J. Am. Chem. Soc.*, 2009, 131, 7524 - 7525.
- [94] D. Farrusseng, J. Canivet, A. Quadrelli, "Design of Functional Metal-Organic Frameworks by Post-Synthetic Modification", in *Metal-Organic Frameworks: Application from Catalysis to Gas Storage*, ed. D. Farrusseng, Wiley-VCH, Weinheim, Germany, 2011, pp. 23 - 48.
- [95] W. Henke, *Liebigs Ann. Chem.*, 1858, 106, 280 - 287.
- [96] F. A. Cotton, F. E. Kühn, *Inorg. Chim. Acta*, 1996, 252, 257 - 264.
- [97] F. A. Cotton, L. M. Daniels, S. C. Haefner, F. E. Kühn, *Inorg. Chim. Acta*, 1999, 287, 159 - 166.
- [98] R. T. Henriques, E. Herdtweck, F. E. Kühn, A. D. Lopes, J. Mink, C. C. Romão, *J. Chem. Soc., Dalton Trans.*, 1998, 1293 - 1298.
- [99] B. N. Storhoff, H. C. Lewis, *J. Coord. Chem. Rev.*, 1977, 23, 1 - 23.
- [100] H. Zhao, R. A. Heintz, K. R. Dunbar, R. D. Rogers, *J. Am. Chem. Soc.*, 1996, 118, 12844 - 12845.
- [101] G. M. Finniss, E. Canadell, C. Campana, K. R. Dunbar, *Angew. Chem. Int. Ed. Engl.*, 1996, 35, 2771 - 2774.
- [102] A. Sen, *Acc. Chem. Res.*, 1988, 21, 421 - 428.
- [103] J. M. Mayer, E. H. Abbott, *Inorg. Chem.*, 1983, 22, 2774 - 2776.
- [104] I. Krossing, I. Raabe, *Angew. Chem. Int. Ed.*, 2004, 43, 2066 - 2090.
- [105] A. Macchioni, *Chem. Rev.*, 2005, 105, 2039 - 2073.

- [106] S. H. Strauss, *Chem. Rev.*, 1993, 93, 927 - 942.
- [107] R. S. Drago, D.W. Meek, M. D. Joesten, L. LaRoche, *Inorg. Chem.*, 1963, 2, 124 - 127.
- [108] D. W. Meek, R. S. Drago, T. S. Piper, *Inorg. Chem.*, 1962, 1, 285 - 289.
- [109] B. J. Hathaway, A. E. Underhill, *J. Chem. Soc.*, 1960, 3705 - 3711.
- [110] B. J. Hathaway, D. G. Holah, J. D. Postlethwaite, *J. Chem. Soc.*, 1961, 3215 - 3218.
- [111] B. J. Hathaway, A. E. Underhill, *J. Chem. Soc.*, 1961, 3091 - 3096.
- [112] B. J. Hathaway, D. G. Holah, A. E. Underhill, *J. Chem. Soc.*, 1962, 2444 - 2448.
- [113] P. Hemmerich, C. Sigwart, *Cell. Mol. Life Sci.*, 1963, 19, 488 - 489.
- [114] A. Sen, T. W. Lai, *J. Am. Chem. Soc.*, 1981, 103, 4627 - 4629.
- [115] A. Sen, T. W. Lai, *Inorg. Chem.*, 1984, 23, 3257 - 3258.
- [116] F. E. Kühn, J. R. Ismeier, D. Schön, W.-M. Xue, G. Zhang, O. Nuyken, *Macromol. Rapid Commun.*, 1999, 20, 555 - 559.
- [117] M. Vierle, Y. Zhang, E. Herdtweck, M. Bohnenpoll, O. Nuyken, F. E. Kühn, *Angew. Chem., Int. Ed.*, 2003, 42, 1307 - 1310.
- [118] S. F. Rach, F. E. Kühn, *Chem. Rev.* 2009, 109, 2061 - 2080.
- [119] B. Bräunlein, F. H. Köhler, W. Strauß, H. Zeh, *Z. Naturforsch.*, 1995, 50b, 1739 - 1747.
- [120] B. V. Ahsen, B. Bley, S. Proemmel, R. Wartchow, H. Willner, F. Aubke, *Z. Anorg. Allg. Chem.*, 1998, 624, 1225 - 1234.
- [121] E. C. Constable, "Homoleptic complexes of 2,2' bipyridine", in *Advances in Inorganic Chemistry*, ed. A. G. Sykes, Academic Press, San Diego, California, 1989, Vol. 34, pp. 1 - 64.
- [122] J. Breu, A. Zwicknagel, *Z. Naturforsch.*, 2004, 59b, 1015 - 1025.
- [123] L. E. Helberg, S. D. Orth, M. Sabat, W. D. Harman, *Inorg. Chem.*, 1996, 35, 5584 - 5594.
- [124] J. Ferguson, F. Herren, E. R. Krausz, M. Maeder, J. Vrbancich, *Coord. Chem. Rev.*, 1985, 64, 21 - 39.
- [125] B. J. Coe, D. W. Thompson, C. T. Culbertson, J. R. Schoonover, T. J. Meyer, *Inorg. Chem.*, 1995, 34, 3385 - 3395.
- [126] R. R. Ruminski, D. Serveiss, M. Jacquez, *Inorg. Chem.*, 1995, 34, 3358 - 3362.
- [127] R. E. Holmlin, J. K. Barton, *Inorg. Chem.*, 1995, 34, 7 - 8.
- [128] G. F. Strouse, J. R. Schoonover, R. Duesing, T. J. Meyer, *Inorg. Chem.*, 1995, 34, 2725 - 2734.
- [129] D. A. Bardwell, F. Barigelletti, R. L. Cleary, L. Flamigni, M. Guardigli, J. C. Jeffery, M. D. Ward, *Inorg. Chem.*, 1995, 34, 2438 - 2446.

- [130] P. Christensen, A. Hamnett, A.V. G. Muir, J. A. Timney, *J. Chem. Soc., Dalton Trans.*, 1992, 9, 1455 - 1463.
- [131] T. Yoshida, K. Tsutsumida, S. Teratain, K. Yasufuku, M. Kaneko, *J. Chem. Soc., Chem. Commun.*, 1993, 7, 631 - 633.
- [132] N. B. Thornton, K. S. Schanze, *Inorg. Chem.*, 1993, 32, 4994 - 4995.
- [133] K. S. Schanze, D. B. MacQueen, T. A. Perkins, L. A. Cabana, *Coord. Chem. Rev.*, 1993, 122, 63 - 89.
- [134] J. F. Endicott, *J. Chem. Educ.*, 1983, 60, 824 - 829.
- [135] S. Sowmiah, V. Srinivasadesikan, M.-C. Tseng, Y.-H. Chu, *Molecules*, 2009, 14, 3780 - 3813.
- [136] J. Lu, F. Yan, J. Texter, *Prog. Polym. Sci.*, 2009, 34, 431 - 448.
- [137] M. C. Buzzeo, R. G. Evans, R. G. Compton, *ChemPhysChem.*, 2004, 5, 1106 - 1120.
- [138] T. Welton, *Chem. Rev.*, 1999, 99, 2071 - 2083.
- [139] A.-O. Diallo, A. B. Morgan, C. Len, G. Marlair, *Energy Environ. Sci.*, 2013, 6, 699 - 710.
- [140] H. Ohno, "Importance and possibility of ionic liquids" in *Electrochemical Aspects of Ionic Liquids*, John Wiley & Sons, Inc., Hoboken, NJ, USA, 2005, pp.1 - 4.
- [141] P. Wasserscheid, W. Keim, *Angew. Chem. Int. Ed. Engl.*, 2000, 39, 3772 - 3789.
- [142] K. C. Lethesh, K. Van Hecke, L. Van Meervelt, P. Nockemann, B. Kirchner, S. Zahn, T. N. Parac-Vogt, W. Dehaen, K. Binnemans, *J. Phys. Chem. B*, 2011, 115, 8424 - 8438.
- [143] Z. C. Zhang, *Adv. Catal.*, 2006, 49, 153 - 237.
- [144] J. F. Wishart, *Energy Environ. Sci.*, 2009, 2, 956 - 961.
- [145] M. Galiński, A. Lewandowski, I. Stępnik, *Electrochim. Acta*, 2006, 51, 5567 - 5580.
- [146] M. Armand, F. Endres, D. R. MacFarlane, H. Ohno, B. Scrosati, *Nat. Mater.*, 2009, 8, 621 - 629.
- [147] A. Lewandowski, A. Świdorska-Mocek, *J. Power Sources*, 2009, 194, 601 - 609.
- [148] H. Sakaebe, H. Matsumoto, K. Tatsumi, *Electrochim. Acta*, 2007, 53, 1048 - 1054.
- [149] F. Endres, *Phys. Chem. Chem. Phys.*, 2012, 14, 5008 - 5009.
- [150] S. Passerini, W. A. Henderson, in *Encyclopedia of Electrochemical Power Sources*, ed. J. Garche, Elsevier B.V., 2009, vol. 5, pp. 85 - 91.

- [151] N. Bucher, S. Hartung, M. Arkhipova, D. Yu, P. Kratzer, G. Maas, M. Srinivasanac, H. E. Hoster, *RSC Adv.*, 2014, 4, 1996 - 2003.
- [152] D. R. MacFarlane, N. Tachikawa, M. Forsyth, J. M. Pringle, P. C. Howlett, G. D. Elliott, J. H. Davis, Jr., M. Watanabe, P. Simon, C. A. Angell, *Energy Environ. Sci.*, 2014, 7, 232 - 250.
- [153] D. C. Grills, Y. Matsubara, Y. Kuwahara, S.R. Golisz, D.A. Kurtz, B.A. Mello, *J. Phys. Chem. Lett.*, 2014, 5, 2033 - 2038.
- [154] L. Sun, G. K. Ramesha, P. V. Kamat, J. F. Brennecke, *Langmuir*, 2014, 30, 6302 - 6308.
- [155] J. Ranke, S. Stolte, R. Störmann, J. Arning, B. Jastorff, *Chem. Rev.*, 2007, 107, 2183 - 2206.
- [156] S. Stolte, J. Arning, U. Bottin-Weber, M. Matzke, F. Stock, K. Thiele, M. Uerdingen, U. Welz-Biermann, B. Jastorff, J. Ranke, *Green Chem.*, 2006, 8, 621 - 629.
- [157] R. P. Swatloski, J. D. Holbrey, R. D. Rogers, *Green Chem.*, 2003, 5, 361 - 363.
- [158] C. Friedel, J. M. Crafts, *Compt. Rend.* 1877, 84, 1392 & 1450.
- [159] M. Freemantle, *An Introduction to Ionic Liquids*, RSC, Cambridge, UK, 2010, pp. 12 - 18.
- [160] P. Walden, *Bull. Acad. Imper. Sci. St. Petersb.*, 1914, 8, 405 - 422.
- [161] F.H. Hurley, U. S. Patent No. 2 446 331, 1948.
- [162] T. P. Wier, F. H. Harley, 1948, U. S. Patent No. 2 446 349, 1948.
- [163] T. P. Wier, U. S. Patent. No. 2 446 350, 1948.
- [164] F. H. Hurley, T. P. Wier, *J. Electrochem. Soc.*, 1951, 98, 207 - 212.
- [165] R. J. Gale, B. Gilbert, R. A. Osteryoung, *Inorg. Chem.*, 1978, 17, 2728 - 2729.
- [166] J. C. Nardi, C. L. Hussey, L. A. King, U. S. Patent No. 4 122 245, 1978.
- [167] J. S. Wilkes, P. Wasserscheid, T. Welton, in *Ionic Liquids in Synthesis*, eds. P. Wasserscheid, T. Welton, Wiley-VCH, Weinheim, Germany, 2007, Vol. 1, pp 1 - 6.
- [168] J. S. Wilkes, J. A. Levisky, R. A. Wilson, C. L. Hussey, *Inorg. Chem.*, 1982, 21, 1263 - 1264.
- [169] T. Welton, *Chem. Rev.*, 1999, 99, 2071 - 2083.
- [170] J. W. Parshal, *J. Am. Chem. Soc.*, 1972, 94, 8716 - 8719.
- [171] *Ionic Liquids in Synthesis*, eds. P. Wasserscheid, T. Welton, Wiley-VCH, Weinheim, Germany, 2007, Vol. 1.
- [172] D. J. Adams, P. J. Dyson, S. J. Tavener, "Ionic liquids" in *Chemistry in Alternative Reaction Media*, Wiley, England, 2004, pp. 75 - 93.

- [173] T. B. Scheffer, C. L. Hussey, K. R. Seddon, C. M. Kear, P. D. Armitage, *Inorg. Chem.*, 1983, 22, 2099 - 2100.
- [174] T. M. Laher, C. L. Hussey, *Inorg. Chem.*, 1983, 22, 3247 - 3251.
- [175] T. B. Scheffer, C. L. Hussey, *Inorg. Chem.*, 1984, 23, 1926 - 1932.
- [176] *Ionic Liquids in Chemical Analysis*, ed. M. Koel, CRC Press, U.S.A., 2008.
- [177] J. S. Wilkes, M. J. Zaworodtko, *J. Chem. Soc. Chem. Commun.*, 1992, 13, 965 - 967.
- [178] H. Prydderch, A. Heise, N. Gathergood, "Toxicity and Bio-Acceptability in the Context of Biological Processes" in *Ionic Liquid Media in Ionic Liquids in the Biorefinery Concept : Challenges and Perspectives*, ed. R. Bogel-Lukasik, RSC, England, 2016, 168 - 201.
- [179] P. Bonhte, A.-P. Dias, M. Armand, N. Papageorgiou, K. Kalyanasundaram, M. Grtzel, *Inorg. Chem.*, 1996, 35, 1168 - 1178.
- [180] R. Hagiwara, Y. Ito, *J. Fluorine Chem.*, 2000, 105, 221 - 227.
- [181] H. Ohno, M. Yoshizawa-Fujita, T. Mizumo, "Ionic conductivity" in *Electrochemical Aspects of Ionic Liquids*, ed. H. Ohno, John Wiley & Sons, Inc., Hoboken, NJ, USA, 2005, pp. 87 - 93.
- [182] M. Nádherná, J. Reiter, J. Moškon, R. Dominko, *J. Power Sources*, 2011, 196, 7700 - 7706.
- [183] B. Ravdel, K. M. Abraham, R. Gitzendanner, J. DiCarlo, B. Luch, C. Campion, *J. Power Sources*, 2003, 119-121, 805 - 1805.
- [184] H. Yang, G.V. Zhuang, P.N. Ross, *J. Power Sources*, 2006, 161, 573 - 579.
- [185] H. Sakaebe, H. Matsumoto, "Li Batteries" in *Electrochemical Aspects of Ionic Liquids*, ed. H. Ohno, John Wiley & Sons, Inc., Hoboken, NJ, USA, 2005, pp. 205 - 220.
- [186] M. Armand, F. Endres, D. R. MacFarlane, H. Ohno, B. Scrosati, *Nat. Mater.*, 2009, 8, 621 - 629.
- [187] M. Galinski, A. Lewandowski, I. Stepniak, *Electrochim. Acta*, 2006, 51, 5567 - 5580.
- [188] I. A. Profatilova, N. S. Choi, S. W. Roh, S. S. Kim, *J. Power Sources*, 2009, 192, 636 - 643.
- [189] J. D. Stenger-Smith, J. A. Irvin, *Mater. Matters*, 2009, 4, 103 - 105.
- [190] A. Farnicola, F. Croce, B. Scrosati, T. Watanabe, H. Ohno, *J. Power Sources*, 2007, 174, 342 - 348.
- [191] S. Seki, Y. Ohno, Y. Kobayashi, H. Miyashiro, A. Usami, Y. Mita, H. Tokuda, M. Watanabe, K. Hayamizu, S. Tsuzuki, M. Hattori, N. Terada, *J. Electrochem. Soc.*, 2007, 154, A173 - A177.

- [192] J. Jin, H. H. Li, J. P. Wei, X. K. Bian, Z. Zhou, J. Yan, *Electrochem. Commun.*, 2009, 11, 1500 - 1503.
- [193] V. Borgel, E. Markevich, D. Aurbach, G. Semrau, M. Schmidt, *J. Power Sources*, 2009, 189, 331 - 336.
- [194] M. Montanino, F. Alessandrini, S. Passerini, G. B. Appetecchi, *Electrochim. Acta*, 2013, 96, 124 - 133.
- [195] J. Sun, M. Forsyth, D. R. MacFarlane, *J. Phys. Chem. B*, 1998, 102, 8858 - 8864.
- [196] M. Egashira, S. Okada, J. Yamaki, D. A. Dri, F. Bonadies, B. Scrosati, *J. Power Sources*, 2004, 138, 240 - 244.
- [197] T. Waldmann, H.-H. Huang, H. E. Hoster, O. Höfft, F. Endres, R. J. Behm, *ChemPhysChem*, 2011, 12, 2565 - 2567.
- [198] S. Fang, Z. Zhang, Y. Jin, L. Yang, S. Hirano, K. Tachibana, S. Katayama, *J. Power Sources*, 2011, 196, 5637 - 5644.
- [199] A. P. Lewandowski, A. F. Hollenkamp, S. W. Donne, A. S. Best, *J. Power Sources*, 2010, 195, 2029 - 2035.
- [200] H. Kunkel, G. Maas, *Eur. J. Org. Chem.*, 2007, 3746 - 3757.
- [201] W. Kantlehner, E. Haug, W. W. Mergen, P. Speh, T. Maier, J. J. Kapassakalidis, H.-J. Braeuner, H. Hagen, *Liebigs Ann. Chem.*, 1984, 108 - 126.
- [202] S. Fang, L. Yang, C. Wei, C. Jiang, K. Tachibana, K. Kamijima, *Electrochim. Acta*, 2009, 54, 1752 - 1756.
- [203] S. Fang, L. Yang, J. Wang, H. Zhang, K. Tachibana, K. Kamijima, *J. Power Sources*, 2009, 191, 619 - 622.
- [204] X. Zhang, S. Fang, Z. Zhang, L. Yang, *Chin. Sci. Bull.*, 2011, 56, 2906 - 2910.
- [205] Y. Jin, S. Fang, L. Yang, S. Hirano, K. Tachibana, *J. Power Sources*, 2011, 196, 10658 - 10666.
- [206] M. Gnahn, C. Berger, M. Arkhipova, H. Kunkel, T. Pajkossy, G. Maas, D. M. Kolb, *Phys. Chem. Chem. Phys.*, 2012, 14, 10647 - 10652.
- [207] J. Reiter, M. Nádherná, R. Dominko, *J. Power Sources*, 2012, 205, 402 - 407.
- [208] M. Montanino, M. Carewska, F. Alessandrini, S. Passerini, G. B. Appetecchi, *Electrochim. Acta*, 2011, 57, 153 - 159.
- [209] H. Matsumoto, M. Yanagida, K. Tanimoto, M. Nomura, Y. Kitagawa and Y. Miyazaki, *Chem. Lett.*, 2000, 29, 922 - 923.
- [210] A. I. Bhatt, I. May, V. A. Volkovich, M. E. Hetherington, B. Lewin, R. C. Thied, N. Ertok, *J. Chem. Soc., Dalton Trans.*, 2002, 4532 - 4534.

- [211] P. C. Howlett, D. R. MacFarlane, A. F. Hollenkamp, *Electrochem. Solid-State Lett.*, 2004, 7, A97 - A101.
- [212] B. Garcia, S. Lavallo, G. Perron, C. Michot, M. Armand, *Electrochim. Acta*, 2004, 49, 4583 - 4588.
- [213] H. Matsumoto, H. Sakaebe, K. Tatsumi, M. Kikuta, E. Ishiko, M. Kono, *J. Power Sources*, 2006, 160, 1308 - 1313.
- [214] M. Ishikawa, T. Sugimoto, M. Kikuta, E. Ishiko, M. Kono, *J. Power Sources*, 2006, 162, 658 - 662.
- [215] M. Holzappel, C. Jost, P. Novak, *Chem. Commun.*, 2004, 2098 - 2099.
- [216] G. H. Lane, *Electrochim. Acta*, 2012, 83, 513 - 528.
- [217] H. Yoon, G. Lane, Y. Shekibi, P. Howlett, M. Forsyth, A. Best, D. MacFarlane, *Energy Environ. Sci.*, 2013, 6, 979 - 986.
- [218] A. Guerfi, M. Dontigny, P. Charest, M. Petitclerc, M. Lagac, A. Vijn, K. Zaghbi, *J. Power Sources*, 2010, 195, 845 - 852.
- [219] J. A. Choi, E.-G. Shim, B. Scrosati, D.-W. Kim, *Bull. Korean Chem. Soc.*, 2010, 31, 3190 - 3194.
- [220] L. Lombardo, S. Brutti, M. A. Navarra, S. Panero, P. Reale, *J. Power Sources*, 2013, 227, 8 - 14.
- [221] H. Matsumoto "Electrochemical Windows of Room-Temperature Ionic Liquids" in *Electrochemical Aspects of Ionic Liquids*, ed. H. Ohno, John Wiley & Sons, Inc., Hoboken, NJ, USA, 2005, pp. 43 - 63.
- [222] M. Hayyan, F. S. Mjalli, M. A. Hashim, I. M. AlNashef, T. X. Mei, *J. Ind. Eng. Chem.*, 2013, 19, 106 - 112.
- [223] S. Randström, G. B. Appetecchi, C. Lagergren, A. Moreno, S. Passerini, *Electrochim. Acta*, 2007, 53, 1837 - 1842.
- [224] D.S. Silvester, R. G. Compton, *Z. Phys. Chem.*, 2006, 220, 1247 - 1274.
- [225] A. Ispas, A. Bund, *Electrochem. Soc. Interface*, 2014, 23, 47 - 51.
- [226] L Grande, J. V. Zamory, S. Koch, J. Kalhoff, E. Paillard, S. Passerini, *ACS Appl. Mater. Interfaces*, 2015, 7, 5950 - 5958.
- [227] Y.-S. Liu, G.-B. Pan, "Ionic Liquids for the Future Electrochemical Applications", in *Ionic Liquids: Applications and Perspectives*, ed. A. Kokorin, InTech, Rijeka, Croatia, 2011, pp. 627 - 642.
- [228] X.-M. Cai, D. Höhne, M. Köberl, M. Cokoja, A. Pöthig, E. Herdtweck, S. Haslinger, W. A. Herrmann, F. E. Kühn, *Organometallics*, 2013, 32, 6004 - 6011.

- [229] C. C. Scarborough, S. Sproules, T. Weyhermüller, S. DeBeer, K. Wieghardt, *Inorg. Chem.*, 2011, 50, 12446 - 12462.
- [230] K. V. Goodwin, W. T. Pennington, J. D. Petersen, *Inorg. Chem.*, 1989, 28, 2016 - 2018.
- [231] A. Hauser, M. Mader, W. T. Robinson, R. Murugesan, J. Ferguson, *Inorg. Chem.*, 1987, 26, 1331 - 1338.
- [232] F. Hein, S. Herzog, *Z. Anorg. Allg. Chem.*, 1952, 267, 337 - 339.
- [233] S. Herzog, K. C. Renner, W. Schön, *Z. Naturforsch.*, 1957, 12b, 809 - 810.
- [234] H. Behrens, A. Müller, *Z. Anorg. Allg. Chem.*, 1965, 341, 124 - 136.
- [235] J. Quirk, G. Wilkinson, *Polyhedron*, 1982, 1, 209 - 211.
- [236] K. R. Ramya, P. Kumar, A. Venkatnathan, *J. Phys. Chem. B*, 2015, 119, 14800 - 14806.
- [237] Y. Katayama, "Electrodeposition of Metals in Ionic Liquids" in *Electrochemical Aspects of Ionic Liquids*, ed. H. Ohno, John Wiley & Sons, Inc., Hoboken, NJ, USA, 2005, pp. 129 - 156.
- [238] N. V. Ignat'ev, P. Barthen, A. Kucheryna, H. Willner, P. Sartori, *Molecules*, 2012, 17, 5319 - 5338.
- [239] P. J. Dyson, T.J. Geldbach, *Metal Catalysed Reactions in Ionic Liquids*, Springer, Dordrecht, The Netherlands, 2005.
- [240] J. D. Holbrey, *Chem. Today*, 2004, 35 - 37.
- [241] R. Hagiwara, *Electrochemistry*, 2002, 70, 130 - 136.
- [242] K. R. Seddon, *J. Chem. Technol. Biotechnol.*, 1997, 68, 351 - 356.
- [243] L. Cammarata, S. G. Kazarian, P. A. Salter, T. Welton, *Phys. Chem. Chem. Phys.*, 2001, 3, 5192 - 5200.
- [244] B. R. Clare, P. M. Bayley, A. S. Best, M. Forsyth, D. R. MacFarlane, *Chem. Commun.*, 2008, 23, 2689 - 2691.
- [245] P. Nockemann, K. Binnemans, K. Driesen, *Chem. Phys. Lett.*, 2005, 415, 131 - 136.
- [246] O. G. Palanna, *Engineering Chemistry.*, Tata McGraw-Hill Education, New Delhi, 2009.

7. Appendix

This section contains crystallographic details of compound $[\text{Cr}(\text{mbipy})_3][\text{BF}_4]_3$ (3b)



Crystal Structure Report for AbbSa9_AP7313123

A clear yellow fragment-like specimen of $\text{C}_{36}\text{H}_{36}\text{B}_3\text{Cl}_0\text{CrF}_{12}\text{N}_6$, approximate dimensions 0.349 mm x 0.362 mm x 0.627 mm, was used for the X-ray crystallographic analysis. The X-ray intensity data were measured on a Bruker Kappa APEX II CCD system equipped with a graphite monochromator and a Mo fine-focus tube ($\lambda = 0.71073 \text{ \AA}$).

Table 1: Data collection details for AbbSa9_AP7313123.

Axis	dx/mm	2 θ /°	ω /°	φ /°	χ /°	Width/°	Frames	Time/s	Wavelength/Å	Voltage/kV	Current/μA
Phi	35.038	10.00	26.37	346.14	-31.870.50	0.50	739	20.00	0.71073	49	31.0
Omega	35.038	20.00	331.25	148.96	55.94	0.50	99	20.00	0.71073	49	31.0
Omega	35.038	-20.00	338.54	10.48	-95.310.50	0.50	64	20.00	0.71073	49	31.0
Omega	35.038	-15.00	343.39	95.19	-68.460.50	0.50	77	20.00	0.71073	49	31.0
Omega	35.038	12.50	9.47	90.27	-33.720.50	0.50	91	20.00	0.71073	49	31.0
Omega	35.038	20.00	320.01	325.67	97.53	0.50	121	20.00	0.71073	49	31.0
Omega	35.038	20.00	308.43	183.21	99.26	0.50	141	20.00	0.71073	49	31.0
Phi	35.038	-10.00	330.92	74.68	85.85	0.50	655	20.00	0.71073	49	31.0
Phi	35.038	-7.50	1.04	285.71	-97.850.50	0.50	739	20.00	0.71073	49	31.0
Phi	35.038	7.50	322.16	64.22	94.04	0.50	739	20.00	0.71073	49	31.0

A total of 3465 frames were collected. The total exposure time was 19.25 hours. The frames were integrated with the Bruker SAINT software package using a narrow-frame algorithm. The integration of the data using a triclinic unit cell yielded a total of 49500 reflections to a maximum θ angle of 25.35° (0.83 Å resolution), of which 8240 were independent (average redundancy 6.007, completeness = 99.7%, $R_{\text{int}} = 4.66\%$, $R_{\text{sig}} = 3.83\%$) and 6626 (80.41%) were greater than $2\sigma(F^2)$. The final cell constants of $a = 12.6950(5) \text{ \AA}$, $b = 13.0714(5) \text{ \AA}$, $c = 15.5782(6) \text{ \AA}$, $\alpha = 90.743(2)^\circ$, $\beta = 96.718(2)^\circ$, $\gamma = 117.9850(10)^\circ$, volume = $2260.33(15) \text{ \AA}^3$, are based upon the refinement of the XYZ-centroids of 9845 reflections above $20\sigma(I)$ with $4.680^\circ < 2\theta < 52.80^\circ$. Data were corrected for absorption effects using the multi-scan method (SADABS). The ratio of minimum to maximum apparent transmission was 0.807. The calculated minimum and maximum transmission coefficients (based on crystal size) are 0.8180 and 0.8920.

The structure was solved and refined using the Bruker SHELXTL Software Package in conjunction with SHELXLE, using the space group P -1, with Z = 2 for the formula unit, $\text{C}_{36}\text{H}_{36}\text{B}_3\text{Cl}_0\text{CrF}_{12}\text{N}_6$. The final anisotropic full-matrix least-squares refinement on F^2 with 567 variables converged at $R1 = 3.65\%$, for the observed data and $wR2 = 9.66\%$ for all data. The goodness-of-fit was 1.055. The largest peak in the final difference electron density synthesis was $0.337 \text{ e}^-/\text{\AA}^3$ and the largest hole was $-0.437 \text{ e}^-/\text{\AA}^3$ with an RMS deviation of $0.055 \text{ e}^-/\text{\AA}^3$. On the basis of the final model, the calculated density was 1.271 g/cm^3 and $F(000)$, 882 e^- .

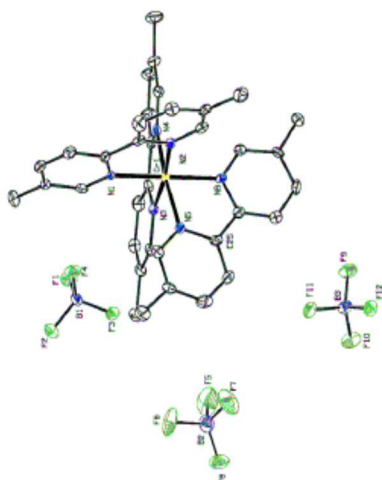


Table 2. Sample and crystal data for AbbSa9_AP7313123.

Identification code	AbbSa9_AP7313123	
Chemical formula	C ₃₆ H ₃₆ B ₃ Cl ₀ CrF ₁₂ N ₆	
Formula weight	865.14	
Temperature	123(2) K	
Wavelength	0.71073 Å	
Crystal size	0.349 x 0.362 x 0.627 mm	
Crystal habit	clear yellow fragment	
Crystal system	triclinic	
Space group	P -1	
Unit cell dimensions	a = 12.6950(5) Å	α = 90.743(2)°
	b = 13.0714(5) Å	β = 96.718(2)°
	c = 15.5782(6) Å	γ = 117.9850(10)°
Volume	2260.33(15) Å ³	
Z	2	
Density (calculated)	1.271 g/cm ³	
Absorption coefficient	0.334 mm ⁻¹	
F(000)	882	

Table 3. Data collection and structure refinement for AbbSa9_AP7313123.

Diffractometer	Bruker Kappa APEX II CCD
Radiation source	fine-focus tube, Mo
Theta range for data collection	1.32 to 25.35°
Index ranges	-15 ≤ h ≤ 15, -15 ≤ k ≤ 15, -18 ≤ l ≤ 18
Reflections collected	49500

Independent reflections	8240 [R(int) = 0.0466]
Coverage of independent reflections	99.7%
Absorption correction	multi-scan
Max. and min. transmission	0.8920 and 0.8180
Structure solution technique	direct methods
Structure solution program	SHELXS-97 (Sheldrick, 2008)
Refinement method	Full-matrix least-squares on F ²
Refinement program	SHELXL-97 (Sheldrick, 2008) and SHELXLE (Huebschle, 2011)
Function minimized	$\Sigma w(F_o^2 - F_c^2)^2$
Data / restraints / parameters	8240 / 42 / 567
Goodness-of-fit on F²	1.055
Δ/σ_{\max}	0.002
Final R indices	6626 data; I > 2 σ (I) R1 = 0.0365, wR2 = 0.0897 all data R1 = 0.0507, wR2 = 0.0966
Weighting scheme	w = 1/[$\sigma^2(F_o^2) + (0.0432P)^2 + 1.2567P$] where P = (F _o ² + 2F _c ²)/3
Largest diff. peak and hole	0.337 and -0.437 eÅ ⁻³
R.M.S. deviation from mean	0.055 eÅ ⁻³

Table 4. Bond lengths (Å) for AbbSa9_AP7313123.

Cr1-N4	2.0465(16)	Cr1-N1	2.0482(16)
Cr1-N2	2.0505(17)	Cr1-N6	2.0519(16)
Cr1-N5	2.0524(16)	Cr1-N3	2.0572(16)
N1-C5	1.343(3)	N1-C1	1.361(3)
N2-C11	1.342(3)	N2-C7	1.363(3)
N3-C17	1.345(2)	N3-C13	1.359(2)
N4-C23	1.346(3)	N4-C19	1.354(3)
N5-C29	1.343(2)	N5-C25	1.362(3)
N6-C35	1.343(2)	N6-C31	1.359(3)
C1-C2	1.383(3)	C1-C7	1.470(3)
C2-C3	1.380(3)	C2-H2	0.95
C3-C4	1.384(3)	C3-H3	0.95
C4-C5	1.389(3)	C4-C6	1.499(3)
C5-H5	0.95	C6-H6A	0.98
C6-H6B	0.98	C6-H6C	0.98
C7-C8	1.378(3)	C8-C9	1.384(3)
C8-H8	0.95	C9-C10	1.385(3)
C9-H9	0.95	C10-C11	1.391(3)
C10-C12	1.502(3)	C11-H11	0.95
C12-H12A	0.98	C12-H12B	0.98
C12-H12C	0.98	C13-C14	1.383(3)
C13-C19	1.473(3)	C14-C15	1.386(3)
C14-H14	0.95	C15-C16	1.387(3)
C15-H15	0.95	C16-C17	1.385(3)
C16-C18	1.505(3)	C17-H17	0.95
C18-H18A	0.98	C18-H18B	0.98
C18-H18C	0.98	C19-C20	1.380(3)
C20-C21	1.382(3)	C20-H20	0.95
C21-C22	1.380(3)	C21-H21	0.95
C22-C23	1.386(3)	C22-C24	1.504(3)
C23-H23	0.95	C24-H24A	0.98

C24-H24B	0.98	C24-H24C	0.98
C25-C26	1.382(3)	C25-C31	1.467(3)
C26-C27	1.386(3)	C26-H26	0.95
C27-C28	1.387(3)	C27-H27	0.95
C28-C29	1.385(3)	C28-C30	1.499(3)
C29-H29	0.95	C30-H30A	0.98
C30-H30B	0.98	C30-H30C	0.98
C31-C32	1.385(3)	C32-C33	1.381(3)
C32-H32	0.95	C33-C34	1.388(3)
C33-H33	0.95	C34-C35	1.386(3)
C34-C36	1.498(3)	C35-H35	0.95
C36-H36A	0.98	C36-H36B	0.98
C36-H36C	0.98	F1-B1	1.398(3)
F2-B1	1.394(3)	F3-B1	1.389(3)
F4-B1	1.396(3)	F9-B3	1.402(3)
F10-B3	1.389(3)	F11-B3	1.392(3)
F12-B3	1.385(3)	B2-F7A	1.245(14)
B2-F8	1.313(9)	B2-F6A	1.361(17)
B2-F5	1.381(4)	B2-F7	1.398(7)
B2-F6	1.405(10)	B2-F5A	1.438(9)
B2-F8A	1.503(16)		

Table 5. Bond angles (°) for AbbSa9_AP7313123.

N4-Cr1-N1	91.72(6)	N4-Cr1-N2	98.20(6)
N1-Cr1-N2	79.92(6)	N4-Cr1-N6	92.09(6)
N1-Cr1-N6	173.79(6)	N2-Cr1-N6	94.69(6)
N4-Cr1-N5	168.55(6)	N1-Cr1-N5	97.28(6)
N2-Cr1-N5	90.36(6)	N6-Cr1-N5	79.58(6)
N4-Cr1-N3	79.89(6)	N1-Cr1-N3	94.05(6)
N2-Cr1-N3	173.64(7)	N6-Cr1-N3	91.45(6)
N5-Cr1-N3	92.39(6)	C5-N1-C1	118.86(17)
C5-N1-Cr1	126.41(14)	C1-N1-Cr1	114.62(13)
C11-N2-C7	118.87(17)	C11-N2-Cr1	126.41(14)
C7-N2-Cr1	114.31(13)	C17-N3-C13	118.71(17)
C17-N3-Cr1	126.76(13)	C13-N3-Cr1	114.49(13)
C23-N4-C19	118.93(17)	C23-N4-Cr1	126.26(14)
C19-N4-Cr1	114.74(13)	C29-N5-C25	118.91(17)
C29-N5-Cr1	126.38(14)	C25-N5-Cr1	114.51(13)
C35-N6-C31	118.92(17)	C35-N6-Cr1	126.30(14)
C31-N6-Cr1	114.79(13)	N1-C1-C2	120.87(19)
N1-C1-C7	115.28(17)	C2-C1-C7	123.82(19)
C3-C2-C1	119.4(2)	C3-C2-H2	120.3
C1-C2-H2	120.3	C2-C3-C4	120.4(2)
C2-C3-H3	119.8	C4-C3-H3	119.8
C3-C4-C5	117.2(2)	C3-C4-C6	122.9(2)
C5-C4-C6	119.9(2)	N1-C5-C4	123.2(2)
N1-C5-H5	118.4	C4-C5-H5	118.4
C4-C6-H6A	109.5	C4-C6-H6B	109.5
H6A-C6-H6B	109.5	C4-C6-H6C	109.5
H6A-C6-H6C	109.5	H6B-C6-H6C	109.5
N2-C7-C8	120.80(19)	N2-C7-C1	115.06(17)
C8-C7-C1	124.13(18)	C7-C8-C9	119.5(2)
C7-C8-H8	120.2	C9-C8-H8	120.2
C8-C9-C10	120.5(2)	C8-C9-H9	119.7
C10-C9-H9	119.7	C9-C10-C11	116.85(19)
C9-C10-C12	122.58(19)	C11-C10-C12	120.55(19)

N2-C11-C10	123.42(19)	N2-C11-H11	118.3
C10-C11-H11	118.3	C10-C12-H12A	109.5
C10-C12-H12B	109.5	H12A-C12-H12B	109.5
C10-C12-H12C	109.5	H12A-C12-H12C	109.5
H12B-C12-H12C	109.5	N3-C13-C14	120.87(18)
N3-C13-C19	115.13(17)	C14-C13-C19	123.94(18)
C13-C14-C15	119.58(19)	C13-C14-H14	120.2
C15-C14-H14	120.2	C14-C15-C16	120.10(19)
C14-C15-H15	119.9	C16-C15-H15	119.9
C17-C16-C15	117.18(19)	C17-C16-C18	120.60(19)
C15-C16-C18	122.22(19)	N3-C17-C16	123.54(19)
N3-C17-H17	118.2	C16-C17-H17	118.2
C16-C18-H18A	109.5	C16-C18-H18B	109.5
H18A-C18-H18B	109.5	C16-C18-H18C	109.5
H18A-C18-H18C	109.5	H18B-C18-H18C	109.5
N4-C19-C20	121.12(19)	N4-C19-C13	115.49(17)
C20-C19-C13	123.39(19)	C19-C20-C21	118.9(2)
C19-C20-H20	120.5	C21-C20-H20	120.5
C22-C21-C20	120.9(2)	C22-C21-H21	119.6
C20-C21-H21	119.6	C21-C22-C23	116.96(19)
C21-C22-C24	122.3(2)	C23-C22-C24	120.7(2)
N4-C23-C22	123.12(19)	N4-C23-H23	118.4
C22-C23-H23	118.4	C22-C24-H24A	109.5
C22-C24-H24B	109.5	H24A-C24-H24B	109.5
C22-C24-H24C	109.5	H24A-C24-H24C	109.5
H24B-C24-H24C	109.5	N5-C25-C26	120.78(18)
N5-C25-C31	115.19(17)	C26-C25-C31	124.03(19)
C25-C26-C27	119.4(2)	C25-C26-H26	120.3
C27-C26-H26	120.3	C26-C27-C28	120.3(2)
C26-C27-H27	119.8	C28-C27-H27	119.8
C29-C28-C27	117.15(19)	C29-C28-C30	121.1(2)
C27-C28-C30	121.80(19)	N5-C29-C28	123.37(19)
N5-C29-H29	118.3	C28-C29-H29	118.3
C28-C30-H30A	109.5	C28-C30-H30B	109.5
H30A-C30-H30B	109.5	C28-C30-H30C	109.5
H30A-C30-H30C	109.5	H30B-C30-H30C	109.5
N6-C31-C32	120.48(18)	N6-C31-C25	115.21(18)
C32-C31-C25	124.27(19)	C33-C32-C31	119.8(2)
C33-C32-H32	120.1	C31-C32-H32	120.1
C32-C33-C34	120.2(2)	C32-C33-H33	119.9
C34-C33-H33	119.9	C35-C34-C33	116.92(19)
C35-C34-C36	120.01(19)	C33-C34-C36	123.06(19)
N6-C35-C34	123.64(19)	N6-C35-H35	118.2
C34-C35-H35	118.2	C34-C36-H36A	109.5
C34-C36-H36B	109.5	H36A-C36-H36B	109.5
C34-C36-H36C	109.5	H36A-C36-H36C	109.5
H36B-C36-H36C	109.5	F3-B1-F2	110.04(18)
F3-B1-F4	109.29(19)	F2-B1-F4	109.97(19)
F3-B1-F1	109.37(19)	F2-B1-F1	108.71(19)
F4-B1-F1	109.45(18)	F12-B3-F10	109.81(19)
F12-B3-F11	108.97(18)	F10-B3-F11	110.16(19)
F12-B3-F9	109.47(19)	F10-B3-F9	109.35(18)
F11-B3-F9	109.06(19)	F7A-B2-F6A	123.0(14)
F8-B2-F5	113.4(4)	F8-B2-F7	112.3(5)
F5-B2-F7	107.2(4)	F8-B2-F6	111.1(6)
F5-B2-F6	108.0(6)	F7-B2-F6	104.4(6)
F7A-B2-F5A	115.1(7)	F6A-B2-F5A	107.3(12)
F7A-B2-F8A	105.5(9)	F6A-B2-F8A	103.8(13)
F5A-B2-F8A	98.7(8)		

Table 6. Torsion angles ($^{\circ}$) for AbbSa9_AP7313123.

C5-N1-C1-C2	1.9(3)	Cr1-N1-C1-C2	178.45(14)
C5-N1-C1-C7	-176.04(16)	Cr1-N1-C1-C7	0.5(2)
N1-C1-C2-C3	-1.4(3)	C7-C1-C2-C3	176.43(18)
C1-C2-C3-C4	-0.6(3)	C2-C3-C4-C5	1.9(3)
C2-C3-C4-C6	-177.2(2)	C1-N1-C5-C4	-0.6(3)
Cr1-N1-C5-C4	-176.62(14)	C3-C4-C5-N1	-1.3(3)
C6-C4-C5-N1	177.83(19)	C11-N2-C7-C8	-2.3(3)
Cr1-N2-C7-C8	170.81(15)	C11-N2-C7-C1	176.96(16)
Cr1-N2-C7-C1	-10.0(2)	N1-C1-C7-N2	6.3(2)
C2-C1-C7-N2	-171.60(18)	N1-C1-C7-C8	-174.48(18)
C2-C1-C7-C8	7.6(3)	N2-C7-C8-C9	1.3(3)
C1-C7-C8-C9	-177.84(19)	C7-C8-C9-C10	0.5(3)
C8-C9-C10-C11	-1.2(3)	C8-C9-C10-C12	-179.3(2)
C7-N2-C11-C10	1.5(3)	Cr1-N2-C11-C10	-170.66(15)
C9-C10-C11-N2	0.2(3)	C12-C10-C11-N2	178.4(2)
C17-N3-C13-C14	0.4(3)	Cr1-N3-C13-C14	-177.44(15)
C17-N3-C13-C19	177.82(17)	Cr1-N3-C13-C19	0.0(2)
N3-C13-C14-C15	0.7(3)	C19-C13-C14-C15	-176.47(19)
C13-C14-C15-C16	-1.0(3)	C14-C15-C16-C17	0.1(3)
C14-C15-C16-C18	-179.84(19)	C13-N3-C17-C16	-1.3(3)
Cr1-N3-C17-C16	176.23(15)	C15-C16-C17-N3	1.0(3)
C18-C16-C17-N3	-178.98(19)	C23-N4-C19-C20	2.4(3)
Cr1-N4-C19-C20	-174.75(16)	C23-N4-C19-C13	-177.15(17)
Cr1-N4-C19-C13	5.7(2)	N3-C13-C19-N4	-3.8(3)
C14-C13-C19-N4	173.53(19)	N3-C13-C19-C20	176.70(19)
C14-C13-C19-C20	-6.0(3)	N4-C19-C20-C21	-2.0(3)
C13-C19-C20-C21	177.5(2)	C19-C20-C21-C22	-0.4(3)
C20-C21-C22-C23	2.3(3)	C20-C21-C22-C24	-176.6(2)
C19-N4-C23-C22	-0.3(3)	Cr1-N4-C23-C22	176.45(15)
C21-C22-C23-N4	-2.0(3)	C24-C22-C23-N4	177.0(2)
C29-N5-C25-C26	3.0(3)	Cr1-N5-C25-C26	-172.20(16)
C29-N5-C25-C31	-176.43(17)	Cr1-N5-C25-C31	8.4(2)
N5-C25-C26-C27	-2.2(3)	C31-C25-C26-C27	177.1(2)
C25-C26-C27-C28	-0.5(3)	C26-C27-C28-C29	2.3(3)
C26-C27-C28-C30	-178.3(2)	C25-N5-C29-C28	-1.1(3)
Cr1-N5-C29-C28	173.47(15)	C27-C28-C29-N5	-1.5(3)
C30-C28-C29-N5	179.01(19)	C35-N6-C31-C32	-0.6(3)
Cr1-N6-C31-C32	178.92(15)	C35-N6-C31-C25	177.20(17)
Cr1-N6-C31-C25	-3.3(2)	N5-C25-C31-N6	-3.4(3)
C26-C25-C31-N6	177.21(19)	N5-C25-C31-C32	174.30(19)
C26-C25-C31-C32	-5.1(3)	N6-C31-C32-C33	0.9(3)
C25-C31-C32-C33	-176.7(2)	C31-C32-C33-C34	-0.4(3)
C32-C33-C34-C35	-0.3(3)	C32-C33-C34-C36	-179.4(2)
C31-N6-C35-C34	-0.2(3)	Cr1-N6-C35-C34	-179.63(15)
C33-C34-C35-N6	0.6(3)	C36-C34-C35-N6	179.75(19)

CURRICULUM VITAE

Sara Abbassi

Gräulingerstr. 109, 40625 Düsseldorf

Tel: +4917663843705

Email: sara.abbassi@yahoo.com

An innovative chemical scientist with experience in all major fields of applied, organic and inorganic chemistry, developing ideas and concepts and managing projects. Creative, self-motivated and pro-active with a proven ability to take concept and turn it into a deliverable result through efficient and persistent project management.

KEY SKILLS & EXPERIENCE

- Familiar with different methods of chemical laboratory techniques and analysis such as Infrared spectroscopy (IR), ultraviolet-visible spectroscopy (UV), nuclear magnetic resonance spectroscopy (NMR), cyclic voltammetry (CV), gas chromatography (GC), Mass Spectroscopy, etc.
- Ability to work with oxygen and moisture sensitive materials and familiar with different methods in this field
- Ability to teach, lead and mentor young students in the field of chemistry
- Familiar with pharmaceutical synthesis tests and their procedures
- Good experience in QC/QA of industrial plants and QA/QC procedures
- Ability to function well within multidisciplinary teams
- Problem solving and troubleshooting skills

CAREER HISTORY

Technical University of Munich

2012 - 2016

Munich, Germany

Worked as research fellow and PhD candidate in the chair of molecular catalysis under the supervision of Prof. Dr. Fritz E. Kühn.

Alborz Plastic Co.

2005 - 2008

Manufacturer of different sizes of Polyethylene pipes of different uses such as sewage, water supply, electric conduits, etc.

Worked as Quality Control Officer & responsible for compliance of raw materials, manufacturing process and product quality with established codes and standards by means of different chemical and physical test methods.

EDUCATION & QUALIFICATION

Ph.D. in Chemistry (Dr. rer. nat.)

2012 - 2016

Technical University of Munich, Germany

- Inorganic Chemistry, Molecular Catalysis, Chemistry Department
- Dissertation Title:
Building Blocks for Organometallic Frameworks and Ionic Liquids
- Scholarship from Bavarian Research Foundation

Master of Science in Organic Chemistry

2005 - 2008

Azad University, Karaj branch, Iran

- Chemistry Department
- Dissertation Title:
Synthesis and Study of Pharmacological Effects of New Derivatives of Phencyclidine Family

Bachelor of Science in Industrial Chemistry

2000 - 2004

Azad University, Karaj branch, Iran

- Chemistry Department
- Dissertation Title:
Quality Control Experiments in Chemical Laboratories of Institute of Standards and Industrial Research of Iran

STUDY & RESEARCH

- Synthesis of different building blocks for metal-organic frameworks and study on their applications
- Synthesis and study on the applications of ionic liquids for Li-ion batteries and electrochemical reduction of carbon dioxide.
- Synthesis and study on analgesic effects of 1-[1-(4-methylphenyl)(cyclohexyl)] 4-piperidinol and 1-[1-(4-methoxyphenyl)(cyclohexyl)] 4-piperidinol as two new phencyclidine derivatives published in *Arzneimittelforschung* (2009;59(4):202-6)
- Research on development and testing of pharmaceutical products

LANGUAGE SKILLS

- Persian: native speaker
- English: Fluent

- German: conversational
- Arabic: basic

EXTRA COURSES PASSED

- Manufacturing process, analysis of characteristics and quality control test of Poly Ethylene pipes - Institute of Standards and Industrial Research of Iran
- Quality control of chemical products including detergents, paints, glues, plastic & other polymer products like PE, PP, PVC, oil & petroleum products like car engine lubricants & grease and organic products like car brake fluid - Institute of Standards & Industrial Research of Iran
- Project management in biopharma industries - Technical University of Munich, Germany
- Biotech quality management - Technical University of Munich, Germany
- Practical IR and Raman spectroscopy - Technical University of Munich, Germany
- Surviving complex projects - Technical University of Munich, Germany
- Discover your strengths - Technical University of Munich, Germany
- Developing entrepreneurial thinking - Technical University of Munich, Germany